

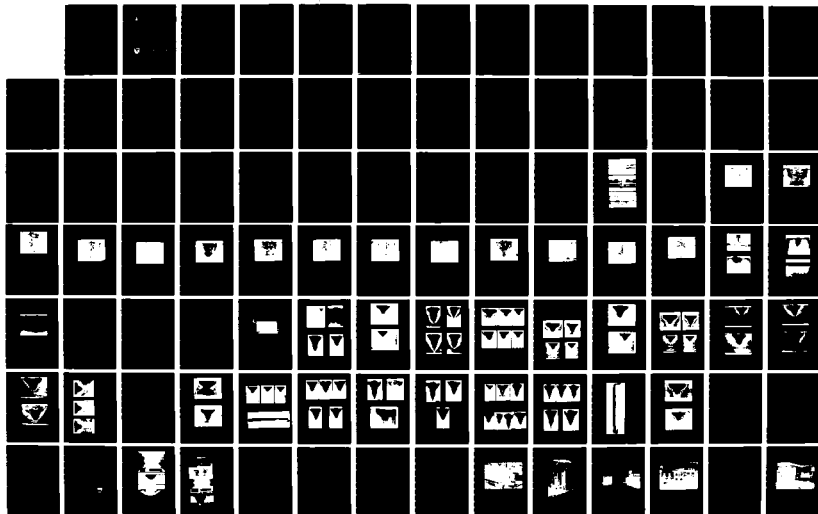
AD-A158 082

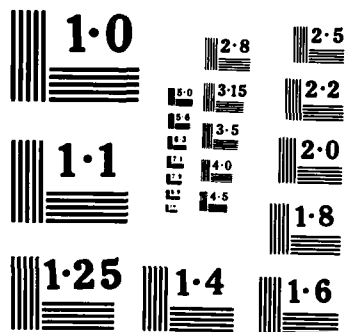
MANUFACTURING METHODS AND TECHNOLOGY APPLICATION OF  
HIGH ENERGY LASER WEL.. (U) ARMY MISSILE COMMAND  
REDSTONE ARSENAL AL STRUCTURES DIRECTORA.. J V MELONAS  
AUG 88 ANSMI/RL-82-2-TR F/G 20/5

1/2

UNCLASSIFIED

NL





NATIONAL BUREAU OF STANDARDS  
MICROCOPY RESOLUTION TEST CHART

AD-A158 082



TECHNICAL REPORT RL-82-2

MANUFACTURING METHODS AND TECHNOLOGY APPLICATION  
OF HIGH ENERGY LASER WELDING PROCESS

John V. Melonas  
Structures Directorate,  
U S Army Missile Laboratory

August 1980

DTIC  
ELECTE  
S JUL 10 1985  
A



**U.S. ARMY MISSILE COMMAND**

*Redstone Arsenal, Alabama 35809*

Approved for public release; distribution unlimited.

DTIC FILE COPY

#### **DISPOSITION INSTRUCTIONS**

**DESTROY THIS REPORT WHEN IT IS NO LONGER NEEDED. DO NOT  
RETURN IT TO THE ORIGINATOR.**

#### **DISCLAIMER**

**THE FINDINGS IN THIS REPORT ARE NOT TO BE CONSTRUED AS AN  
OFFICIAL DEPARTMENT OF THE ARMY POSITION UNLESS SO DESIGNATED BY OTHER AUTHORIZED DOCUMENTS.**

#### **TRADE NAMES**

**USE OF TRADE NAMES OR MANUFACTURERS IN THIS REPORT DOES  
NOT CONSTITUTE AN OFFICIAL INDORSEMENT OR APPROVAL OF  
THE USE OF SUCH COMMERCIAL HARDWARE OR SOFTWARE.**

REPORT DOCUMENTATION PAGE		READ INSTRUCTIONS BEFORE COMPLETING FORM
1. REPORT NUMBER MMT 3441	2. GOVT ACCESSION NO. AD-A158082	3. RECIPIENT'S CATALOG NUMBER
4. TITLE (and Subtitle) Manufacturing Methods and Technology Application of High Energy Laser Welding Process		5. TYPE OF REPORT & PERIOD COVERED Final Technical Report 16 Oct 78 - 30 Sep 79
		6. PERFORMING ORG. REPORT NUMBER
7. AUTHOR(s) John V. Melonas		8. CONTRACT OR GRANT NUMBER(s) DAAK40-79-C-0004
9. PERFORMING ORGANIZATION NAME AND ADDRESS Commander US Army Missile Command ATTN: DRSMI-RL, Redstone Arsenal, AL 35898		10. PROGRAM ELEMENT, PROJECT, TASK AREA & WORK UNIT NUMBERS
11. CONTROLLING OFFICE NAME AND ADDRESS Commander US Army Missile Command DRSMI-ET, Redstone Arsenal, AL 35898		12. REPORT DATE August 1980
		13. NUMBER OF PAGES 159
14. MONITORING AGENCY NAME & ADDRESS (if different from Controlling Office)		15. SECURITY CLASS. (of this report)  UNCLASSIFIED
		15a. DECLASSIFICATION/DOWNGRADING SCHEDULE
16. DISTRIBUTION STATEMENT (of this Report)  <div style="border: 1px solid black; padding: 5px; width: fit-content; margin: 10px auto;"> This document has been approved for public release and sale; its distribution is unlimited. </div>		
17. DISTRIBUTION STATEMENT (of the abstract entered in Block 20, if different from Report) Approved for public release; distribution unlimited		
18. SUPPLEMENTARY NOTES		
19. KEY WORDS (Continue on reverse side if necessary and identify by block number) Highpower Laser; Laser Welding; Welding; Sheet Steel alloy welding; aluminum alloy plate welding; CO <sub>2</sub> continuous-wave laser; T-joint welds; lap welds; butt welds.		
20. ABSTRACT (Continue on reverse side if necessary and identify by block number) A 50 Kw CW CO <sub>2</sub> laser was used to establish: Optimum welding parameters for common joint configurations for both steel and aluminum alloys; and economic factors which prevail in a production environment. Feed-rate, heat ranges, special tooling, and economic considerations were evolved for each metal. A significant breakthrough in the control of weld heat in the aluminum workpiece was evolved with the development of a reflecting shield which		

UNCLASSIFIED

SECURITY CLASSIFICATION OF THIS PAGE(When Data Entered)

essentially increased the heat in the workpiece by a factor of two. Thus, greater depth and quality of the weld bead resulted.

The work reflected in this report contributes significantly to the establishment of essential data and information which are required in accomplishing optimum laser welds in steel and aluminum at a favorable cost.

*Reynolds*

Accession For	
NTIS GRA&I	<input checked="" type="checkbox"/>
DTIC TAB	<input type="checkbox"/>
Unannounced	<input type="checkbox"/>
Justification	
By	
Distribution/	
Availability Codes	
Dist	Avail and/or Special
A-1	

RE: Distribution Statement, Rept. MMT-3441  
Unlimited per Mr. Parker, USAMICOM/AMSMI-ET

UNCLASSIFIED

SECURITY CLASSIFICATION OF THIS PAGE(When Data Entered)

## CONTENTS

	PAGE
INTRODUCTION . . . . .	3
 PART I - LASER WELDING OF STEEL . . . . .	5
A. Objective. . . . .	3
B. Equipment . . . . .	3
C. External Optics . . . . .	8
D. Automatic Laser Control for Welding . . . . .	8
E. Gas Shielding . . . . .	9
F. Materials . . . . .	9
G. Welding Trails . . . . .	10
H. Application of the Laser to Storage Containers . . . . .	21
I. Demonstration of Capability of Laser Welding to Produce Types of Joints Found in Missile Containers. . . . .	32
J. Conclusions . . . . .	54
K. Recommendations. . . . .	54
 PART II - LASER WELDING OF ALUMINUM . . . . .	55
A. Introduction . . . . .	55
B. Procedure . . . . .	55
C. Results. . . . .	56
D. Summarized Bar Chart . . . . .	79
E. Summary . . . . .	80
F. Conclusions . . . . .	80
G. Recommendations. . . . .	81
 APPENDIX . . . . .	85

## I. Introduction

The objective of this project was to establish the feasibility of applying multi-watt continuous wave CO<sub>2</sub> lasers for welding of missile shipping and storage containers. These containers are currently manufactured by cutting, forming, and welding sheet steel but future design will probably include aluminum. A high power CO<sub>2</sub> laser originally designed and developed to operate at a peak power of 50 Kw as a prototype mobile weapon test system was modified for use in this project. The laser was operated in the continuous wave mode with an annular beam configuration.

A significant portion of this project was conducted at two other facilities possessing Avco high power lasers and actively engaged in applying these lasers to metalworking applications including welding. ITT Research Institute, Chicago, Illinois and Avco-Everett Metalworking Lasers, Somerville, Massachusetts, made significant contributions in defining welding parameters and in particular, effects of beam geometry and focal distance, as well as providing other technical support. Others participating in this project included Sperry Systems Management, Huntsville, Alabama, who operated and maintained the 50 kw laser; Lanson Industries, Cullman, Alabama, manufacturers of missile containers, who provided manufacturing data and access to their manufacturing facility for analysis of the feasibility of applying laser welding to missile container fabrication, as well as material for laser welding experiments; Marshall Space Flight Center, NASA, Huntsville, Alabama, who provided technical welding consultation and some of the materials used in this project; and several laser consulting firms who provided support in control system development and optics. Other technical support was provided by various elements of MICOM including the Directed Energy Directorate, who provided operational support and technical assistance on all aspects of laser technology.

This report is divided into two parts. Part I is devoted to laser welding of sheet steel and describes the equipment, optics, gas shielding and weld trials; and contains an economic analysis of the laser manufacturing process applied to missile containers. Part II covers the work done in aluminum welding, the development of a welding shield that significantly improves aluminum laser welding efficiency, and optimizing parameters for welding of aluminum. The Appendix describes the many technical aspects of the MICOM 50 Kw laser, the operating procedures, welding fixtures and the modifications made to the laser to provide welding capability.

Laser welding of missile containers is shown to be feasible, but to be economically effective, extensive modification of weld joints, current manufacturing sequences, and possibly design standardization of the multitude of types of shipping containers would be necessary in order to maintain a simple mode of external optics. Complex optics systems would not be economically suitable for the quantities of containers currently manufactured.

A most significant technical contribution of the project is the development of a welding shield which greatly enhances heat input of the laser beam in welding aluminum and other highly reflective materials.





## PART I LASER WELDING OF SHEET STEEL

### A. OBJECTIVE

The objective of this study was to establish the feasibility of laser welding missile shipping containers and to establish welding procedure data, energy density, power settings, welding speeds, etc., for steel sheet materials. Feasibility of this process is determined by economics and the capability of the equipment to produce a reliable weld consistently in a production environment. This dictates that the equipment itself must operate reliably in between scheduled maintenance periods to prevent massive nonproductive labor costs.

In accordance with the objective, an analysis was made of the MICOM high power laser (50 Kw) whereby welding procedure data was generated for welding sheet steel. In addition, the manufacturing of missile storage containers at Lanson Industries was analyzed. These containers are a moderately high production welded structural unit consisting of 20,000 units of various configurations per year. The welds must be of an acceptable quality to endure severe service conditions. These characteristics suggest the need for a rapid, high quality welding process.

### B. EQUIPMENT

The equipment used in this effort was a very large, high power (50 Kw HPL) laser built by Avco Everett Laboratories, Everett, Massachusetts, and installed at Redstone Arsenal, Alabama.

In this discussion, the elements of the overall system will be briefly described. Technical aspects, operating procedures, welding fixtures and modifications made to this laser to provide welding capability are described in the Appendix. Those that influence its application in a production situation are discussed in greater detail.

Additional lower power welding studies were conducted on IITRI's industrial CO<sub>2</sub> Avco laser. Its power ranges from 1 to 15 Kw.

#### 1. Transverse Flow Laser Head

This portion of the MICOM laser is similar to the industrial HPL series lasers produced by Avco Everett Laboratories in two respects: first, the use of a closed cycle gas-handling system (wind tunnel) in which a mixture of CO<sub>2</sub>, CO, He, and N<sub>2</sub> is circulated, and, second, the fact that the electric current, which produces the laser energy, is conducted through the gas stream at right angles (transverse) to the direction of flow.

Such transverse flow systems are industrially attractive because they can be built to produce greater power levels than the alternative axial (tubular) lasers and are more compact.

## 2. Electron Stabilization

Another area of similarity between the MICOM laser and the Avco industrial lasers is the broad area electron beam (EB) source which is built onto the throat of the wind tunnel. This broad area EB gun provides a control over beam power, which is essential to industrial applications. The EB does this by introducing electrons into the gas, so that the transverse electric current, which produces and sustains the laser discharge, can pass easily from one side of the throat to the other, transverse to the gas stream, at lower voltages than would be the case if the extra electrons were not present.

The power of the laser is proportional to the electron beam output because the light-producing sustainer current flow is enhanced or suppressed as the number of electrons from the electron beam increases or decreases. Therefore, the EB feature provides a means for computerizing the laser output to assure that the amount of power is applied at each point along the weld joint, and for maintaining a constant closed loop control over beam power. To establish closed loop control, however, the beam must be sampled continuously. The EB can then respond to this sampling of the laser beam so that any tendency of the lasing action to rise or fall can be countered by lowering or raising, respectively, the output of the broad area electron beam.

Two key components that permit the realization of the desirable electron beam stabilization and control concept are:

a. The laser beam sampling system operates by exposing a rotating reflector surface of small area to the main laser beam as that beam leaves the laser head. The small amount of reflected beam energy is directed into the infrared detector. The detector output can then be calibrated (e.g., through the use of calorimeters) so that it bears a known relationship to the main laser beam.

b. The metallic foil "window" separates the high-vacuum (one-millionth atmosphere) environment of the electron beam system from the higher pressure environment of the laser gas stream into which the electrons must be directed. The need to perform satisfactorily as a window for electrons, and as a barrier for gas molecules, results in the need for a number of compromises in terms of material, material thickness, and ultimately, the life of the window. A 0.00050 in. (1/2 mil) aluminum foil, mounted in a hard-to-reach location underneath the laser head, is used in this particular system.

A stabilizing circuit was developed and built to control the laser output power. In the open loop, sustainer current control, and beam current control mode, the laser output power varies by approximately 40 percent during a 30 second lasing operation. In the power feedback mode the stabilizing circuit maintains the power within a 10 percent variation of the nominal power setting.

The electron beam foil "window" brings up a more fundamental question with respect to industrial utilization of this laser. The foil of the window constitutes a degradable element in the process. Thus, it has an impact on productivity. In the laser used in this program, loss of effectiveness of the foil was difficult to detect and failure hard to predict. Thus, replacement must be conducted at predetermined intervals, or upon complete failure and shutdown.

The arguments for arbitrary replacement relate to the fact that several hours are required to bring the system back on line after replacement. Production is best served if this "conditioning" is conducted off shift.

In the industrial version of the HPL, the actual changing of the foil requires only a few minutes. However, with the equipment used in this program, both the changing and conditioning are more complex. The downtime for a foil change would become excessive in a production shop environment.

	<u>Standard Industrial HPL</u>	<u>MICOM Laser Used in Program</u>
Hours for foil change	0.5	2.0
Hours for conditioning	3.5	18.0

In the program, the conditioning time consisted of six hours of the eight-hour day. However, the equipment is allowed to stand overnight accounting for 12 of the 18 hours before the laser is put into use again.

#### c. Auxiliary Components

The CO<sub>2</sub> laser system used in these studies includes many other subsystems. They are:

- Aerodynamic window--which allows the beam to exit the laser head without the need for a solid window.
- Refrigeration systems--which cool and maintain the temperature of the circulating gas.
- Internal optics--which produce the coherent laser beam.
- Coolant systems--which control the temperature of the internal optics and the current-conducting electrodes (while permitting the latter to be isolated electrically).
- Gas circulating system--high-capacity, axial blowers operating in the gas stream and powered by a motor generator set that converts 60 cycle line current to a frequency of 440 cycles.
- Sustainer power supply.
- Electron beam power supply.

These subsystems have been adapted to the present installation from the initial equipment application. They are, therefore, more complex than needed for general industrial usage. For example, a three-page checklist is required for daily start-up. In industrial systems the start-up function is more or less automatic.

### C. EXTERNAL OPTICS

The optical elements of the systems can be divided into two groups; internal optics (beam forming), and external optics (beam management). During these tests, two external optical systems were employed at MICOM. (The commercial external optics employed in the industrial trial laser are described in the Appendix.)

Initial welding trials were accomplished using a vertical welding beam. It should be noted that the MICOM laser, like its industrial counterpart, is configured to produce a hollow pipe-like beam of infrared light which is roughly parallel to the floor. This beam geometry permitted the use of an annular flat, upward deflecting mirror. The mirror feeds an overhead spherical (focusing) mirror. The focus mirror then directs the beam downward to a minimum point (focus), which is used to form the weld in metal which is transversed beneath the focus mirror.

The welding beam passes through the annular flat mirror. This means that the beam can feed back upon itself. Its folding angle is  $0^\circ$ . Low folding angles reduce astigmatism and produce the smallest, most concentrated focal point for a given condition.

Measurements of the impingement diameter at the face of the focusing mirror and of the distance between the focus mirror and focal point indicate that the MICOM optics could be characterized by an f/number between f/8 and f/12.

Avco has suggested that, for their industrial laser cavities, the multiplication of the f/number by 0.006 inches gives an approximation of the spot size. They have not related this to the distribution of energy within the beam. For purposes of this discussion, it will be assumed that it approximates the half-height diameter of a standard Gaussian distribution. In other words, under this assumption, the beam spot is at least 0.072 inches in diameter with an average specific energy of  $6 \times 10^6$  watts/in.<sup>2</sup> when the laser is operating at 25,000 watts.

### D. AUTOMATIC LASER CONTROL FOR WELDING

The laser control was converted from manual operation to automatic operation because manual control required attention to be placed in too many areas at one time. After designing the necessary equipment and connecting the logic controls, minimum operator control required for the laser operation for welding is limited to activating a start switch. The speed of the workpiece is checked automatically before activating the laser and shield gas. At the end of the weld cycle the laser is automatically turned off. Details of the automatic control system are given in the Appendix. All laser manual controls can override the automatic sequencing such as when the laser needs to be shut down prematurely.

Several advantages are provided with the automatic system as follows:

1. The laser is more closely controlled because viewing parallax causes a problem when controlling the laser manually and at the same time watching a closed circuit TV monitor.

2. The shielding gas is only on while the laser is on which provides a cost saving on shielding gas.
3. Laser operating time is significantly reduced during automatic operation.
4. Automatic operation releases the operator to monitor metering functions and be more aware of safety requirements; otherwise, a second person is required to handle the extra activities.

#### E. GAS SHIELDING

Unlike other high-intensity beams, such as electron and ion beams, the laser welds in normal room atmosphere. However, considerable improvement in rates of welding can be realized if the air around the beam impingement point is rapidly displaced by a gas of low atomic number.<sup>1</sup> The movement of displaced gases removes metal vapor from the weld area, yielding better access of the beam to the work. Of more importance, the vapor, which is a natural consequence of the interaction between high-intensity beams and the workpiece, appears to trigger an energy-absorbing plasma. If allowed to remain above the impingement point, the plasma blocks the beam. Moving gas displaces (and perhaps suppresses) the plasma for greater beam efficiency.

Shielding can provide further benefits if light gases, such as helium, are used to displace air. In these tests, a stream of helium was directed across the beam impingement point and its associated molten weld pool. The method of shielding the metal was adapted from conventional fusion welding. The gas nozzles used were adapted for commercial practice. These nozzles projected a coherent gas stream about 1 inch, and thus they could be set well out of the beam path. Gas was projected back over the solidifying weld. During the latter part of the program, an improved gas shield was developed with an integrally designed mirror which deflected laser beams reflected from the workpiece. Details of this shield appear in Part II of this report.

#### F. MATERIALS

Three materials were considered: Cor-Ten Grade A steel sheet, hot rolled rimmed steel sheet, and carbon steel plate.

##### 1. Cor-Ten Grade A Sheet

Thickness of 0.062 and 0.118 inches were evaluated. This material appears to be weldable. The chemical composition of Cor-Ten Grade A (Type 1) is:

D (max)	0.15%
Mn (max)	1.00%
P (max)	0.15%
S (max)	0.05%
Cu (max)	0.20%

It conforms to ASTM A242; SAE 7410B, grade 950D; and MIL-S-1250A.

<sup>1</sup>F. D. Seaman, "The Role of Shielding Gas in High Power CO<sub>2</sub> (CW) Laser Welding", SME Technical Paper No. MR77-982, 1977.

## 2. Hot Rolled Rimmed Steel Sheet

Thicknesses of 1/16 and 1/8 inch were evaluated. The making of rimmed steel leaves the remains of a core of solidified metal containing large amounts of nitrogen in the sheet. Severe evolution of gas was observed when the beam interacted with the core of this steel. The reaction could be controlled by coating the surface with aluminum, but because of the added operation, the welding of hot rolled steel was not pursued.

## 3. Carbon Steel Plate

Because of the uniquely high power level available to the program (24 Kw), welds were attempted in thick section plate. A plate 1 1/4 inches thick was used, so that the maximum weld thickness could be maintained and measured within the plate.

## G. WELDING TRIALS

The MICOM laser system described in the Appendix had not been used for welding prior to this manufacturing technology program. Therefore, before any comparisons or analyses could be made, a welding data base had to be established. This action describes the welding trials that build the base.

The existence of a focal point in beam welding procedures (EB and laser) has a special significance in terms of the effectiveness and efficiency of the process. Early investigators assumed that the focal point should always be placed on top of the work surface and maintained at this position very precisely - regardless of the cost of doing so. At the present, results indicate this is not necessary.

At some maximum speed (for a given power and thickness) only one focal point placement will exhibit full penetration. This unique combination of maximum full-penetration speed and optimum focus serves as an excellent point of reference with which to relate other processes or to compare materials but, as will be shown, it is not necessarily the best operating condition. Because it can serve as a reference, it can be called the bench mark condition (of optimum focus and maximum speed). The bench mark speed would be expected to change with the beam power, material, and material thickness.

### 1. Using the Bench Mark to Study Processes

Although the single invariable focus placement associated with the so-called bench mark will produce an acceptable weld, the bench mark speed-focus condition is a very poor selection as an operating procedure. It does not permit variations in either speed or telescope/work position. Nevertheless, the bench mark does serve as an anchor for a survey of experimentally determined "off-mark" conditions (Figure 1).

Off-mark conditions, as shown in Figure 1, reveal a great deal more about practical laser welding processes than does the bench mark. The first observation that can be made from such a survey of off-mark conditions is that speeds below the bench mark result in full penetration over an increasingly broad range of focal point settings.

The above proportions may be slightly distorted. Operations 5 and 6 involve more complex welding access problems than the other operations. Nevertheless, it appears reasonable to assume that the principal potential for savings lies in the development of a plate/channel welding concept (operations 3 and 6). These two similar configurations involve 54% of the welding time, - almost one hour of labor. They also represent a classic approach to the transition from arc to laser welding.

As a point of departure, it is necessary to point out that the rail, as presently joined to the channel, must go into the assembly before the inner plate can be put on. Otherwise, access to the operation 6 weld areas becomes limited, even for a laser beam. Approaches which would allow the rail to be welded into the narrow space between inner plates will not be considered here. The assumption will be made that it is most efficient to weld the two channels onto the rail (one at either end, to form an "H" shaped subassembly), using the present GMAW process as an initial operation in the sequence while there is maximum access to the rail/channel joint. However, fabrication of the "H" shaped rail/channel(s) subassembly (Figure 11) limits the work-handling approaches available to the system because it prevents the rotation of the individual channels under the beam. The beam now has to be moved around the plate/channel weld area in some manner while the subassembly is clamped on a tooling plate. Two joint configurations are available: (1) reaching into a "carriage" (Figure 12), or corner weld with the beam, and (2) a 2 ply lap. The 2-ply lap joint was selected for this study because (1) beam/joint alignment is not critical, and (2) the large spot available from the high power laser provides a joint which apparently has an adequate shear area. The resulting process is shown, for one quarter of the "H" shaped cradle assembly, in Figure 13 where it is compared with the current GMAW methods. The resulting total welding time for this operation (plate/channel welding) is: GMAW: 0.864 hr (est.); Laser: 0.100 hr.

Figure 14 suggests an optical/mechanical tooling concept for handling the awkward 32 x 48 in. "H" shaped assembly. The sequence minimizes redundant moves, as follows:

1. Operator assembles plate into tooling which locates them accurately at the proper intervals along the channel. (This tooling is conventional and not shown.) The "H" shaped channel weldment is then locked over the plate so that the plate and channel surfaces touch at the weld areas.
2. Loaded tooling is moved into the laser welding station. The door latches automatically. The laser will not start until the latching takes place.
3. The tooling is indexed (toward the viewer in Figure 14) to the plane of one of the plate/channel joints in what can be termed "Channel A", and a flat mirror is positioned to redirect the beam to the side of the channel.
4. The first of the 2 ply lap welds occurs when the tooling moves the work-piece downward with the beam impinging horizontally onto the side of the channel. The tooling in Figure 15 is just starting this downward stroke, using the three vertical, chain-driven lead screws shown under the tooling carriage.

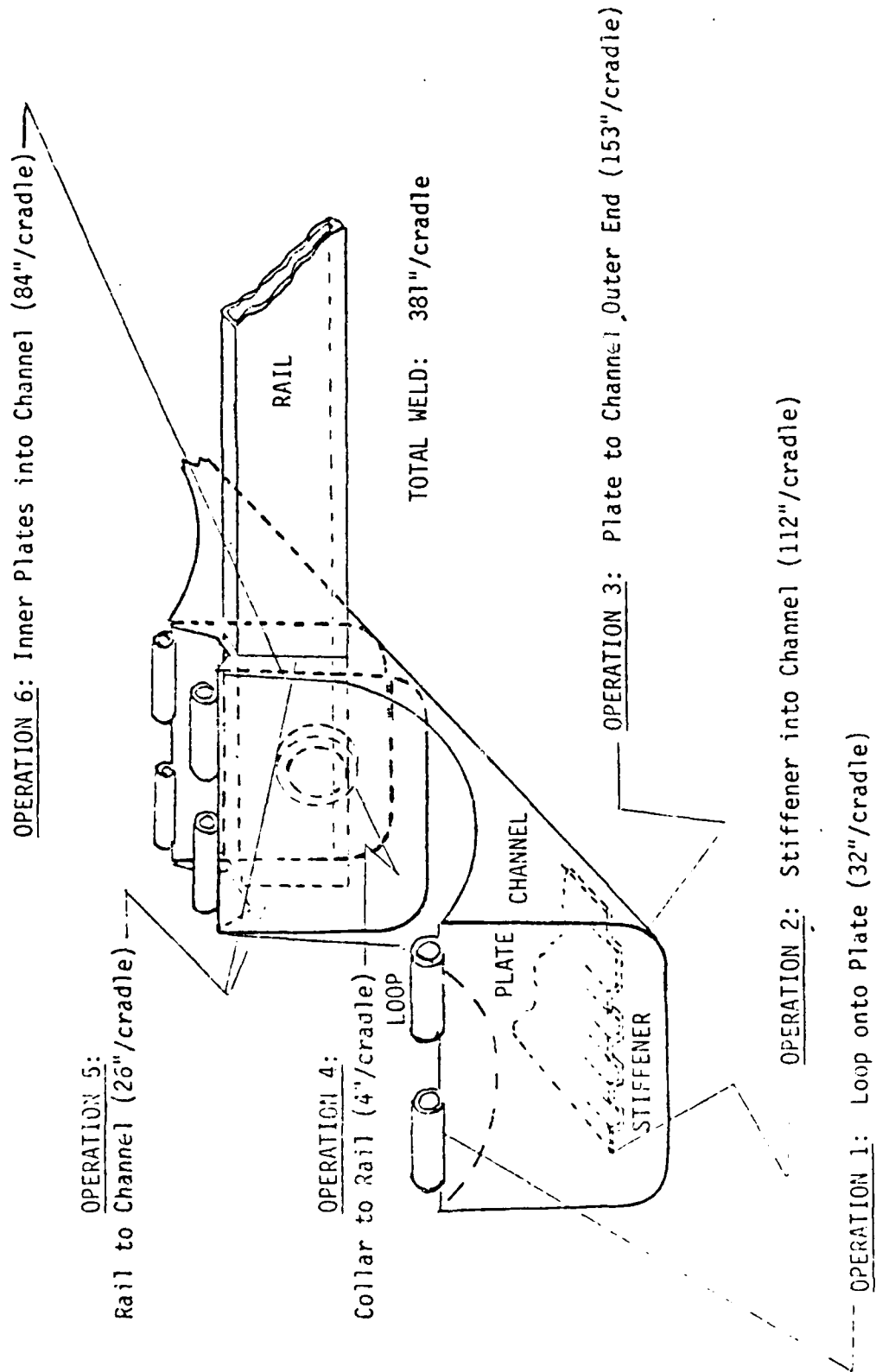


Figure 10. Current manufacturing sequence for cradle fabrication.



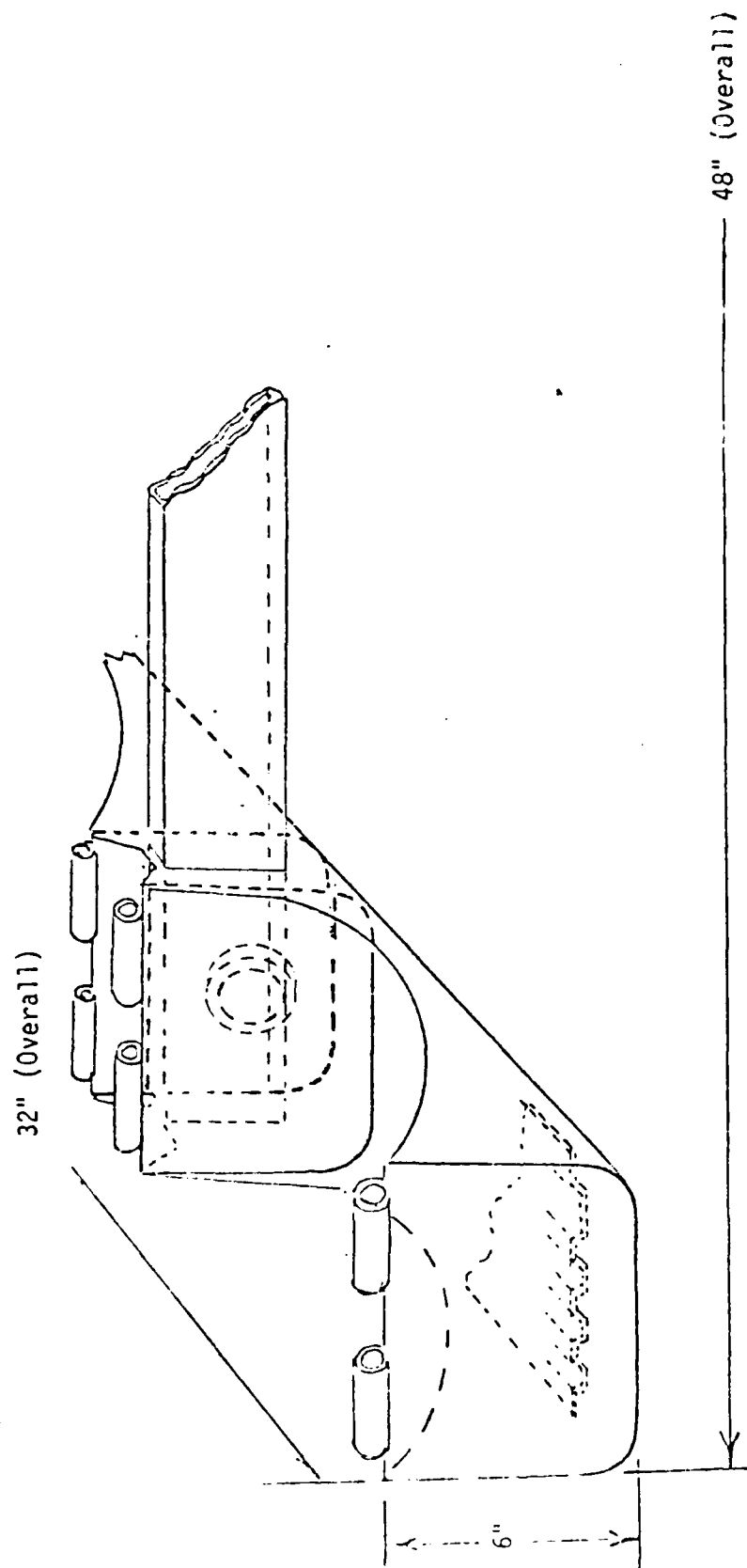


Figure 9. Detail of cradle fabrication.

#### H. Application of the Laser to Storage Containers

The CMU 238E storage container was analyzed for potential application of laser welding. The distinctively high welding labor content associated with the cradle subassembly suggested it as a candidate for the applications study carried out in this section. The welding labor content of the other subassemblies is listed below:

H-frame	0.639 hr
Body	0.508 hr
End panel	0.226 hr
Cradle	1.600 hr

As shown, the cradle takes 1.60 hr to build, compared with 0.508 hr to fabricate the entire main body weldment of the CMU 238E storage containers. Almost all of the 1.60 hr is used for producing the required 381 in. of weld. Weld placement is difficult, bringing the effective joint completion rate down from 14 ipm (typical for the body) to 4 ipm in the more complex cradle weldment.

Such slow productivity, relating as it does to joint accessibility, coupled with the large amount of welding per weldment, makes the cradle (Figure 9) a classic application for laser beam welding. To fully understand the application, it is necessary to consider the geometry of the cradle (Figure 9) and the present manufacturing sequence. This sequence is built around the Gas Metal Arc Welding (GMAW) process in which metal from a bare wire electrode is deposited by an arc into the joint.

In the cradle application, all welding is manual and each weld requires the operator to perform a number of separate operations which include: the visual alignment of the welding gun with the joint; dropping the operator's eye protection shield; starting of the arc; welding; and termination of the arc. Welds are short, usually 4-6 in., so that the actual welding time is dominated by the complex start-and-stop operations. This explains the low productivity and suggests an automated process, such as the laser.

Figure 10 defines the present manufacturing sequence, in which six operations are required. Operation 6 involves two welders. The other operations are carried out by a single welder, or by a welder working between short operations, such as Nos. 1 and 4. As previously noted, the total time is 1.60 hr. If the linear inches of weld in each operation are used as a criterion for breaking down the total time into operation increments, the following distribution occurs:

<u>Operation</u>	<u>Time/Hr.</u>
1. Loop/plate	0.144
2. Stiffener (corrugated)/channel	0.464
3. Plate/channel (outer ends)	0.512
4. Collar/rail	0.016
5. Rail/channel	0.112
6. Plate/channel (inner)	0.352
TOTAL	1.600

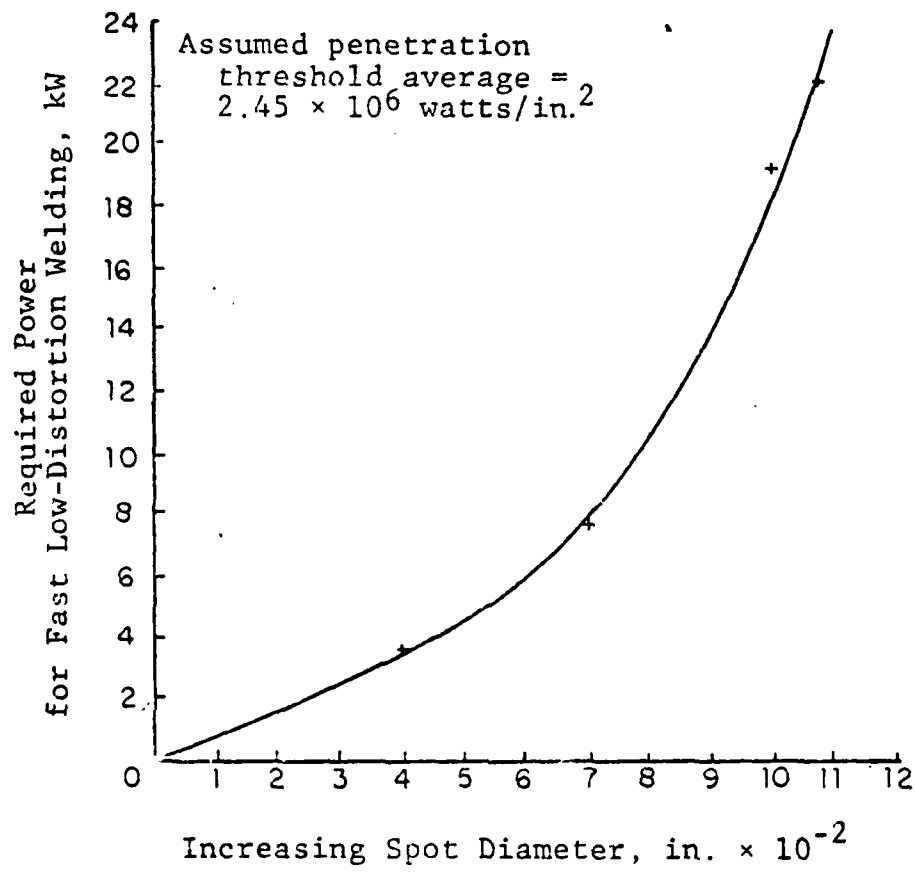


Figure 8. Influence of spot diameter on capital costs.

The broad latitude is significant in that it greatly reduces the need for an expensive, hard-to-maintain, precision relationship between the optics and the workpiece. A stamped sheet metal weldment, for example, demands this type of latitude if the laser is to be applied because it cannot be precision formed. But these high f/No. optics involve a large diameter spot. A large spot welding technique is valuable for lap joints of the type welds in Figure 7 because they provide a commercially useful shear area at the sheet interfaces. For sheet metal, this is an additional advantage over the tolerance to workpiece variances that also characterizes the high f/Nos.

The realization of these broad-spot advantages brings the role of the large laser into perspective. The productive advantages of a laser welding process - speed and precision - stem from the special way in which a laser weld is formed.

In producing a weld with a laser, the focused beam literally blasts a hole to the desired depth, or through the workpiece if a full penetration joint is required. This hole is called a cavity. The width of the cavity is closely related to the diameter of the beam at the impingement point on the work. Hence, if a broad weld zone is desired, a broad cavity must be formed and a broad beam spot must be used. Reducing speed can also be used to broaden the weld since the welding process has time to transmit more energy to the cavity walls and to the metal surrounding the cavity. But the effect is not as pronounced upon bead width as the changing of the spot size, and distortion increases greatly.

There is, however, a limitation placed upon the increased spot size if the cavity type of weld is to be obtained. The energy density within the spot must stay above some threshold value,\* generally believed to be  $1-5 \times 10^6$  watts/in<sup>2</sup>. Figure 8 shows a calculated relationship between required laser power and the spot size, assuming the beam energy threshold has to be  $2.45 \times 10^6$  watts/in<sup>2</sup>. Because the spot area is related to the square of the spot diameter, the curve increases rapidly as the spot diameter increases. Following is a summary of the technical/economic relationship derived herein.

a. Large spots, when produced by high f/No. optics, have two advantages when sheet metal joints are considered: (1) Broad shear areas in 2 ply overlap welds, and (2) Tolerance for work/telescope distance.

b. The larger the spot, the larger the spot areas (as a function of the square of the diameter).

c. The larger the spot diameter, the greater the need for higher power levels.

Therefore, realization of the advantages of large spot laser welding will involve lasers with relatively high power levels.

---

\*For the bench marks obtained, the threshold appeared to be  $3.6 \times 10^6$  and  $1.3 \times 10^6$  watts in<sup>2</sup>. for the 5 and 12 kw experiments, respectively. Spot diameters were estimated from manufacturer's data.

Material: Cor-Ten steel  
 Thickness: 0.236 in. (total)  
 Type of Weld: Two-ply assembly  
 Optics: f/8-f/12  
 Power: 24 kW (est.)  
 Beam Configuration: Concentric

Symbols: F = Full penetration  
 S = Some evidence of penetration  
 N = No evidence of penetration

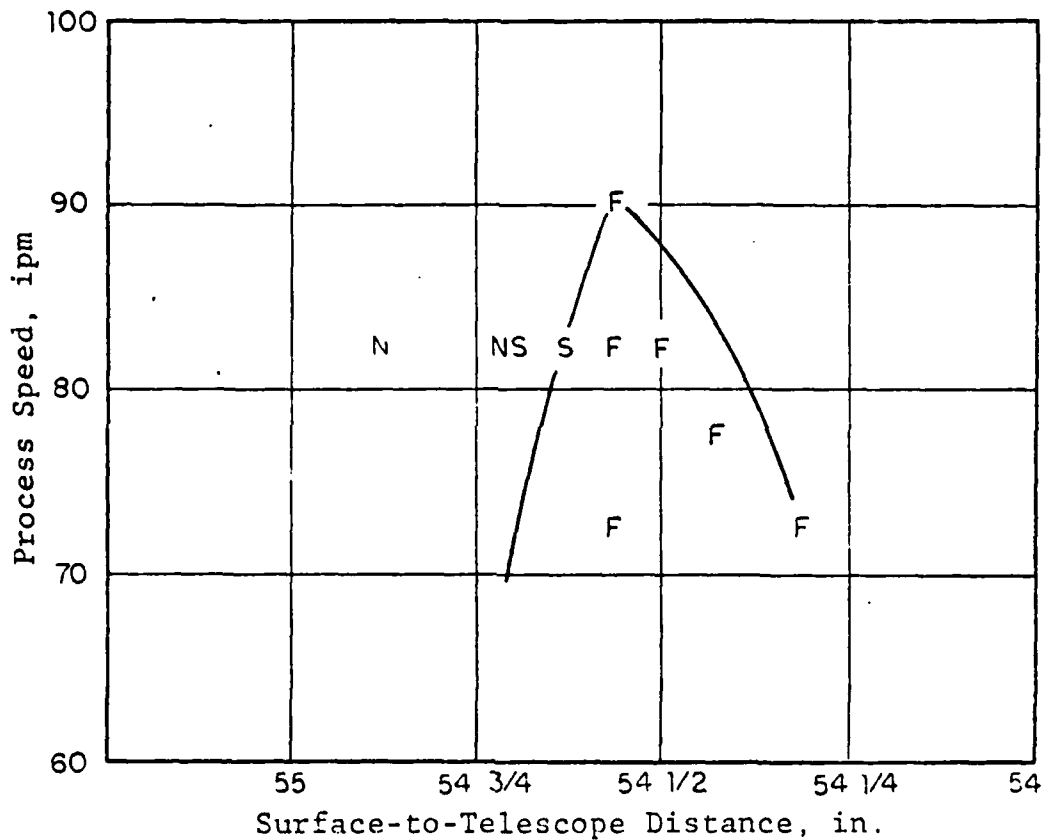


Figure 7. 13 kW bench mark survey on Cor-Ten steel.

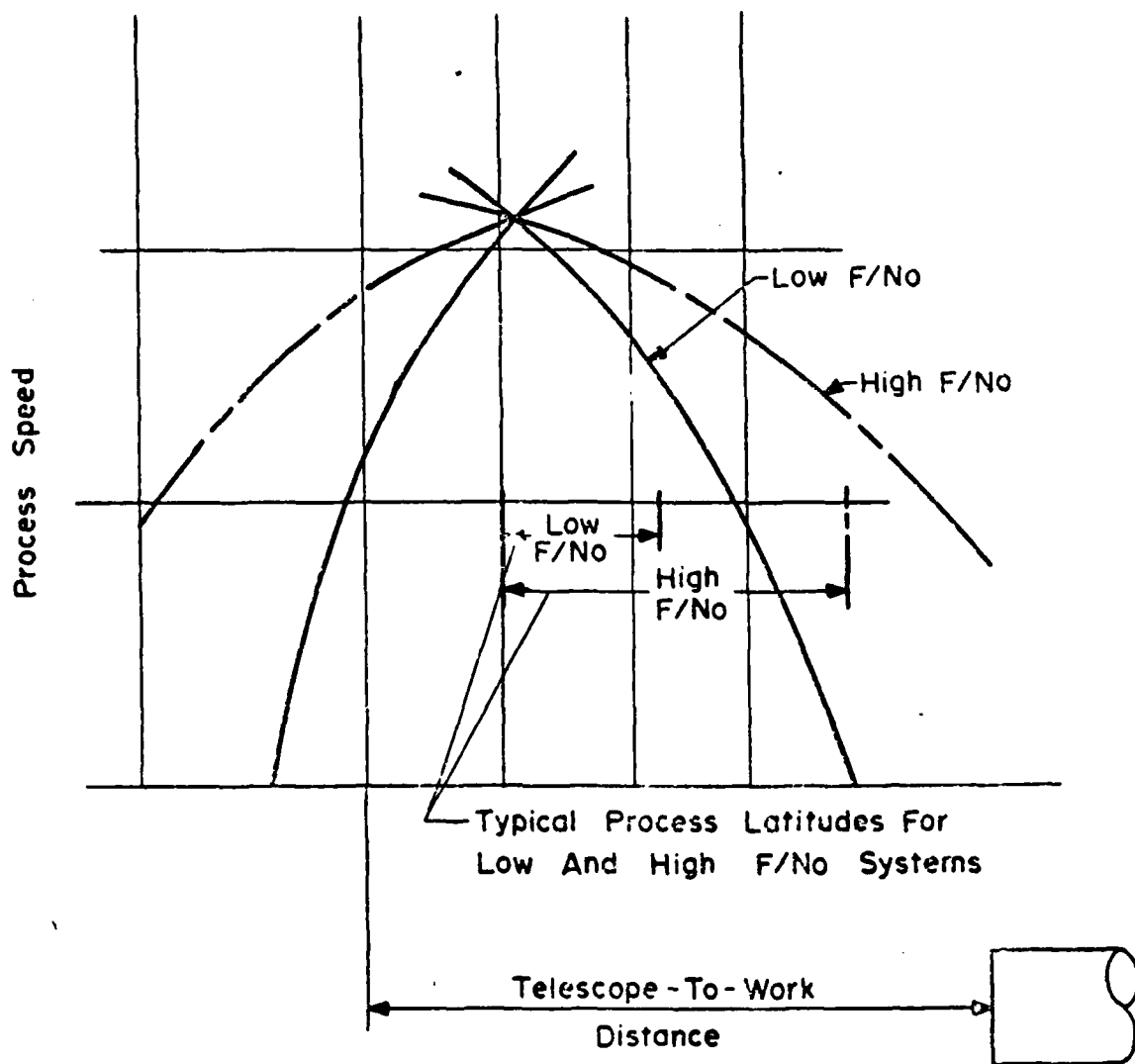


Figure 6. Increased tolerance in telescope-to-work distance with increasing  $f/\text{No.}$ , as shown in full-penetration boundaries of bench mark survey.

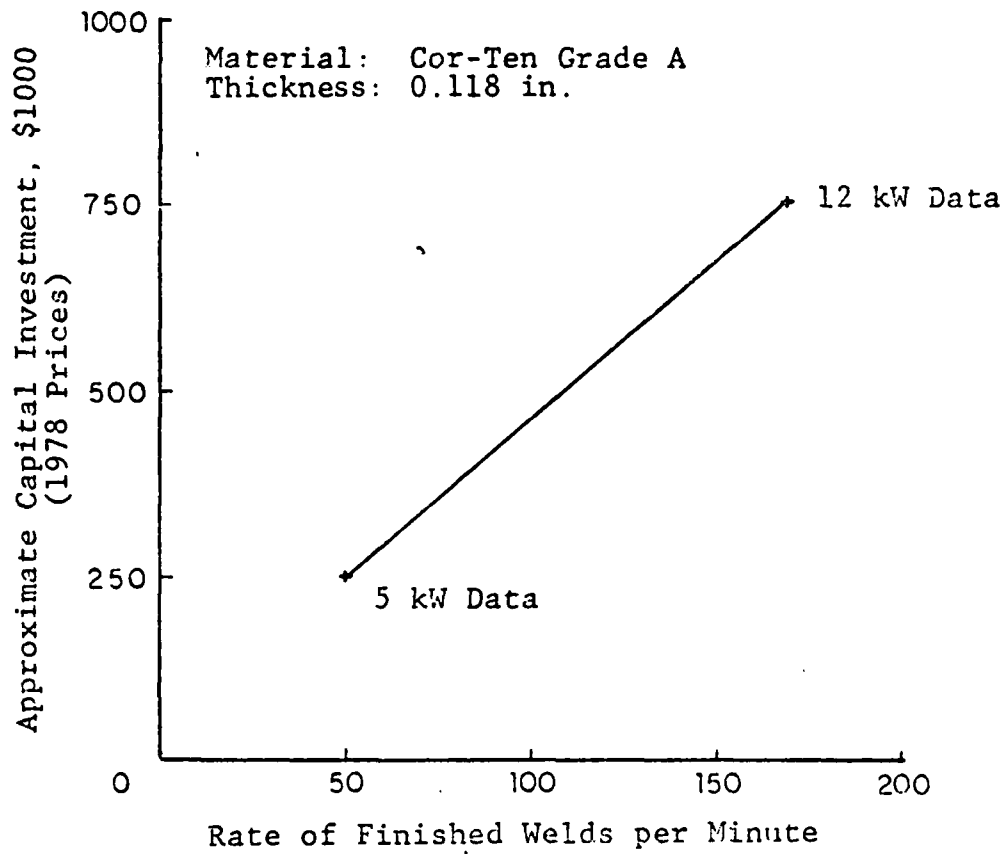


Figure 5. Equipment cost vs production.

Material: Cor-Ten steel  
Thickness: 0.118 in.  
Type of Weld: Bead-on-plate  
Optics: f/7 best focus  
Power: 12 kW  
Beam Configuration: Concentric

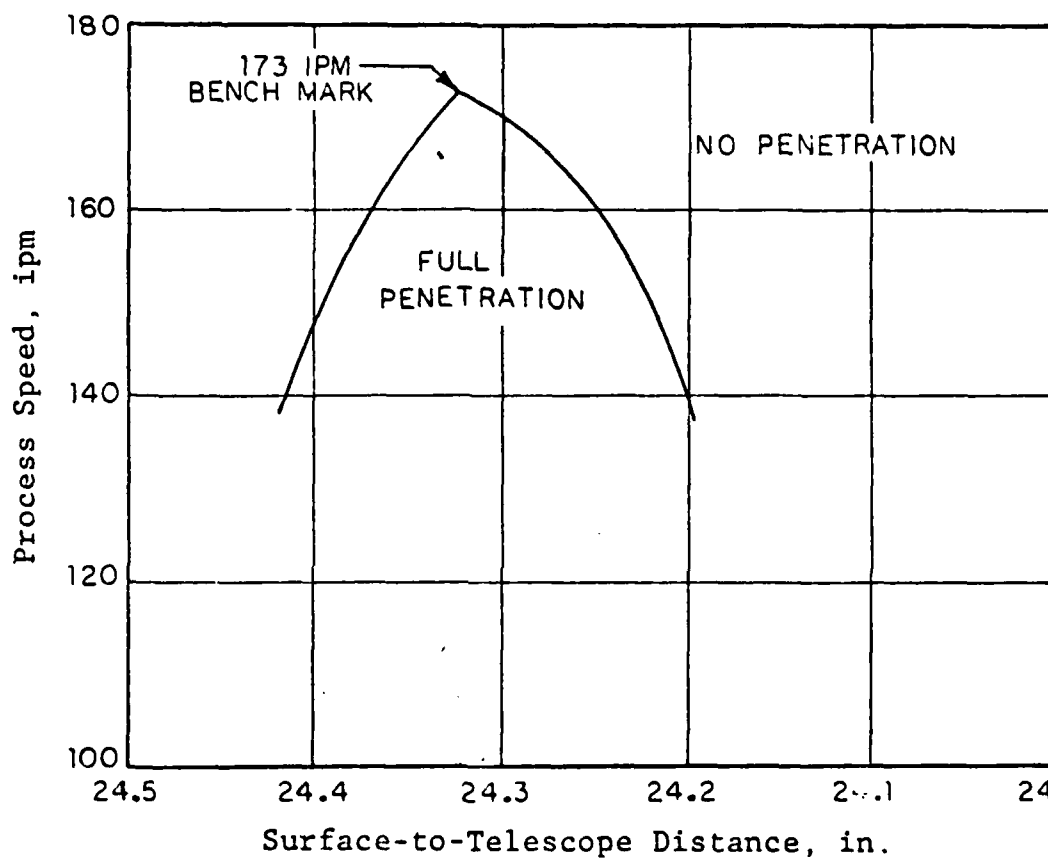


Figure 4. Limited 12 kW bench mark survey on Cor-Ten steel.



Material: Cor-Ten steel  
Thickness: 0.118 in.  
Type of Weld: Bead-on-plate  
Optics: f/7  
Power: 5 kW  
Beam Configuration: Concentric

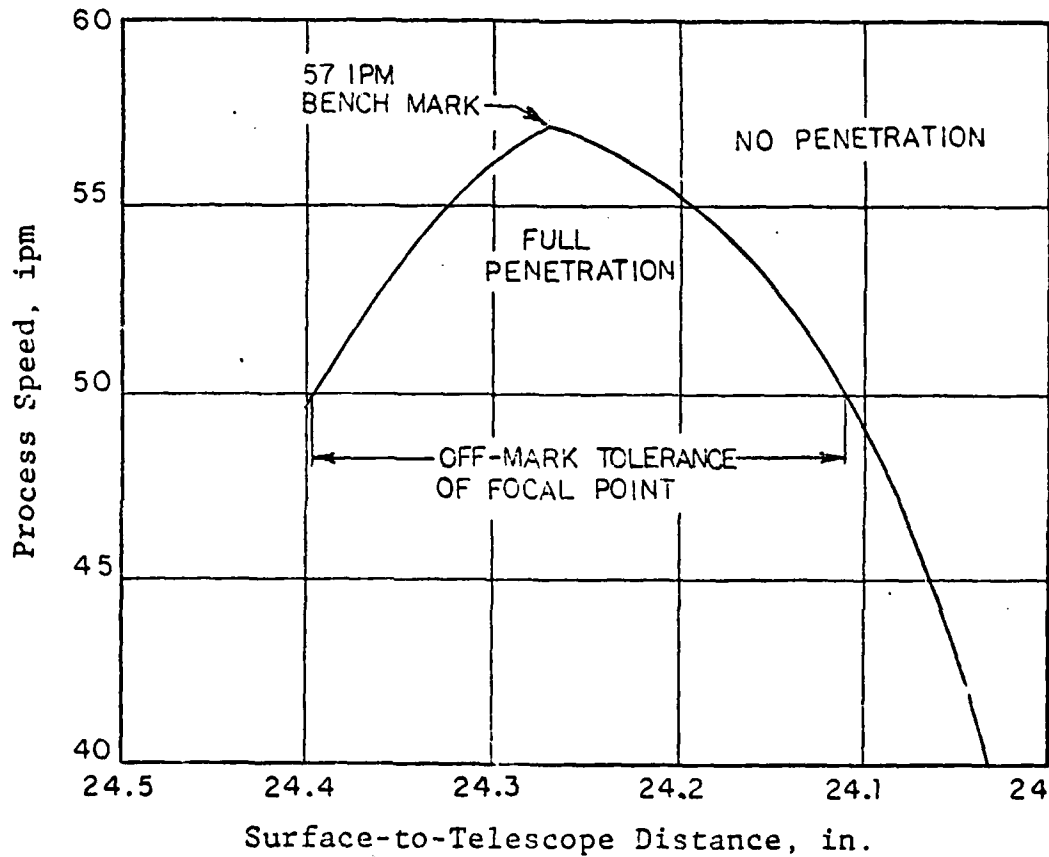


Figure 3. 5 kW bench mark survey on Cor-Ten steel.

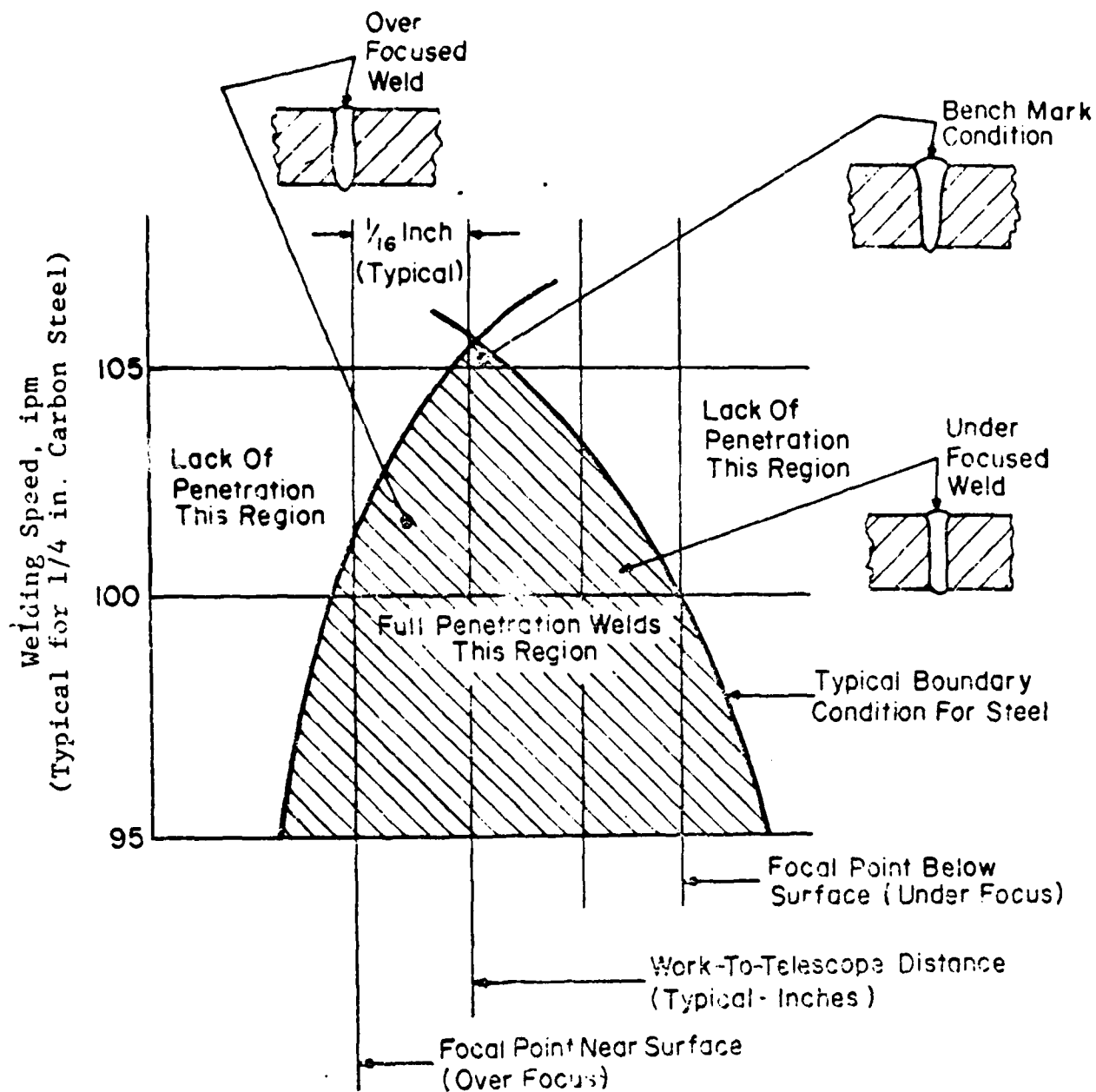


Figure 2. Changes in weld cross section with focal point setting.

To date, a limited number of weld cross-sections at the extremes of the full penetration zone in plots, such as Figure 2, suggest that the shape changes in the cross-section as the focal point is driven into the work, and also as the welding speed increases. The quality can be drastically affected. It is important to note that actual experimentation is required with the materials and optical configurations that are to be used.

## 2. Experimental Bench Mark Surveys

Figure 3 shows a 5 Kw bench mark survey for 0.118 inch Cor-Ten A steel. The bench mark at this low power level is 57 ipm. By a slight reduction in speed (about 10%) the gross tolerance for focal point placement becomes almost 0.3 in. However, as noted, quality requirements may reduce the useful range by about 50%.

Figure 4 presents a limited survey to establish a 12 Kw bench mark in the same material. At this high-power bench mark, speed increases to 173 ipm while a reduction in speed of 10% indicates a gross tolerance of 0.2 in. in focal point placement. When Cor-Ten bench mark points derived from Figures 3 and 4 are compared in terms of speed resulting from a given power level, a curve showing the trade-off between equipment cost and rate of production can be drawn (Figure 5). In preparing this curve, the following assumptions were made with respect to the capital cost of several commonly produced laser beam sources (exclusive of such specialized individual systems elements as sequence timers, external optics, work-handling equipment):

<u>Power, kw</u>	<u>Manufacturer</u>	<u>Cost, \$1000</u>
5	Sylvania	230-260
5	Ferranti	260
15	Avco	600-800

The bench mark surveys used to produce the preceding rate/cost data used low f/No. optics. Such optics produce small spots. If a broader beam spot could be tolerated (for example, because a high-power laser was available), then higher f/Nos. could be used. Figure 6 shows that a greatly increased tolerance for focal point placement can be expected as the f/No. increases.

Figure 7 shows a bench mark that was produced on Cor-Ten A steel using an optical system with a high f/No. — f/14. A 0.24 inch thick (2 ply; 0.118 inch ply) lap joint in Cor-Ten was used to produce Figure 7.

Full penetration welds were obtained at 90 ipm under the focal point placement conditions. The best focal point placement of the surfaces of the joint, with respect to a reference point on the focusing mirror mounts, appears to be 54-9/16 in. at the above speed. Thus, the bench mark speed and focus are 90 ipm and 54-9/16 in., respectively. The full penetration process boundaries (solid line in Figure 7) show the previously observed broad tolerance for workpiece position; as speed is reduced, the tolerance increases, as follows:

At bench mark speed (90 ipm)	= no tolerance
Bench mark speed, minus 5%	= 0.15 in. tolerance
Bench mark speed, minus 10%	= 0.28 in. tolerance

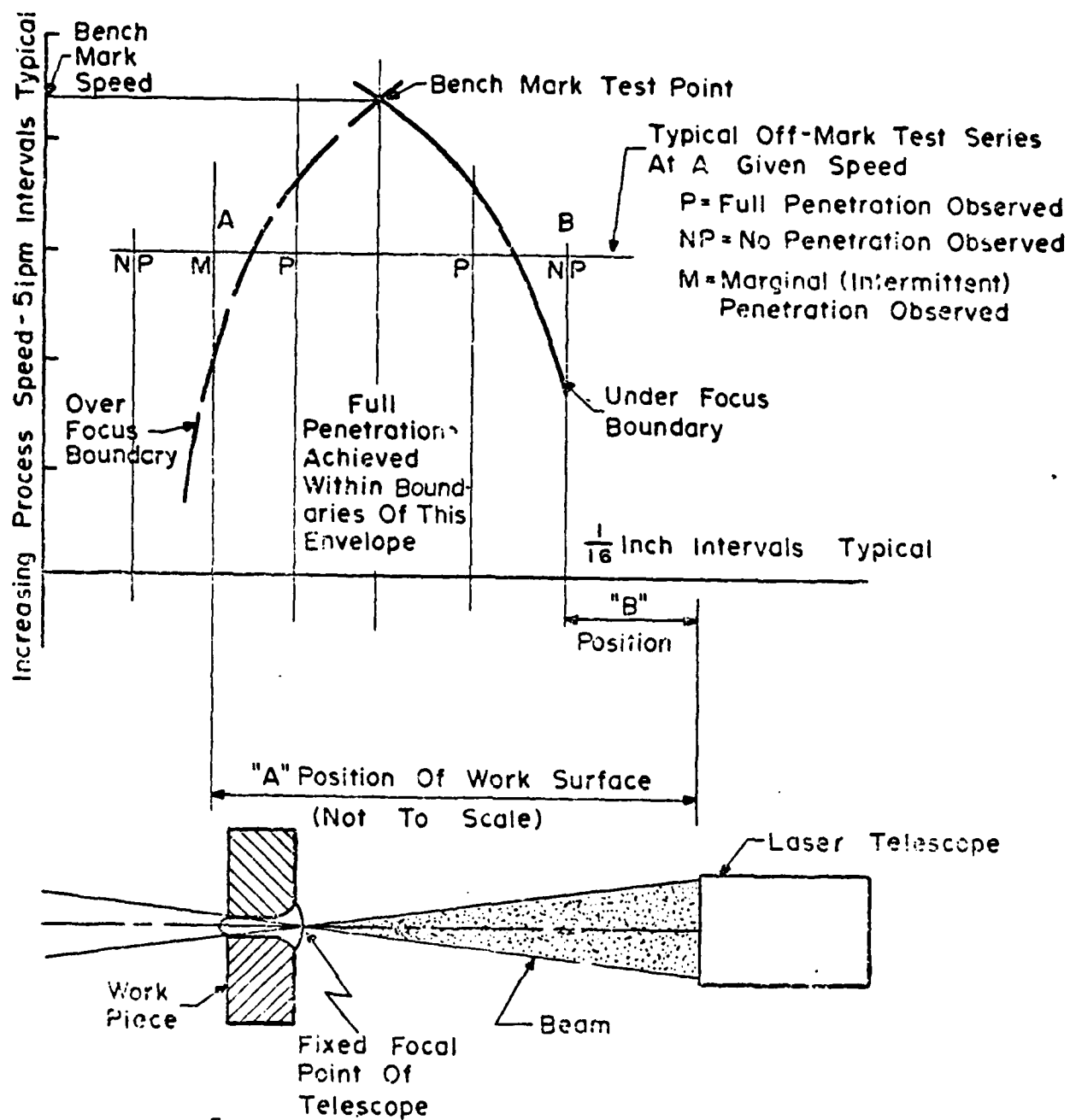


Figure 1. Bench mark test point and off-mark survey of full-penetration laser welding conditions.

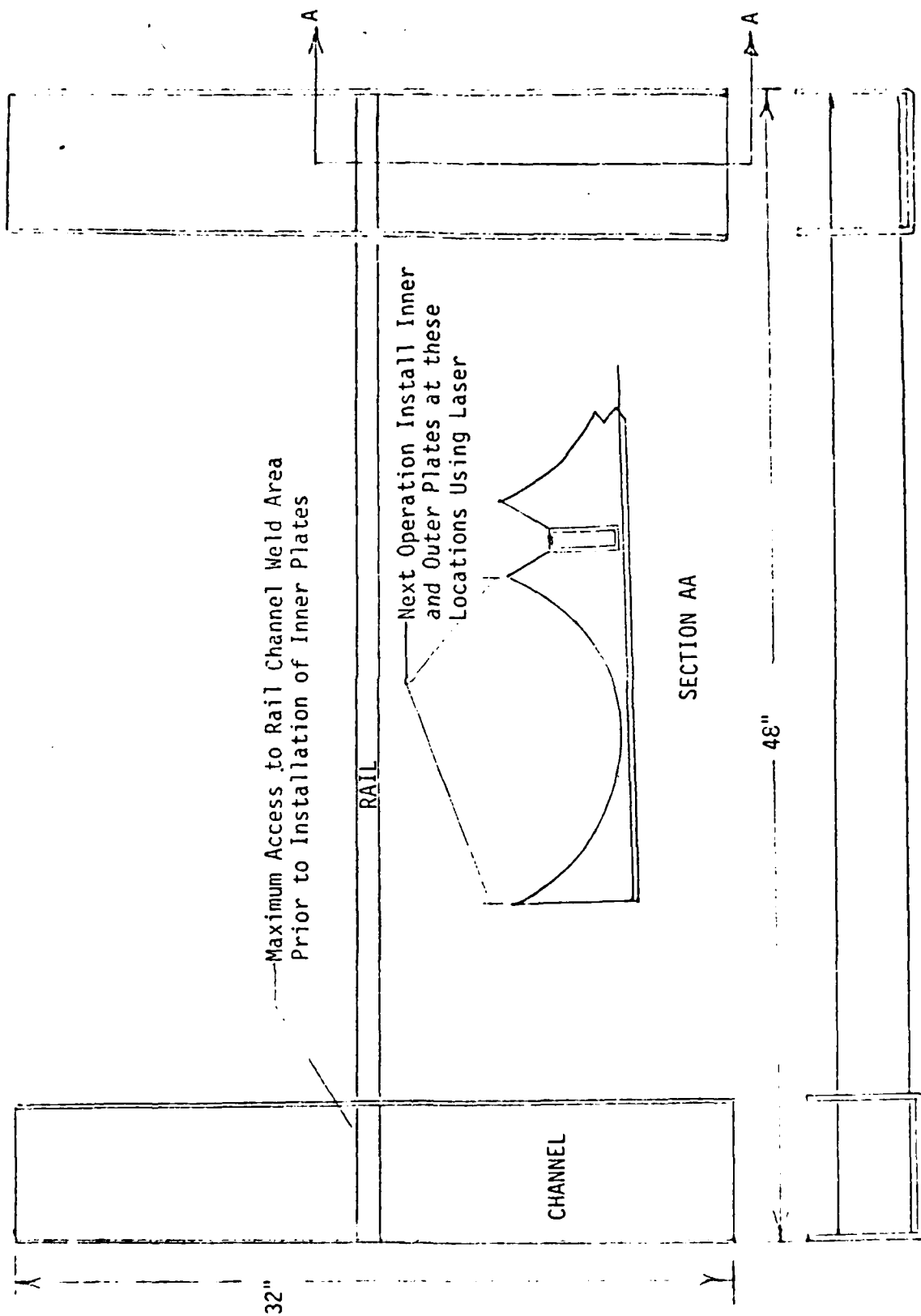


Figure 11. Initial "h" shaped fabrication ready for plates.

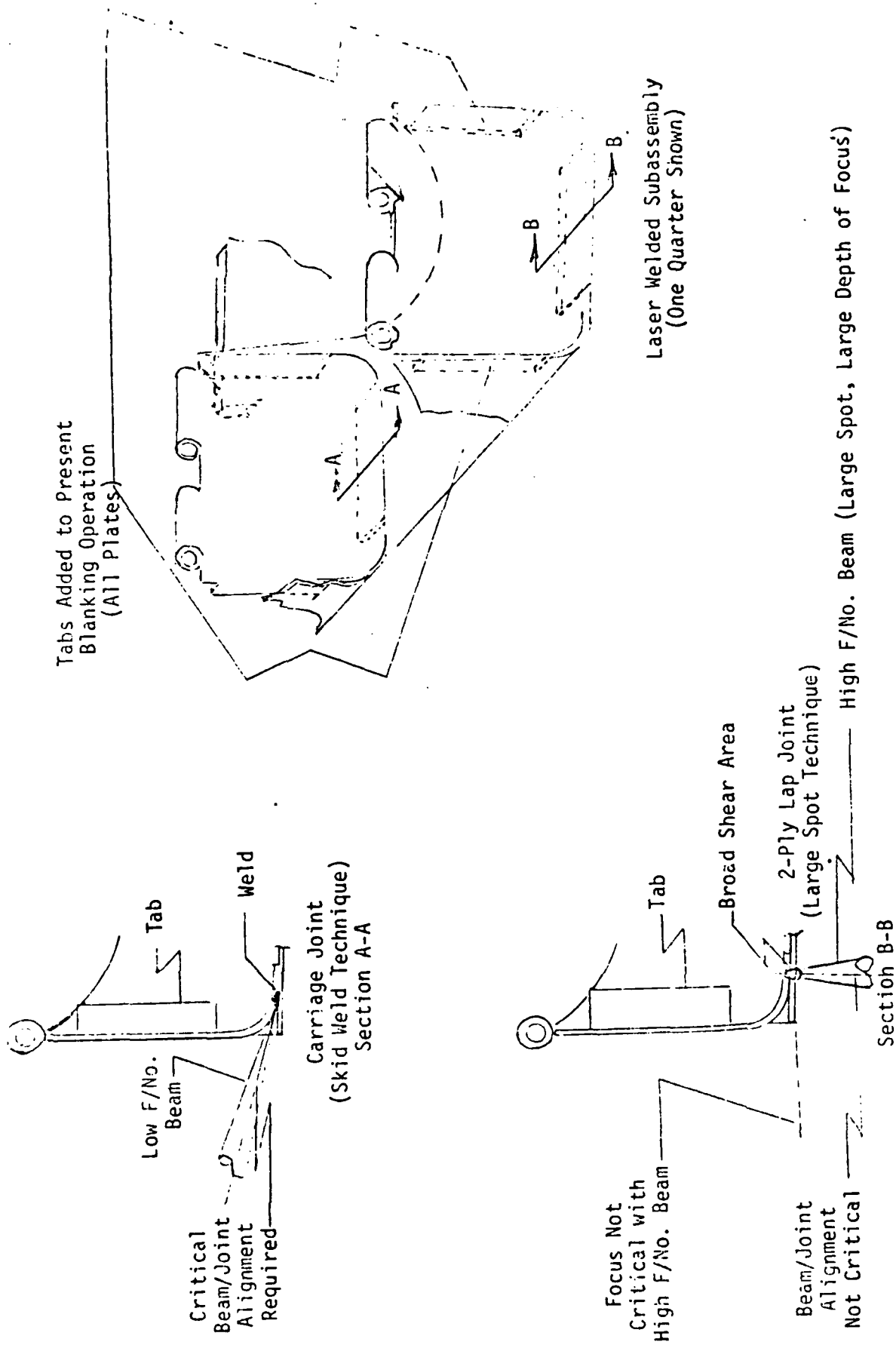


Figure 12. Alternative laser welded joint configuration.

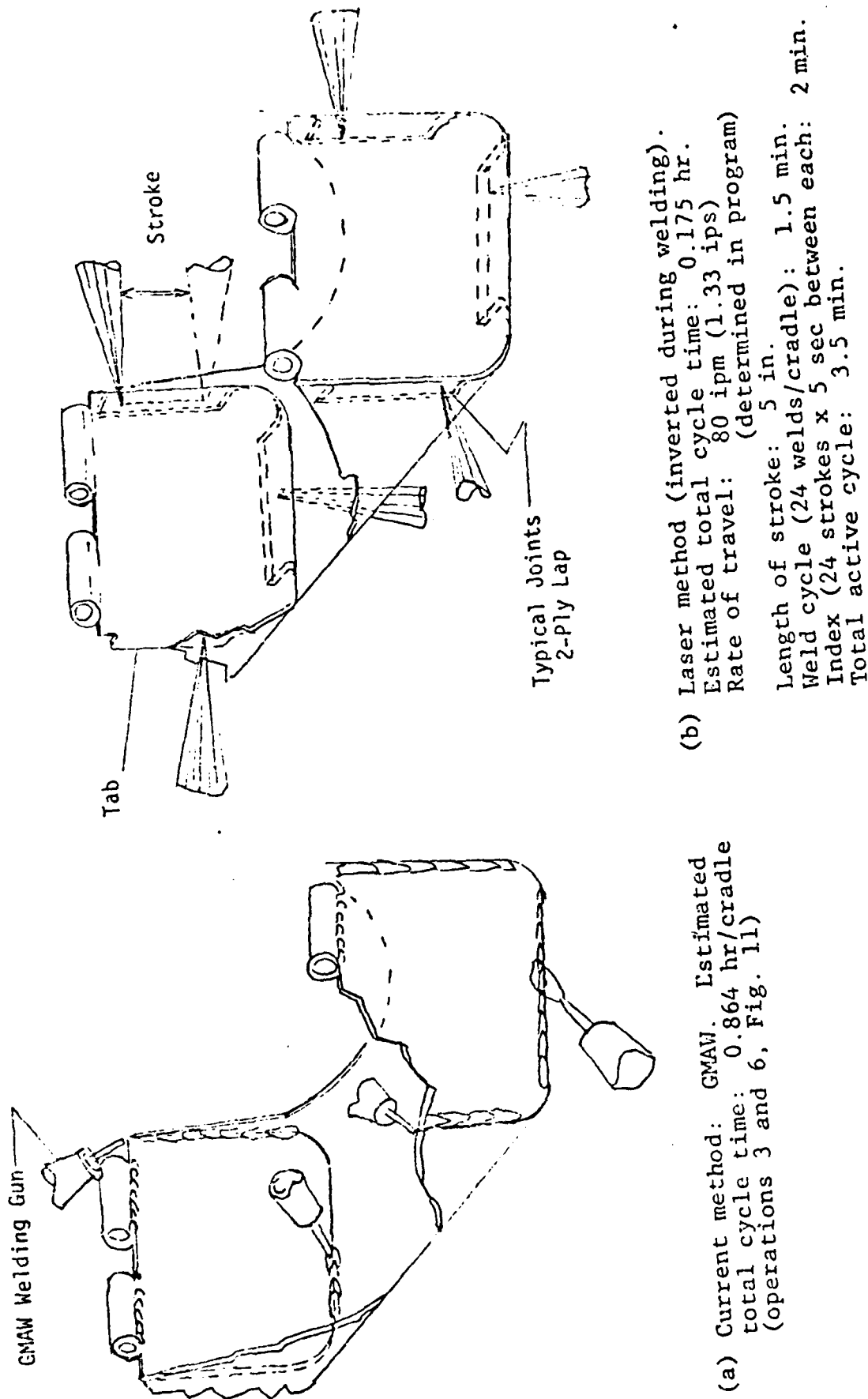


Figure 13. Comparative processes for plate/channel welding (GMAW vs Laser).

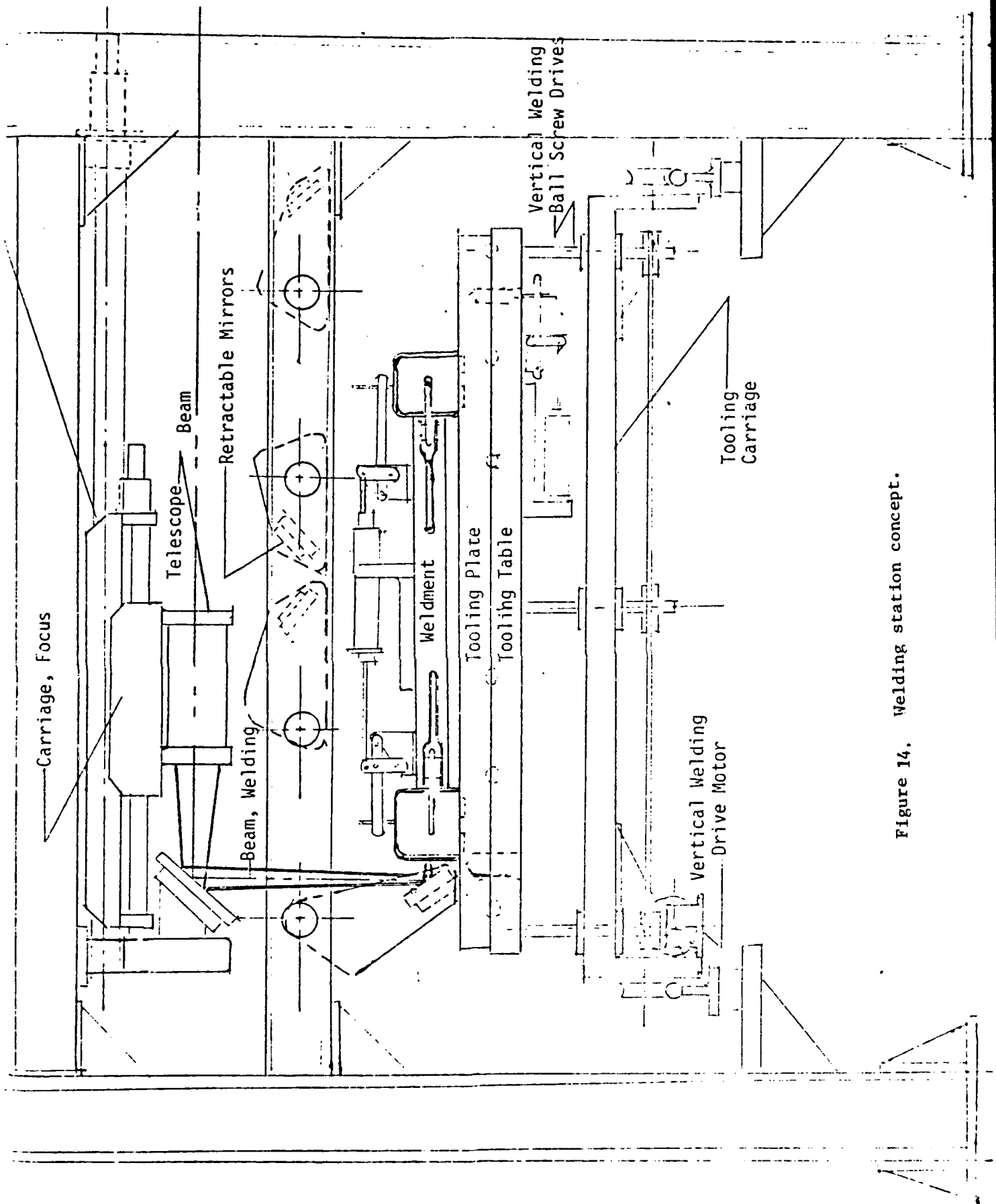


Figure 14. Welding station concept.



Rate of travel: 80 ipm (1.3 ips determined in program)  
 Length of stroke: 10 in.  
 Weld cycle (8 welds/cradle): 1 min (0.01 hr max)  
 Index (8 strokes, 7 sec between strokes): 1 min  
 Additional cycle time to weld loop/plate: 1 min  
 Total active time: 3 min

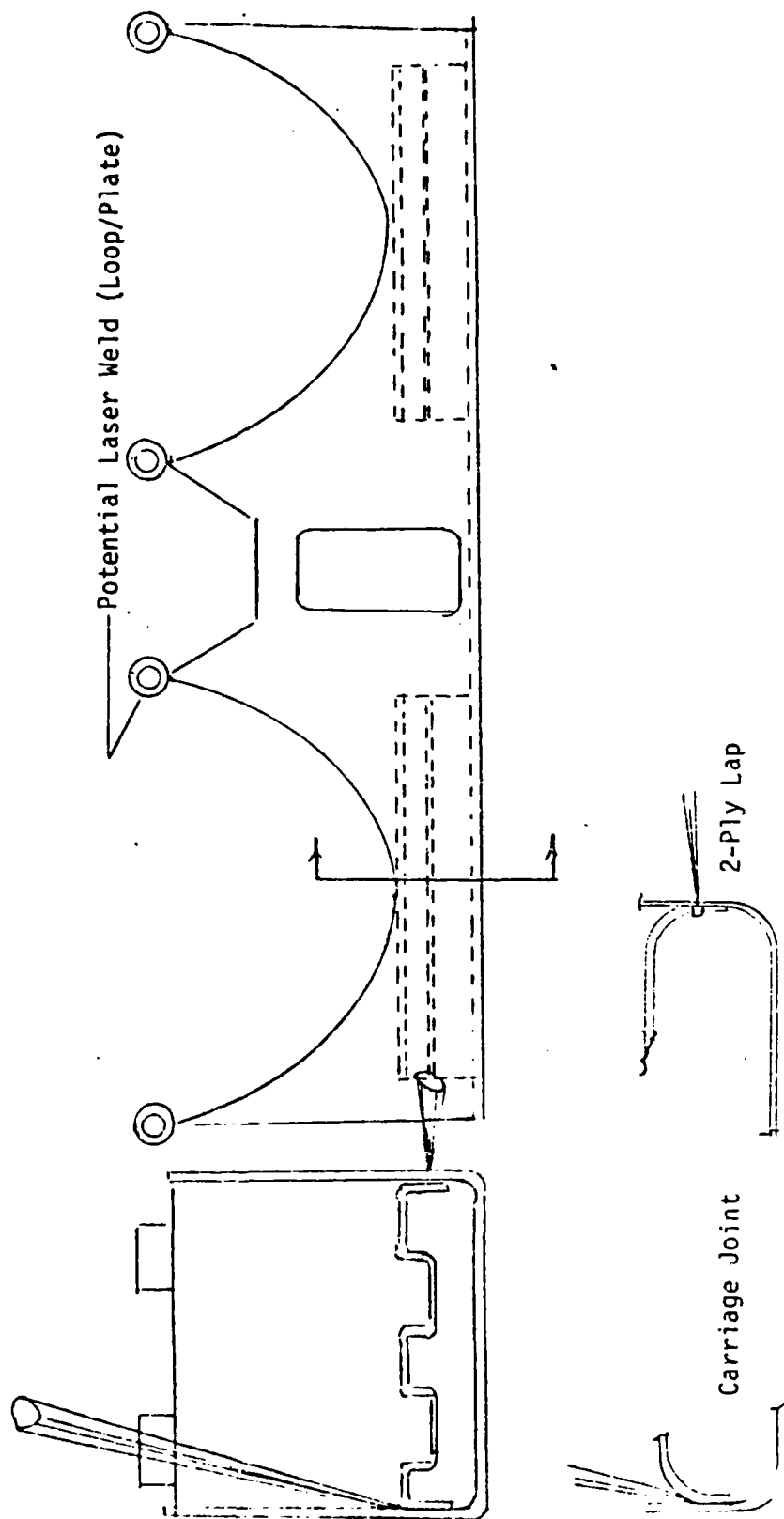


Figure 15 Alternative methods of attaching the corrugated stiffener.

5. Next, the telescope automatically backs away from the downhand mirror to produce a downhand beam impinging on the top of the channel. The mirror retracts. The beam is moved over the top of the channel to form the weld when the main telescope carriage moves to the right, as illustrated in Figure 14.

6. The welding action required to complete the precision attachment of one plate into the channel takes place when the telescopic optics go back to the initial configuration impinging horizontally on the side of the channel, but with a second retractable mirror pointing into a direction opposite to the first weld, so that this final weld can be made on the second side of the channel.

7. The tooling moves toward the viewer to the second plate/channel joint in Channel A and repeats steps 1 to 6.

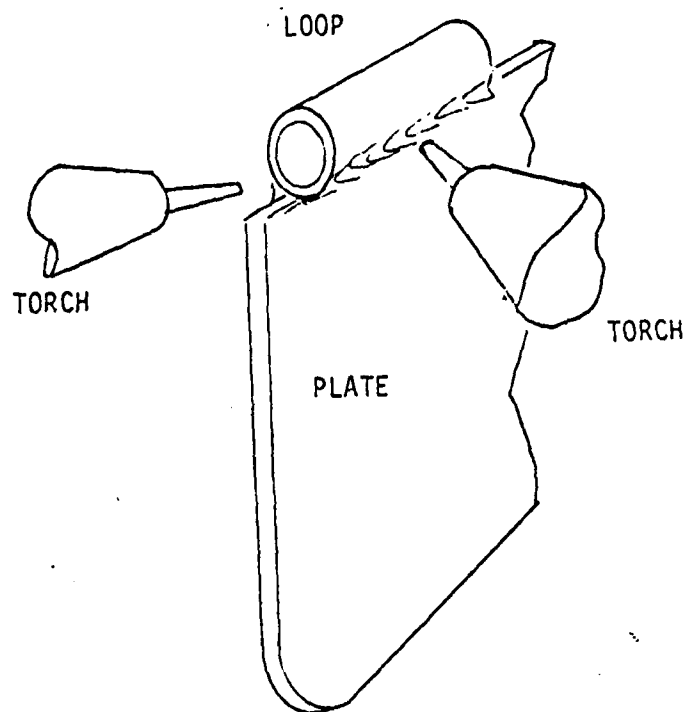
8. After all four plate/channel joints in Channel A have been completed, the tooling indexes approximately 42 in. to the near side of a plate/channel joint in the second channel (Channel B) and steps 1 to 6 are repeated four times.

As noted, the total cycle to weld the plates into the "H" shaped cradle assembly is estimated to be 0.1 hr. (compared with an estimated 0.825 hr for GMAW), but there is a further potential for saving in labor.

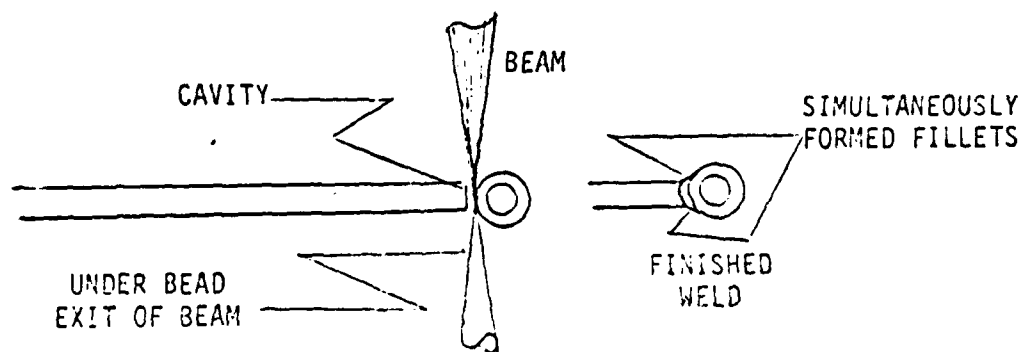
A second welding machine, similar to the one illustrated in Figure 14, could be used to attach the corrugations in a separate step. A separate operation is recommended because the channel/plate weld is most easily made with the channel lying face down in the tooling, so that the carriage weld shown in Figure 16 can be made. More important, placing too many operations in the Figure 14 station would have a tendency to unbalance the load/weld cycle. The work performed by the operator in loading (and unloading) should take the same amount of time as the work going on in the station.

The weld cycle for the cradle/corrugation weld (Figure 15) requires about 5 minutes. As in the case of the plates, assembly in the tooling and disassembly after welding would be paralleled with the automated welding cycle. The term "load" refers to the automatic movement of the loaded tooling into the station. Although it is not a major element in the present manual welding operation, the attachment of the loops to the plates might also be accomplished in the second welding station, possibly in the same fixture as the corrugation/channel weld. This is suggested by the unique weld which the laser beam makes possible in a plate/cylinder configuration.

Figure 16 illustrates the weld. It should be noted that the beam need only impinge upon one side of the joint. The optical properties of the joint, plus the drilling action of the beam, permit the fusion process to continue through the joint thickness. The unusual cavity penetration phenomenon associated with the laser beam can be refined to form a fillet on the side opposite from which the beam enters. Thus, in one pass, the laser is capable of firmly joining the loop to the upper plate edge. It is estimated that the loop/plate welding operation on the eight plates needed for the cradle would increase the floor-to-floor time for the welding corrugation operation from 5 to 6 minutes (0.1 hr) if it were added to the corrugation/channel tooling. It is necessary to work out the production sequence prior to making a final assessment of the required hours of labor for these new laser operations (replacing GMAW operations 1, 2, 3, and 6 shown in Figure 10).



(a) Manual GMAW method



(b) Laser welding method

Figure 16. Comparative processes for loop/plate welding (GMAW vs Laser).

Figure 17 illustrates the entire work flow sequence, including the two station time shared system using a single large laser, in addition to the GMAW joining station for the initial welding of the rail to the channels. The beam is directed into only one station at a time. This switching of direction is accomplished in the periscope housing of the laser by sliding or rotating mirrors. This feature is currently available on industrial lasers.

Only one operator is needed for the two station laser system. It is estimated that such a person could load and unload the A station in 3.5 minutes, while the welds in the B station are being completed automatically. Figure 18 shows the load/weld cycle for both stations over a 30 minute period, during which time production has been completed for five cradles. The following is a comparison of labor for five cradles:

<u>Operation (Weld)</u>	<u>GMAW Production Line hr (Figure 10)</u>	<u>Laser/GMAW Welding Center hr (Figure 13)</u>
Loop/plate	0.114	N/A
Stiffener/channel	0.464	N/A
Plate/channel (outer)	0.512	N/A
Plate/channel (inner)	0.352	0.5
Laser weld all joints	N/A	0.016
Collar/rail	0.016	0.016
Rail/channel	<u>0.112</u>	<u>0.112</u>
TOTAL	1.600	0.628

Thus, the laser could effect a 60% reduction in labor savings per cradle. This corresponds to 0.972 hr. per cradle, or 19,440 hr. per year at a rate of 20,000 storage containers per year.

#### I. Demonstration of capability of Laser Welding to Produce Types of Joints Found in Missile Containers

##### 1. Welding Procedure

Welding procedure used in generating optimum laser weld parameters for types of joints used in construction of the missile container structure was to maintain the weld power constant at 15 Kw, vary the distance between focusing mirror and weld surface from 54 5/16" to 54 7/8", and vary the welding speed from 67 to 114 inches per minute (IPM).

Figure 19 illustrates typical good structural weld joints welded on .118 in. Cor-Ten A steel. Helium gas was the shielding gas introduced in the form of a jet at 160 cubic ft/hour (CFH).

After successfully completing the welding test samples for Cor-Ten A steel lap welds, a modification was made to place a spacer of 0.030 in. between the plates. Typical welds are described in the following section.

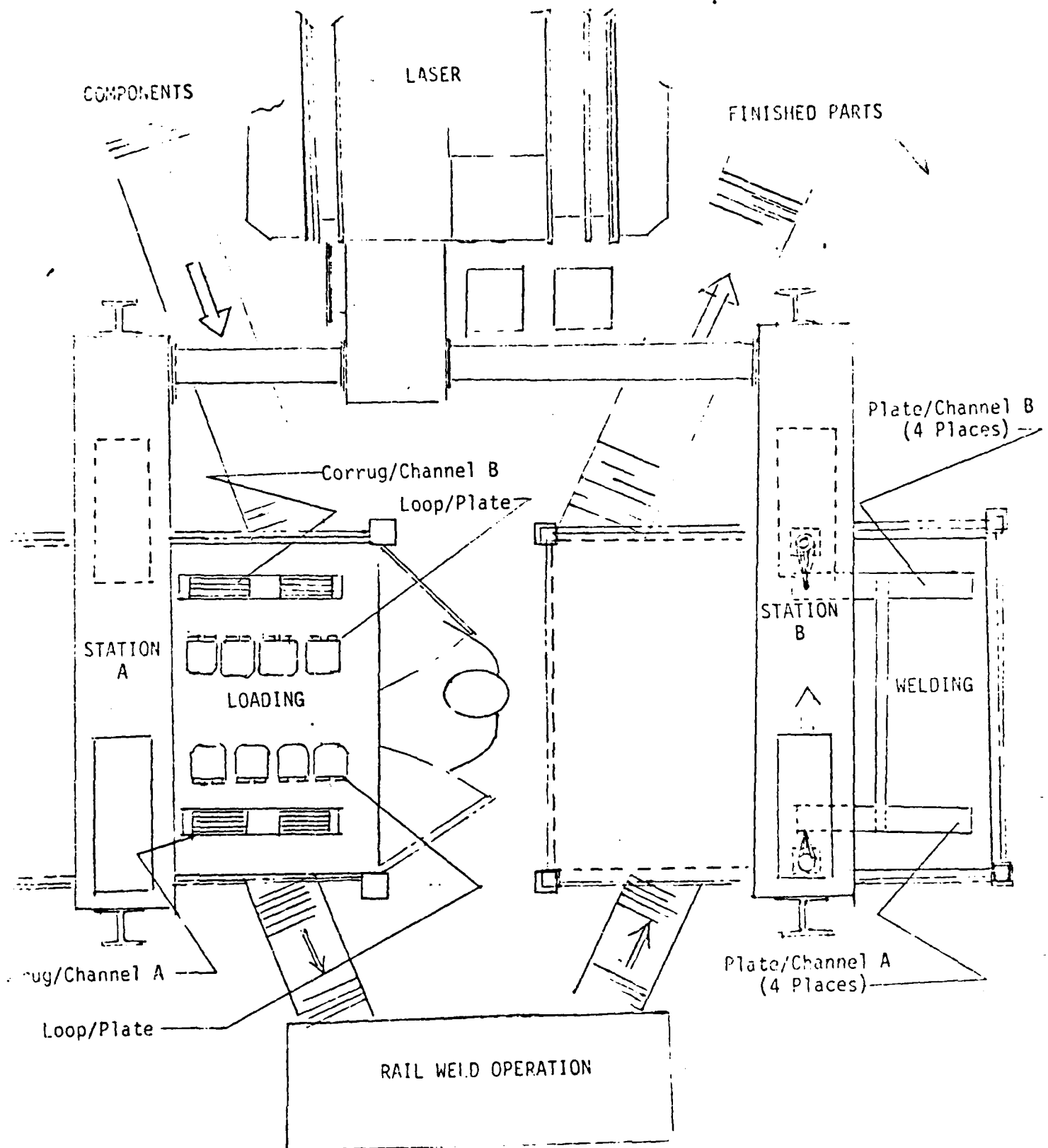


Figure 17. Layout of laser cradle welding operations.

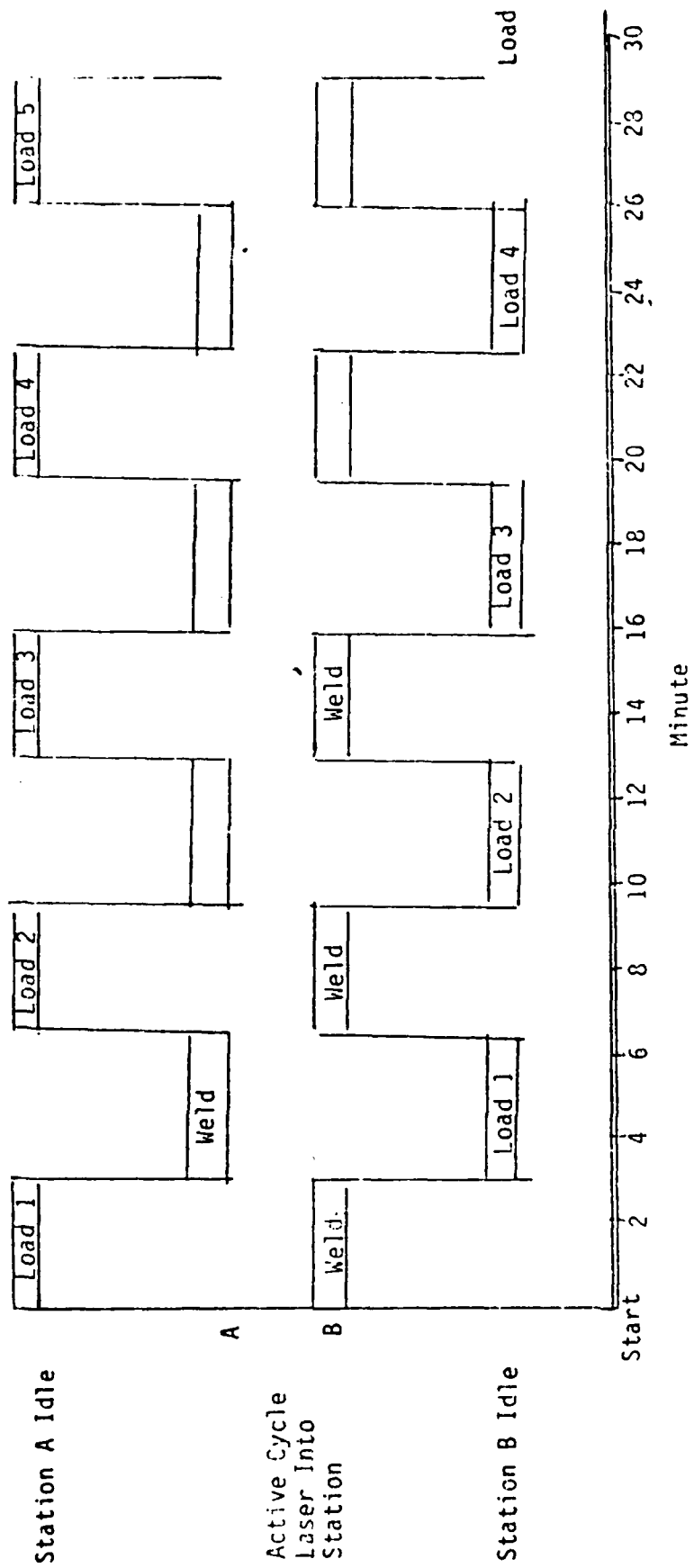


Figure 18. Laser station cycle.

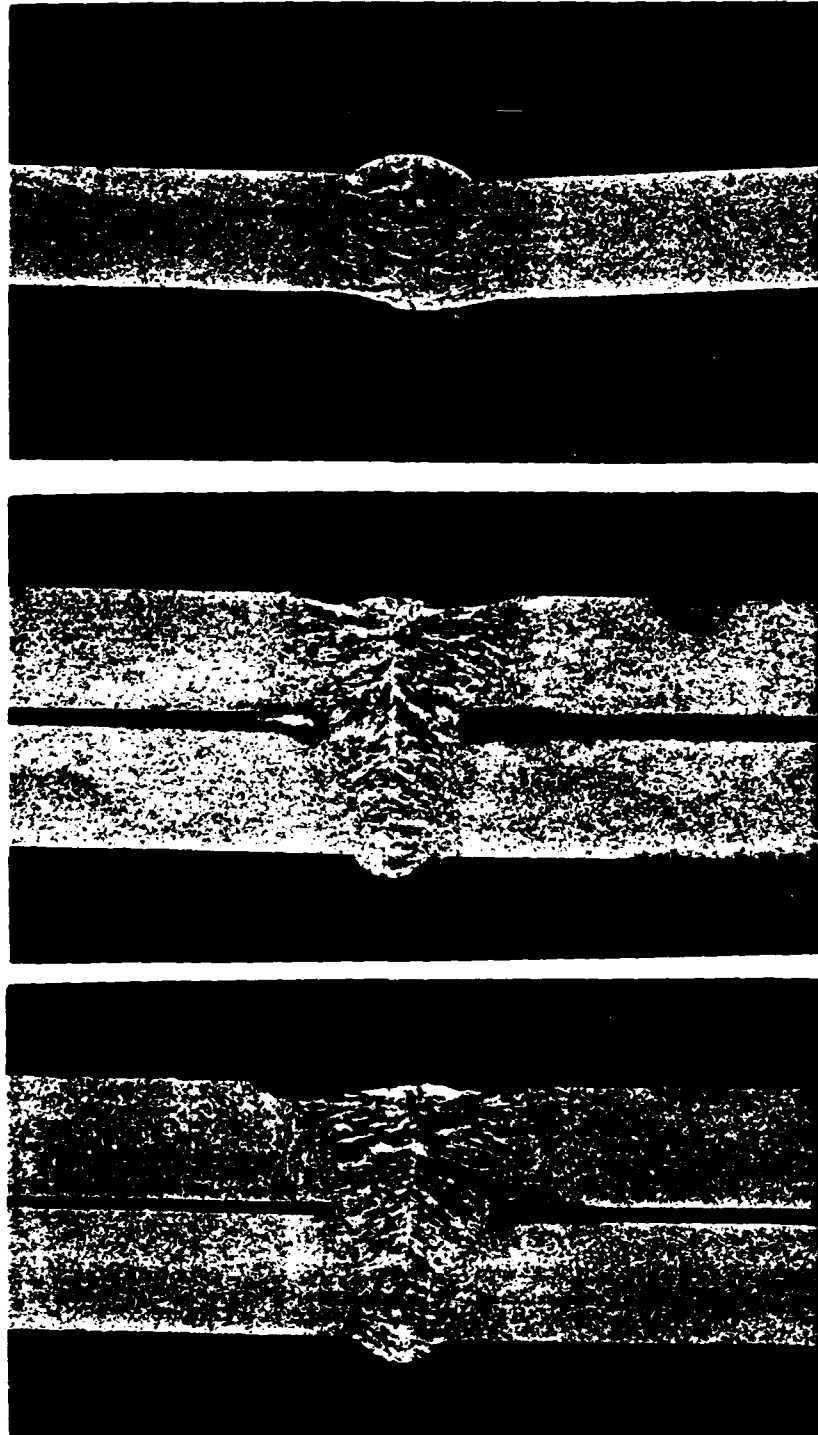


Figure 19 . Typical cross-sections of laser welds on 1/8" steel missile container material welded at optimum parameters.

## 2. Lap Weld Joints

Figures 20 through 33 illustrate the effect of change in focal length and speed on weld penetration and nugget appearance. All welds were made at the same power level, 15 Kw. Examination of the weld nugget appearance suggests that a focal length of 54 9/16" to 54 3/4" is optimum for these weldments (Figures 26, 27, and 31). These welds were made at identical weld settings (power, speed and focal length) and illustrate not only a desirable weld nugget, but the ability to reproduce weld conditions. Figures 20 and 21 illustrate the effect of shorter focal length on undercut. The deeper penetration in Figure 20 is probably due to the slower speed. A slight increase in focal length (1/16 inch) improves penetration and the condition of undercut (Figure 21 vs Figure 26). The effect on undercut by an increase in speed at the lower fringe of focal length is depicted by Figure 23 - a condition which does not seem to occur at the longer focal length (Figure 28).

Figures 32 and 33 illustrate the ability of the laser to weld two sheets intentionally separated approximately 1/32 inch to reproduce imperfect abutted conditions which might prevail in production. Again, penetration occurs at the lower speed but at the expense of drop-through of the top portion of the weld beam, which is due to the space between the two sheets. The effect of higher speed, Figure 32, is seen in lack of adequate penetration and the formation of a crack due to faster freezing. Figures 29, 30, and 31 also depict desirable weldments, though penetration is not complete as in Figures 26, 27, and 31. Deducing the conditions best suited for the laser beam used in generating these weldments:

Focal Length:	54 9/16 to 54 3/4 inches
Weld Speed:	70 to 80 IPM
Weld Power:	15 kw

## 3. T-Joints Welds

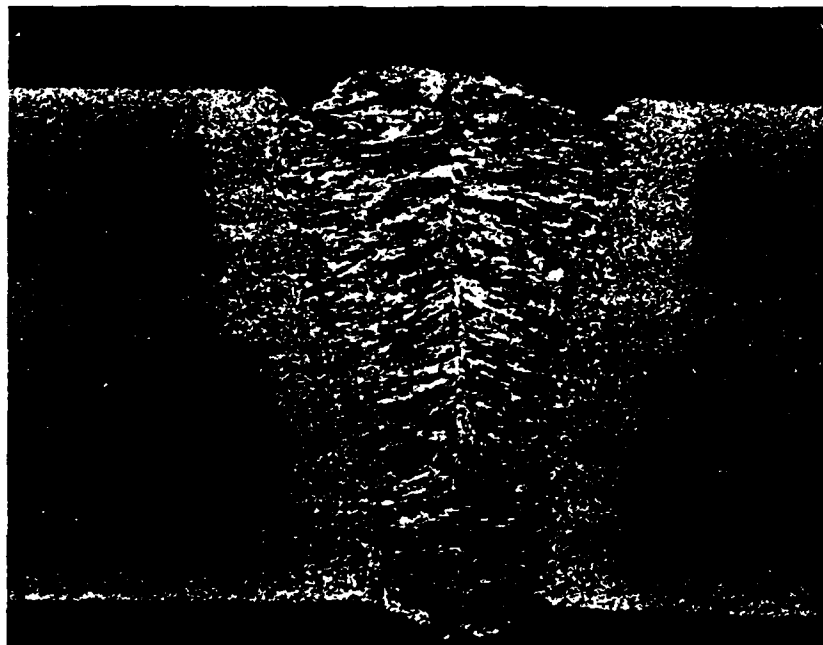
The second most common type of weld joint used in producing missile containers is the inverted "T" joint which is formed by joining two "L" shaped sheet edges. (See Figure 34.) Because the height and the gap of the "L" sections vary somewhat in production, welds were made with a shorter than optimum focal length. Reducing the focal length, of course, increases the spot size and thereby insures weld "tie-in" of parts with poor fit-up. This is accomplished at the expense of reduced energy concentration of the laser beam; the main advantage of the laser welding system.

This joint does not require deep penetration since it is only a semi-structural joint. The main function is to seal against atmosphere; therefore, less emphasis was placed in generating precise welding parameters. An acceptable range of welding parameters, however, is 10 Kw, 54 in. focal length  $\pm 1/8$  and a welding speed of 50 to 80 IPM.

## 4. Penetration Capability of the MICOM Laser

Figure 36 demonstrates the ability of the laser to penetrate thick sections of steel. Thick section welding is not applicable to this program; however, the illustration is offered as a point of interest.





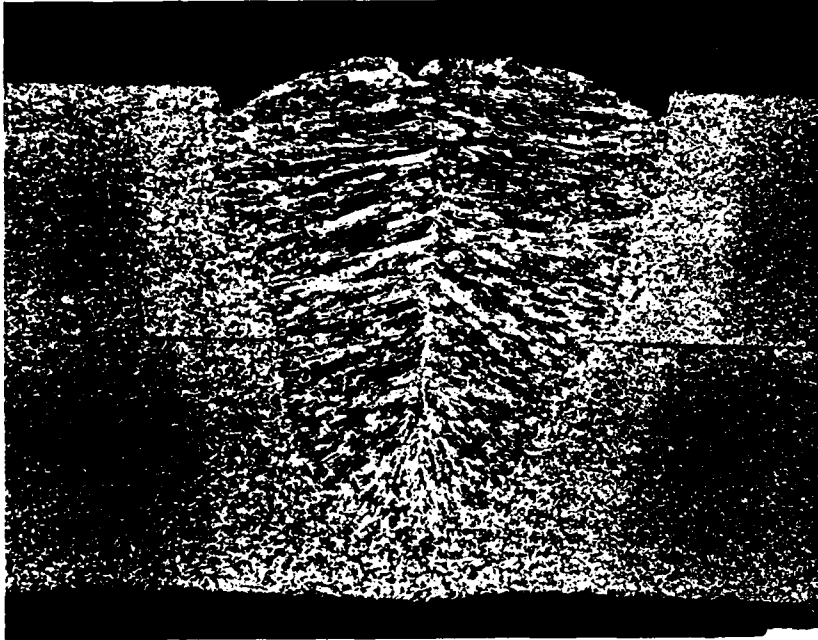
Corten Material ~ Thickness 0.118 in. each

Focal Length: 54 5/16 in.

Welding Speed: 71 inches per minute

Magnification: 11 X

Figure 20. Lap weld; full penetration.



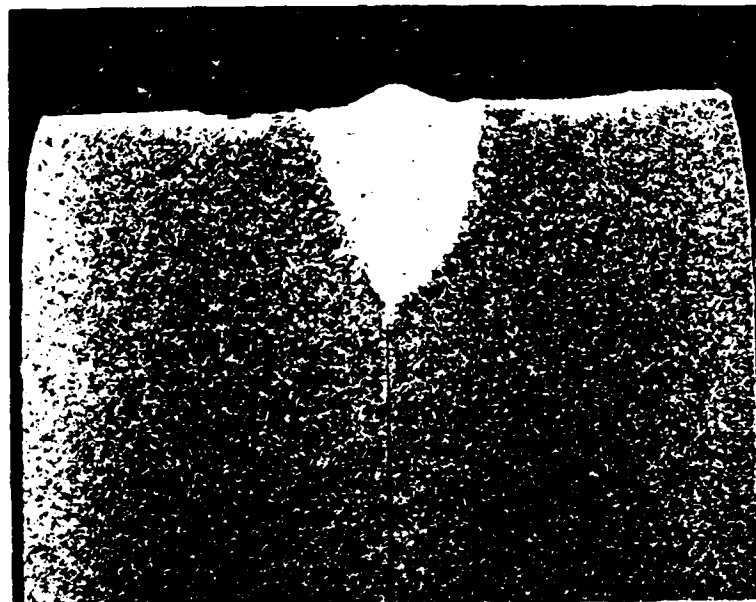
Corten Material - Thickness 0.118 in. each

Focal Length: 54 7/16

Welding Speed: 75 inches per minute

Magnification: 11 X

Figure 21. Lap weld; partial penetration.

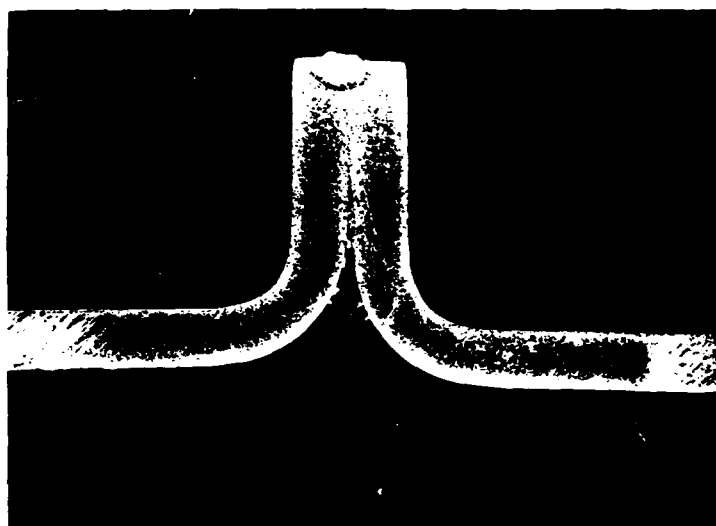


MAG: 11 X

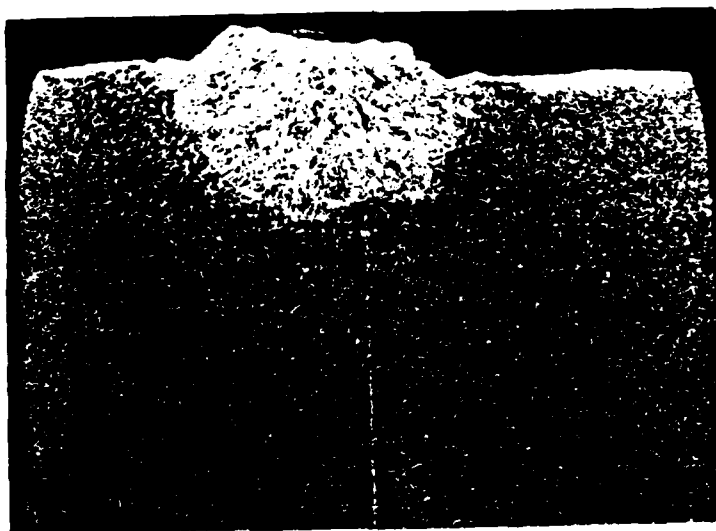


MAG: 6.6 X

Figure 35 . Laser welded Corten "T" joint,  
showing transverse (top) and  
longitudinal (bottom) macrosections.  
Focal Length: 53 15/16 in.  
Weld Speed: 78 in/min  
Weld Power: 10 kW  
Material: Corten; thickness .185 in.



MAG: 1.7X



MAG: 10X

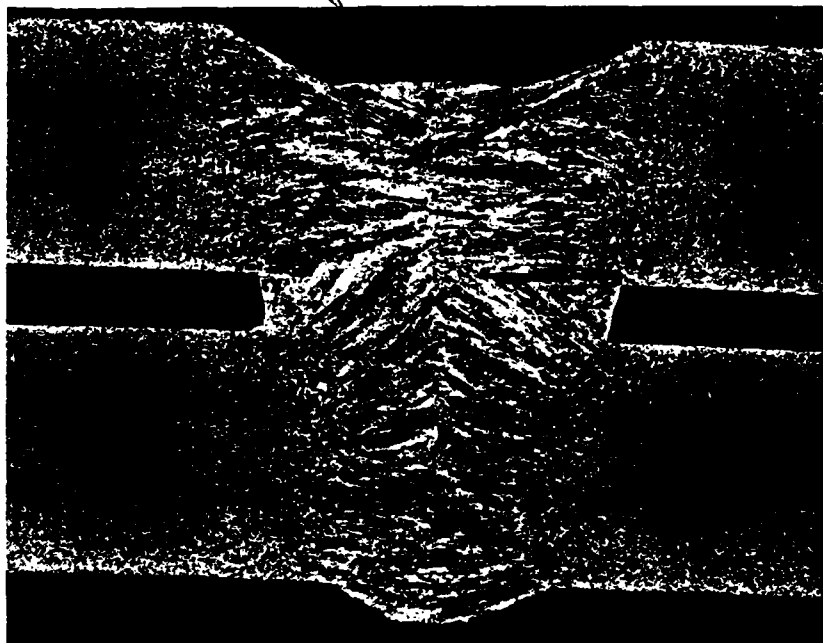
Figure 34 . Laser welded Corten "T" joint.

Focal Length: 54 1/8

Welding Speed: 54 in/min

Welding Power: 10 kW

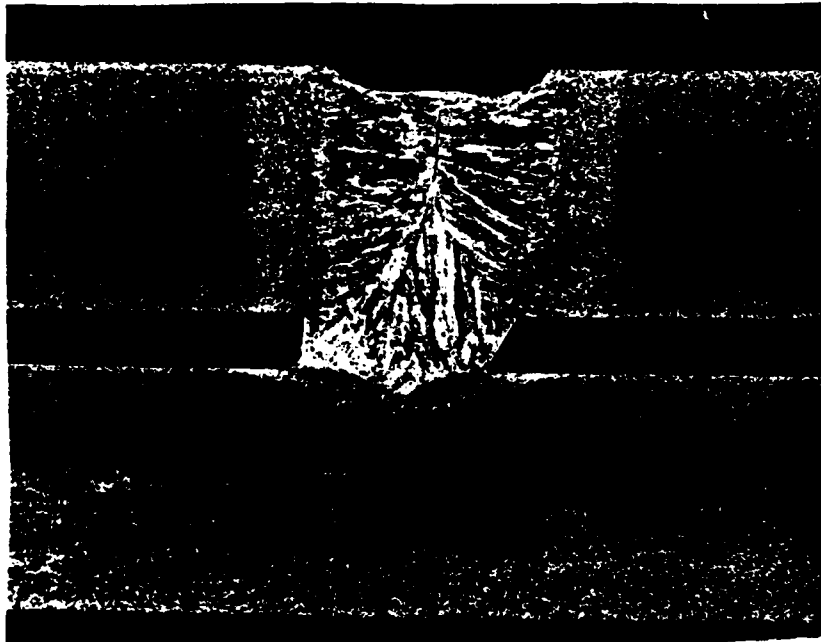
Material: Corten Thickness; 0.185 in.



Material: Corten    Thickness: 0.118 in. ea  
Focal Length: 54 9/16  
Welding Speed: 75 in/min  
Magnification: 11 X

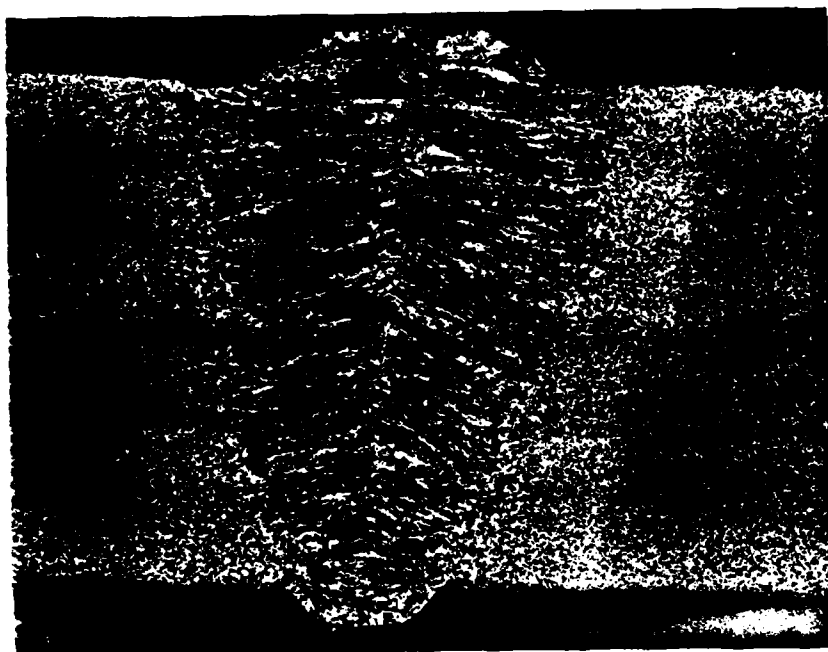
Figure 33 . Lap weld with sheet to be welded intentionally spaced apart. Complete penetration.

After successfully completing the welding test samples for Corten Lap Welds, a modification was made to place a spacer of 0.030 in. between the plates. Typical welds are shown in the pertinent data.



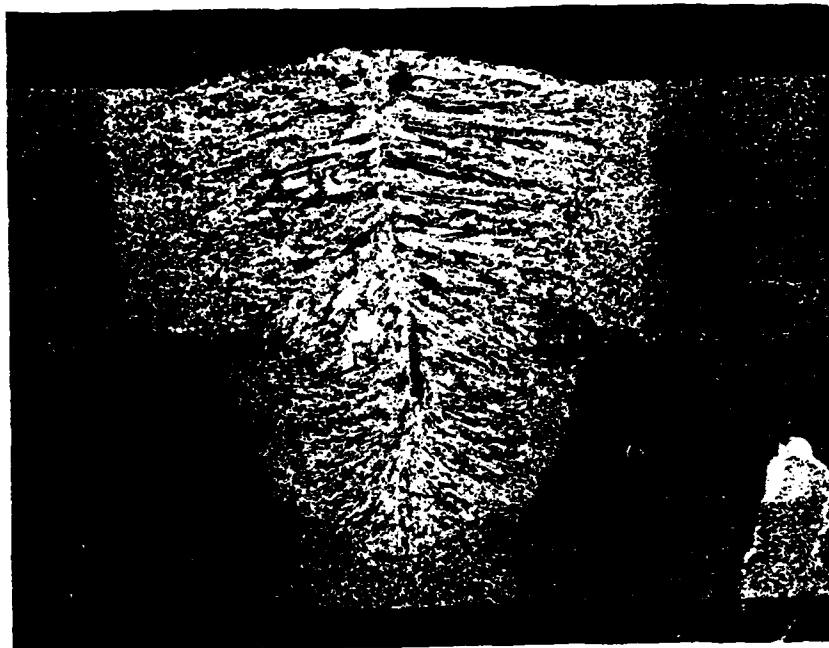
Material: Corten    Thickness: 0.118 in. ea  
Focal Length: 54 9/16  
Welding Speed: 106 in/min  
Magnification: 11 X

Figure 32 . Lap weld, with sheets to be welded intentionally spaced apart. Incomplete penetration.



Material: Corten    Thickness: 0.118 in. ea  
Focal Length: 54 3/4  
Weld Speed: 75 in/min  
Magnification: 11 X

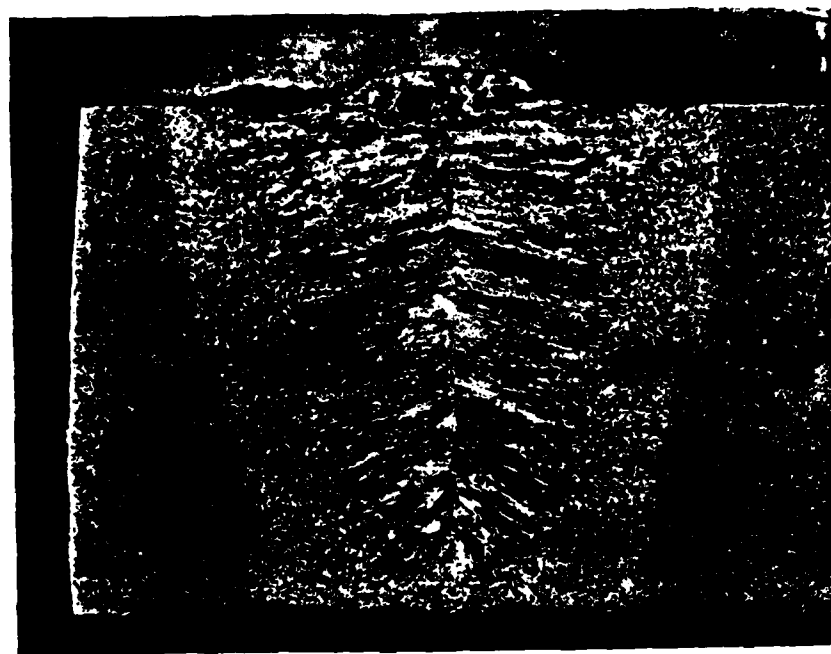
Figure 31 . Lap weld. Full penetration.



Material: Corten      Thickness: 0.118 in ea  
Focal Length: 54 3/4 in.  
Welding Speed: 85 in/min  
Magnification: 11 X

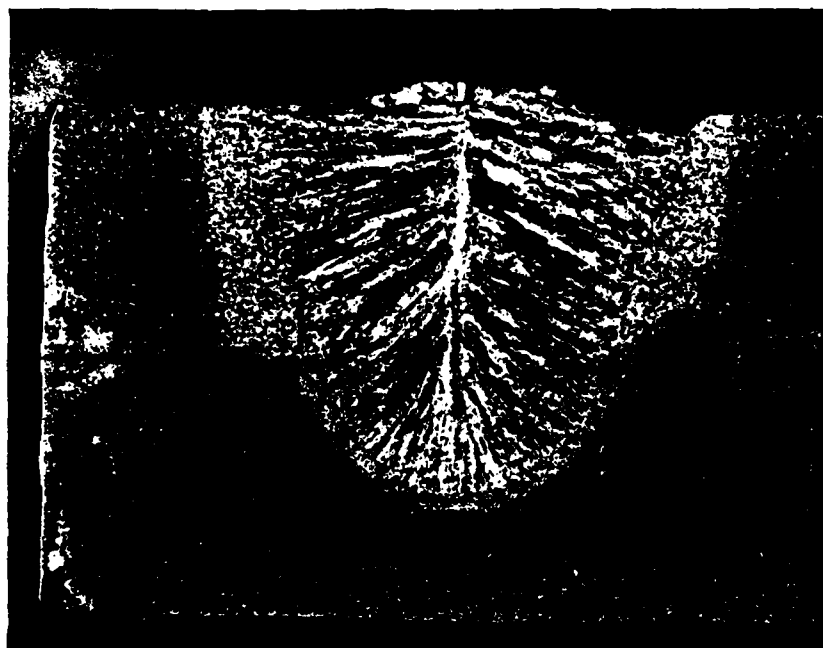
Figure 30 . Lap weld. Partial penetration.





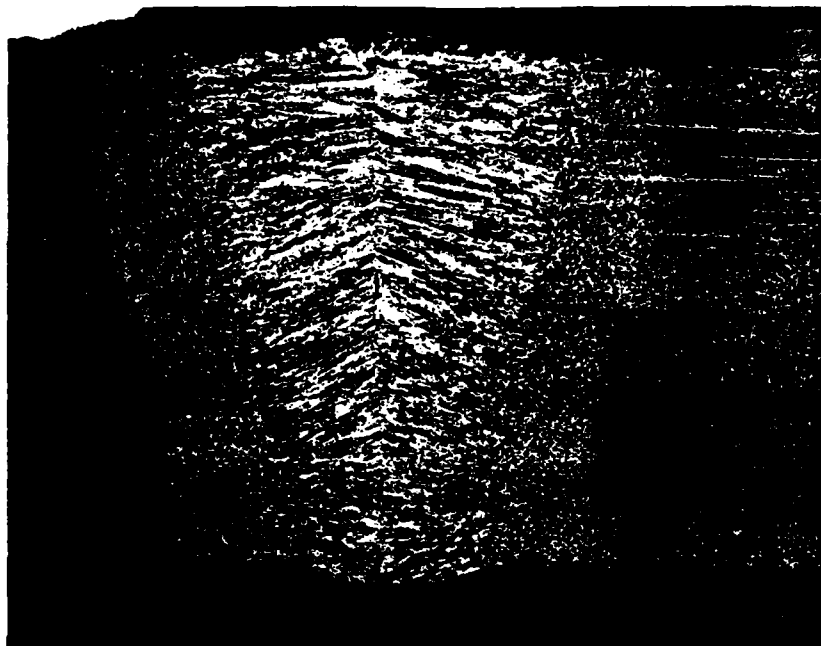
Material: Corten      Thickness: 0.118 in. ea.  
Focal Length: 54 11/16 in  
Welding Speed: 84 in/min  
Magnification: 11 X

Figure 29 . Lap weld. Full penetration.



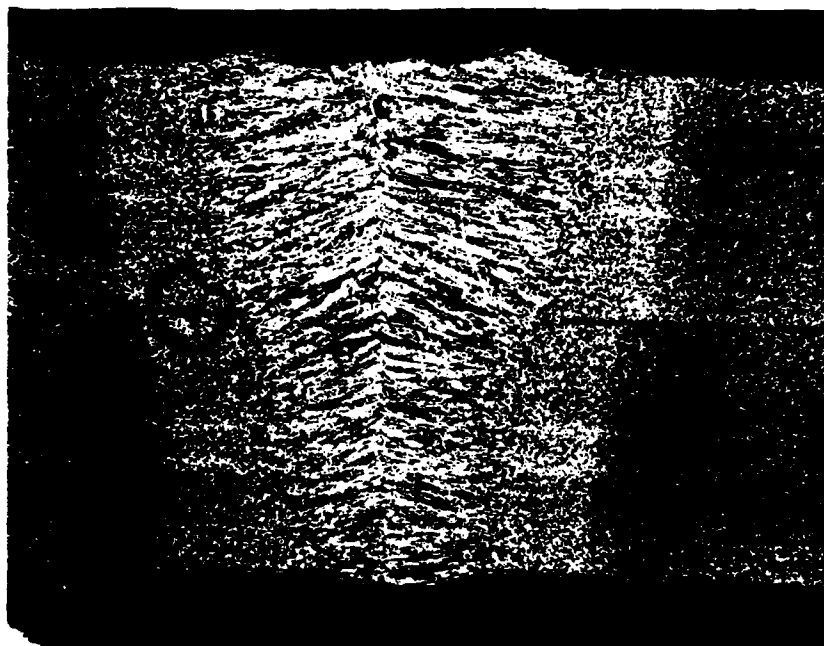
Material: Corten                      Thickness: 0.118 in. ea.  
Focal Length: 54 11/16  
Weld Speed: 105 in/min  
Magnification: 11 X

Figure .28 . Lap weld. Partial penetration.



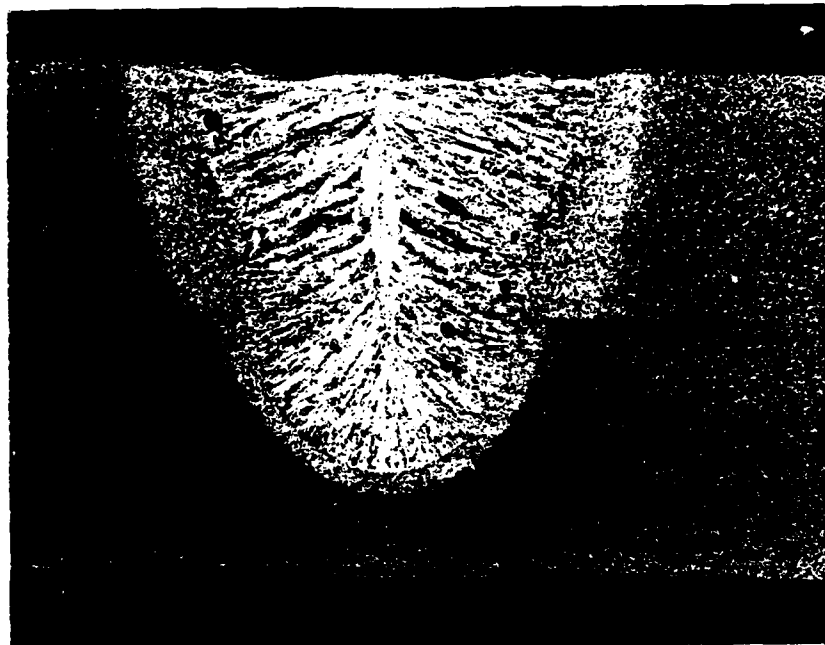
Material: Corten      Thickness: 0.118 in. ea.  
Focal Length: 54 9/16  
Welding Speed: 75 in. per minute  
Magnification: 11 X

Figure 27 . Lap weld. Full penetration.



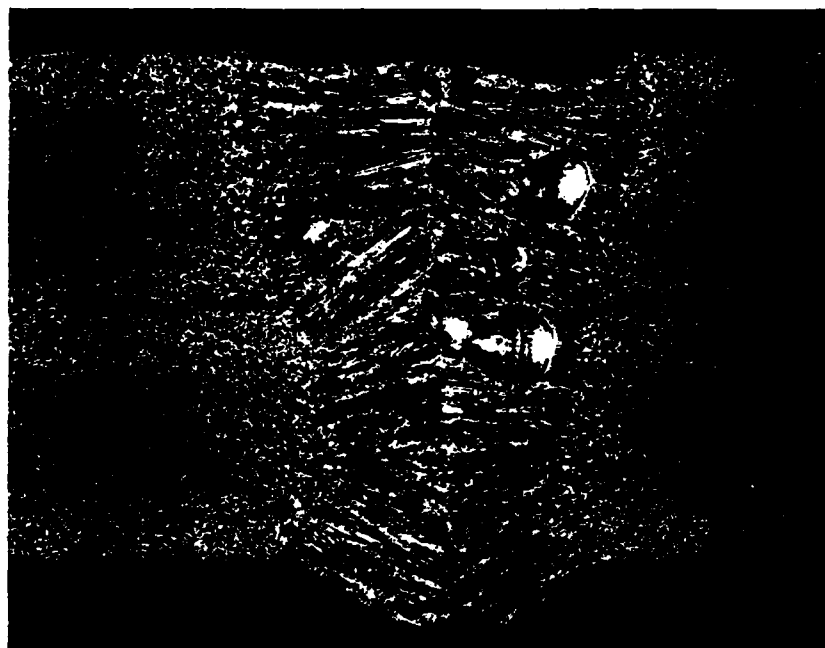
Material: Corten      Thickness: 0.118 in. ea.  
Focal Length: 54 9/16 in.  
Welding Speed: 75 in. per minute  
Magnification: 11 X

Figure 26. Lap weld. Full penetration.



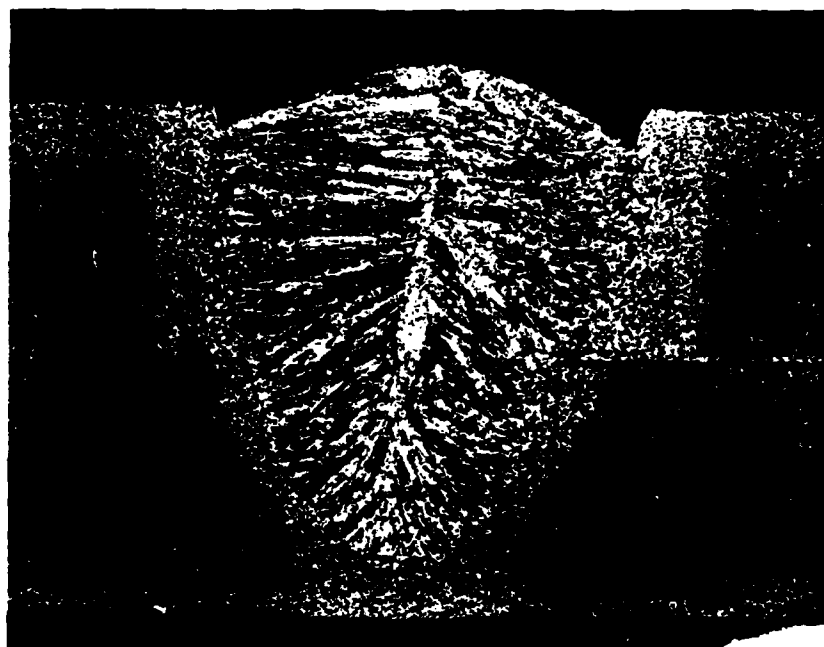
Material: Corten      Thickness: 0.118 in. ea.  
Focal Length: 54 9/16 in.  
Welding Speed: 84 in. per minute  
Magnification: 11 X

Figure 25 . Lap weld. Partial penetration.



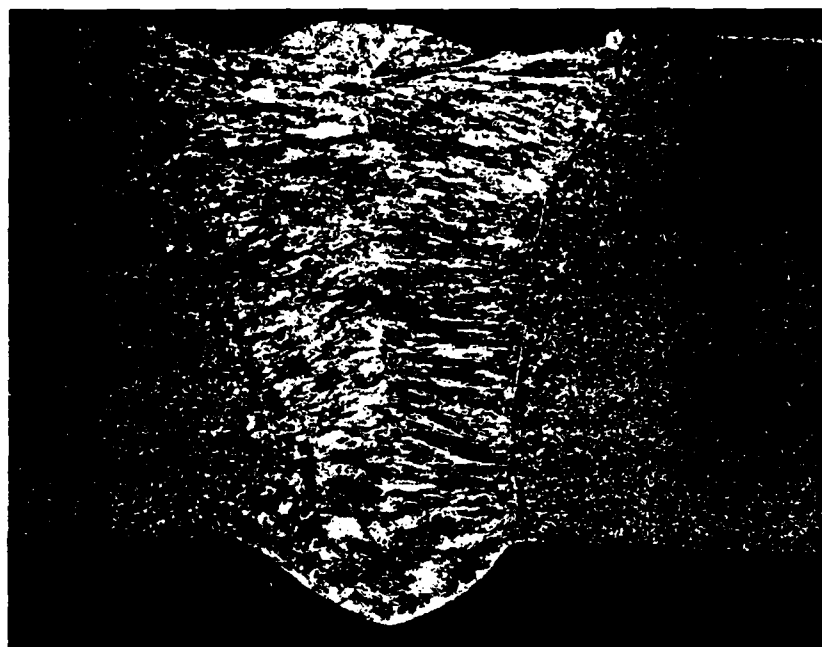
Material: Corten                      Thickness: 0.118 in. ea.  
Focal Length: 54 1/2 in.  
Welding Speed: 75 in/min  
Magnification: 11 X

Figure 24. Lap weld. Full penetration.



Material: Corten      Thickness: 0.118 in. ea.  
Focal Length: 54 1/2 in.  
Welding Speed: 98 in/min  
Magnification: 11 X

Figure 23 . Lap weld. Partial penetration.



Corten Material Thickness 0.118 in. each

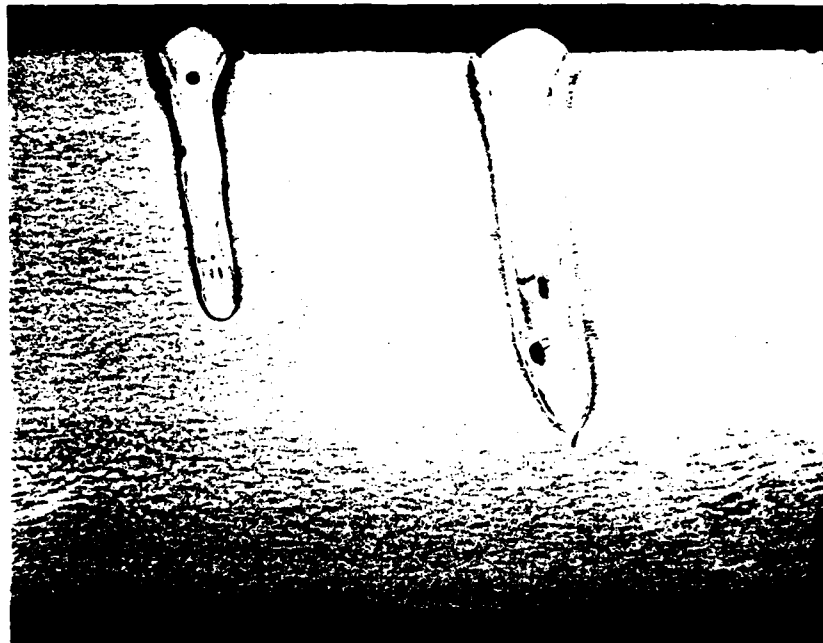
Focal Length: 54 7/16

Welding Speed: 71 in. per minute

Magnification: 11 X

Figure 22 . Lap weld; full penetration.





MAG: 11 X

Figure 36 . Bead on plate laser beam weld passes in 1.25 " thick steel plate 25 kW, left: 60 IPM; right: 30 IPM.

## J. Conclusions

As a result of this investigation, it was determined that a high power laser using an unusually high f/No. (broad spot) optical system could accomplish two things; it could produce a commercially important 2 ply weld in 0.118 in. Cor-Ten Grade A steel, and it could be adapted for missile storage container subassemblies, such as the cradle, to effect a 60% reduction in labor (0.972 manhours out of 1.60 manhours in each cradle assembly).

## K. Recommendations

It is important that a number of observations and conclusions from this study be more closely evaluated, demonstrated and, if viable, verified under actual test conditions. These include:

- Optimization of the broad spot, 2 ply weld on which the conclusions are based.
- Determination of the shear and tensile strengths for several spot sizes (f/7 and f/18) to verify the value of the high power, broad spot concept.
- Verification of the substitution of 2 ply welds for the present GMAW procedures through the fabrication and testing of an initial set of cradles.
- Improvement of performance in test through modifications of the concept based on the results of the verification mentioned above.
- Verification of the production concept through the prototype manufacturing of at least 100 cradles, using tooling and welding techniques that simulate those suggested in this report.

## PART II LASER WELDING OF ALUMINUM

### A. INTRODUCTION

Welding parameters were developed for aluminum in anticipation of utilizing aluminum alloys for missile container fabrication. The art of laser welding of aluminum has not been perfected. Some success has been achieved in welding sheet thicknesses of aluminum, but attempts so far have produced welds of poor quality and erratic reproducibility. The problem seems to be attributed to poor coupling of the laser beam due to the high reflectance characteristic of aluminum.

In this program, various techniques were investigated to counter the reflectance. Aluminum alloys were painted with carbon black, various paints, and anodized coatings. Results indicated that coupling of the laser beam was a function of the type and thickness of the coating. For example, anodic coatings coupled much better than paints. However, as with other coatings which differ from the base metal constituents, weld quality is impaired.

The most efficient coupling was one whereby the reflected beam from the workpiece was redirected back to the workpiece via a copper mirror located just above the weld zone. This arrangement, in addition to a helium jet gas shielding design, significantly improved coupling efficiencies; often it more than doubled the heat input over the conventional gas shielding system. The design of the shield, the resulting welds, and a bar chart summarizing the results, appear in illustrations in this part of the report.

### B. PROCEDURE

Laser welding of aluminum has met with little success, especially in plate thicknesses, i.e., thicknesses exceeding 1/8 inch. In this program, investigation of the effects of material type, beam shape, focal length, and other parameters was necessary before generating weld data for the production environment of missile container manufacturing. To this end, various types of aluminum alloys were subjected to laser welding conditions whereby the parameters of the laser were investigated. The method of evaluation was bead-on-plate welding which provided weld parameter data on a gross scale at high energy levels and optimum travel speeds.

Considerable effort was expended in modifying the laser to perform as a welder, such as incorporating a closed loop feedback control. Details appear in the Appendix. A significant effort was also expended in improving coupling efficiency with aluminum alloys. The latter effort resulted in a gas-shielding design which improved heat transfer into aluminum. The design was checked out in principle at two different high power laser installations whereby welding parameters were generated for various devised weldment configurations. This device is referred to as the MICOM shield.

Helium gas was selected for use in shielding both steel and aluminum during laser welding because of the known advantage of deeper penetration afforded by helium over other shielding gases. For steel, a simple jet of helium was directed over the top side of the weld area through a conventional plasma arc shielding nozzle. For aluminum, a much more sophisticated technique was necessary to achieve the required shielding. The technique developed was one whereby two inches forward and aft of the weld area was covered by helium. The

underside of the weld was also shielded by helium flowing through perforations in the back-up plate. Flow rates of 200 CFH and 150 CFH were found to be satisfactory for top and bottom shielding respectively.

The MICOM shield which was fabricated from a copper block is shown in Figure 1. Operationally, the beam enters through a hole in the center of the block and on the underside of the hole is a hemispherical cavity polished to a mirror finish which counteracts the high reflectance characteristics of the aluminum surface by re-reflecting the portion of the beam which is reflected from the workpiece into the cavity back to the workpiece. A shielding gas jet located at the edge of the cavity blows away the plasma, (formed above the weld) where it escapes via a trough cut on the opposite side of the cavity. To prevent air from being aspirated into the weld zone, a second source of shielding gas is introduced via holes located peripherally around the cavity.

Four aluminum alloys in plate thicknesses were investigated for comparison of a conventional shield with the MICOM shield. Focal distances, travel speed, power input into the workpiece, lens f/numbers, and beam configurations were all varied to establish the effect of each parameter on weldments. Before each weld pass was made, the workpiece was cooled to room temperature in order to assure an initial baseline temperature for proper comparison. The bead-on-plate technique was used in most cases. However, some butt welds were prepared.

Carbon black, various paints and anodized coatings were investigated very briefly for their ability to minimize reflectance of the laser beam. Only the anodized coatings showed any significant response. In this study, clad aluminum and two anodized aluminum specimens were exposed to the laser beam at constant power and at two travel speeds. Results are illustrated in Figures 22 and 23.

### C. RESULTS

Figures 1 through 9 illustrate the effect of shielding techniques on weld heat input. The advantage of the MICOM shield is readily seen in Figures 2, 3, 7, and 8. Figures 4 and 5 also illustrate the improved penetration but to a lesser extent. The referenced figures show that the greatest increase in weld heat input occurred with the f/18 lens and a pure annular beam. The MICOM shield, used with an f/7 lens, and an annular beam, failed to produce noticeable differences in weld heat input (Figure 6). With the f/18 lens and a crescent beam, the shield was more effective than with the f/7 lens, (Figures 4 and 5). Since more energy is concentrated in an f/7 than an f/18 lens, and in a crescent rather than an annular beam, it appears that the effectiveness of the MICOM shield is somewhat related to the energy concentration. Unfortunately, the beam spot size was not measured for these tests. Nevertheless, the f/18 lens is more efficient in transferring energy into aluminum than the f/7, with or without the MICOM shield. The phenomena is admittedly not understood but future investigations should include this aspect as a subject for study.

#### 1. Weld Quality

There was no attempt to optimize weld quality from the standpoint of porosity or cracking. However, weld quality was better with the f/18 lens and the annular beam. Heaviest cracking occurred with 6061 aluminum and, although 6061 aluminum is considered highly weldable by most reference sources, previous

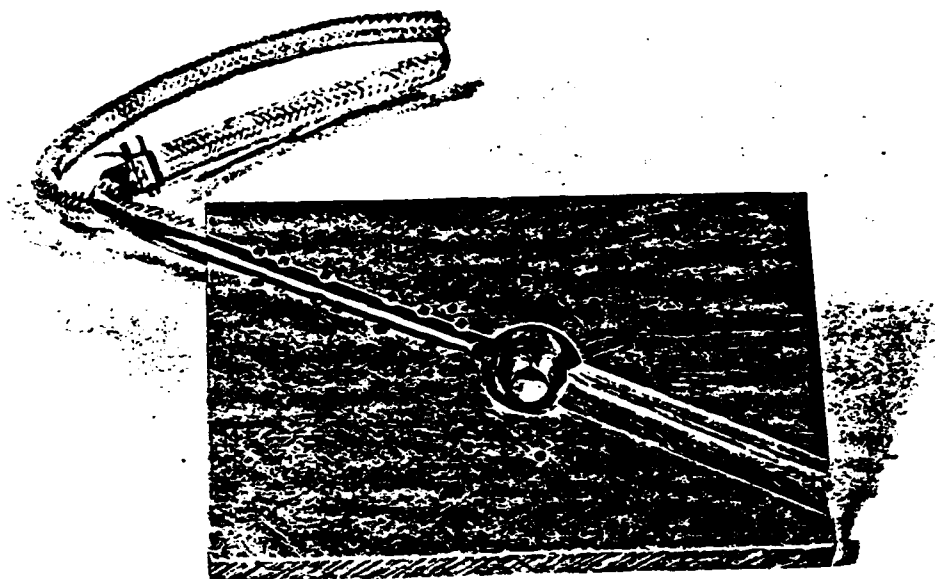
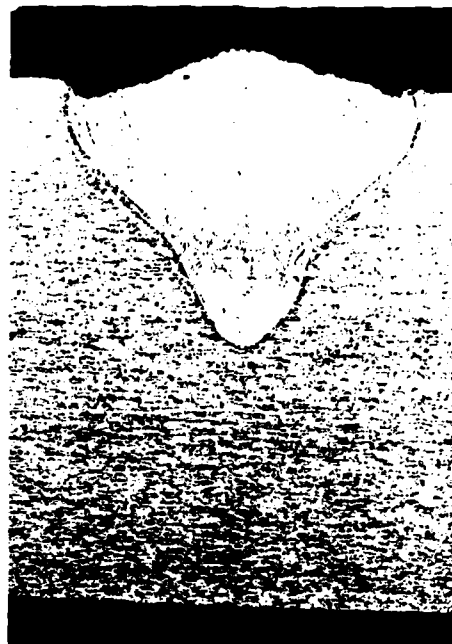
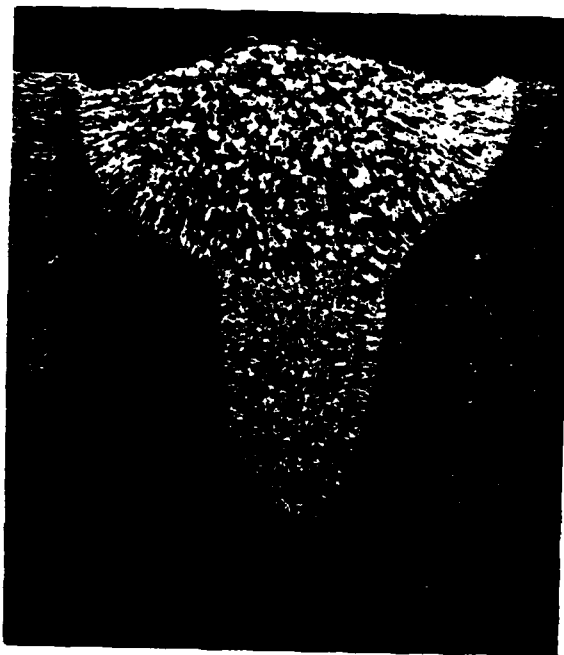


Figure 1.  
MICOM Gas welding shield used in laser welding of aluminum.  
Reflected rays of the laser beam from the workpiece  
are re-directed from the shield back to the workpiece.



BEAM: f/18 SHIELD: MICOM SHIELD (left)  
One-sided Conventional(right)  
Annular

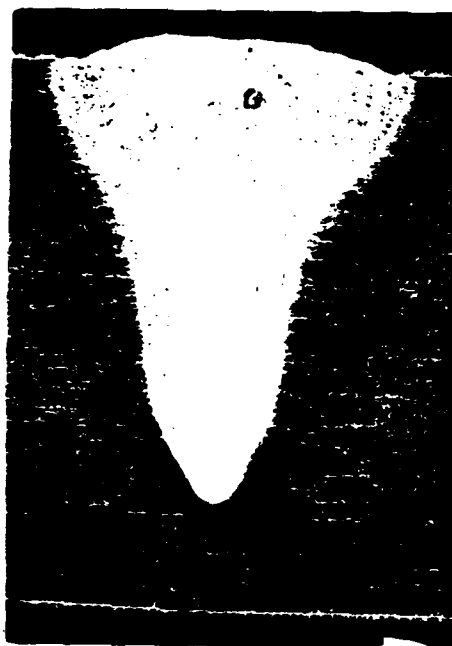
GAS FLOW RATE: 200 CFH

KW: 8

WELD SPEED: 40

FOCUS: Optimum

MATERIAL: 1/2" 5052



BEAM: f/18 SHIELD: MICOM Shield (left) GAS FLOW RATE: 150 CFH  
One-sided Conventional right  
Annular

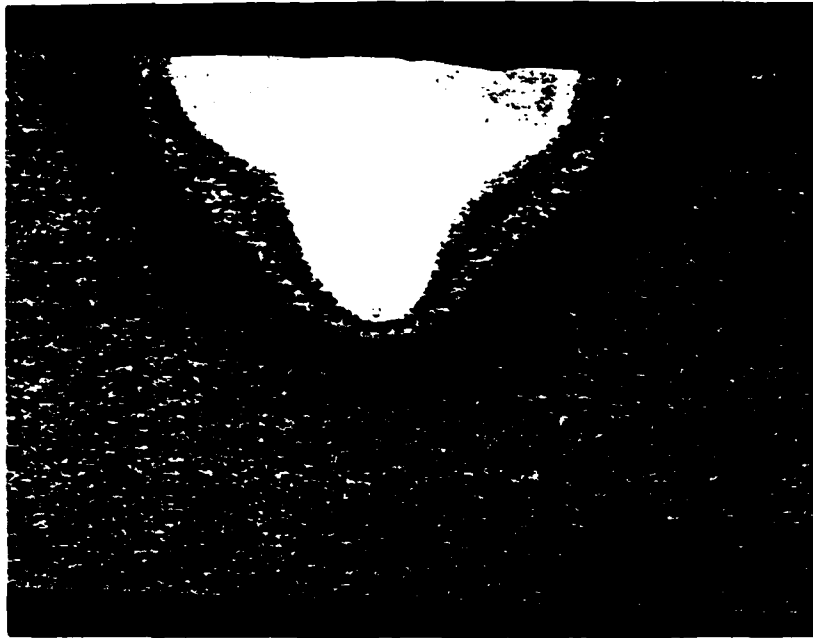
KW: 3

WELD SPEED: 40

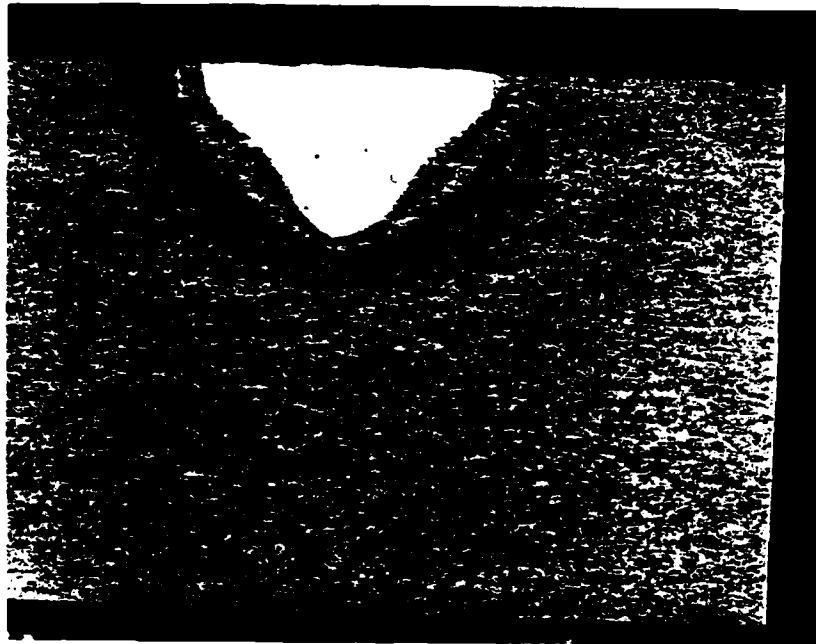
FOCUS: 23 13/16

MATERIAL: 1/2" CLAD 7075

Figure 2. Macrosections of bead on aluminum plate laser welds showing the effect of shielding techniques on weld heat input. Mag 6X



BEAM: Annular f/18 SHIELD: MICOM Shield GAS FLOW RATE: 200 CFH  
 KW: 10 WELD SPEED: 40 IPM FOCUS: Optimum MATERIAL: 1/2" 2219



BEAM: Annular F-18 SHIELD: Conventional GAS FLOW RATE: 200 CFH  
 KW: 10 WELD SPEED: 40 IPM FOCUS: Optimum MATERIAL: 1/2" 2219

Figure 3. Macrosections of bead on aluminum plate laser welds illustrating the effect of shielding techniques on weld heat input and bead shape. Mag 6X



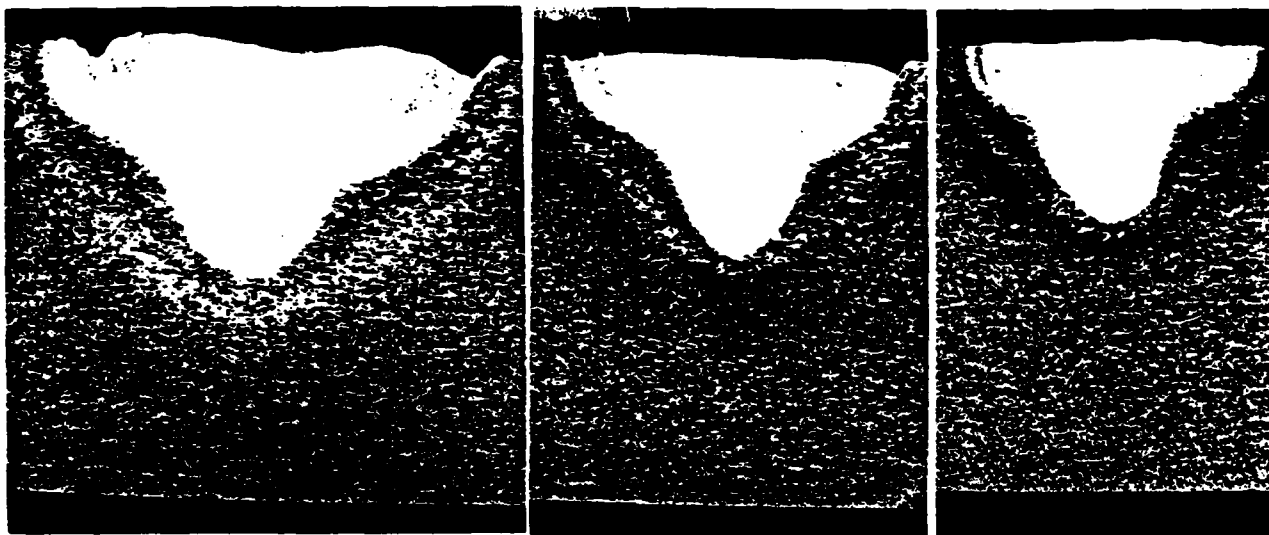
f/18 SHIELD: MICOM Shield(left)  
 BEAM: Crescent Conventional Shield (right) GAS FLOW RATE: 150 CFH  
 KW: 10 WELD SPEED: 40 IPM FOCUS: Optimum + 1/8 MATERIAL: 1/2" 6061



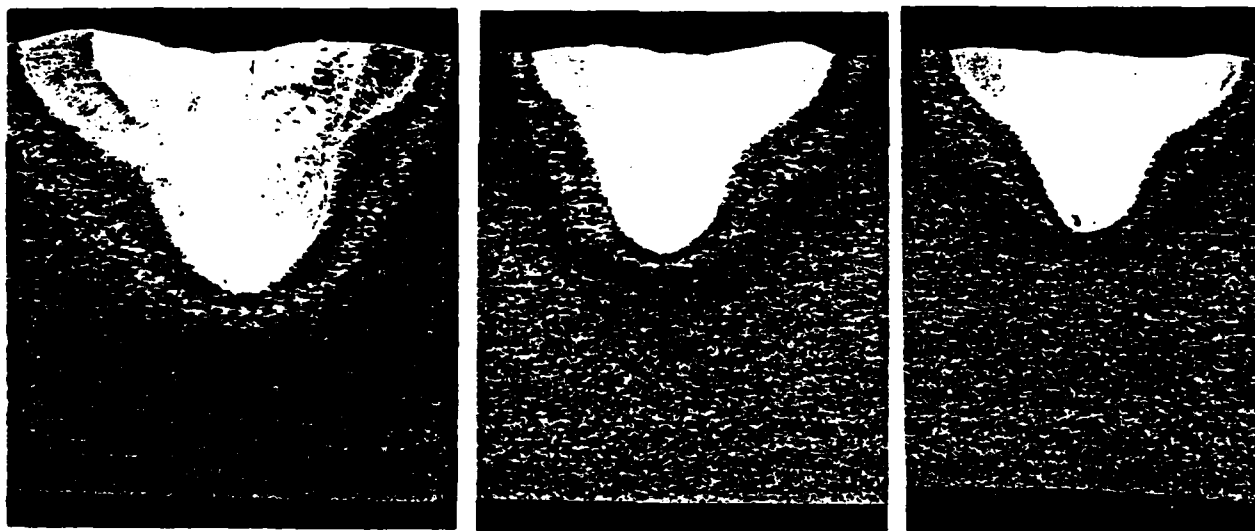
f/18 SHIELD: MICOM SHIELD (left)  
 BEAM: Crescent Conventional Shield (right) GAS FLOW RATE: 150 CFH  
 KW: 10 WELD SPEED: 40 IPM FOCUS: Optimum MATERIAL: 1/2" 6061

Figure 4. Macrosections of bead on aluminum plate laser welds illustrating the effect of shielding techniques on weld heat input and bead shape. Mag 6X

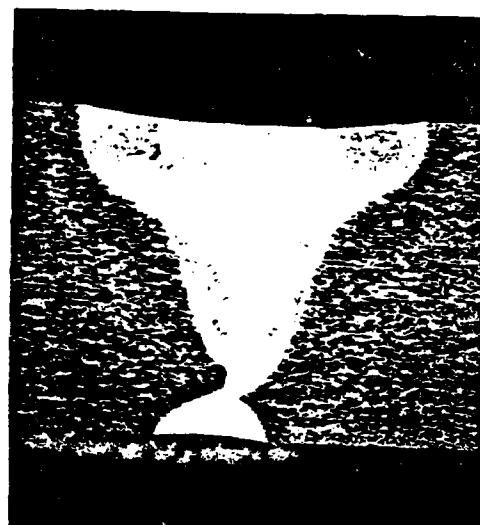
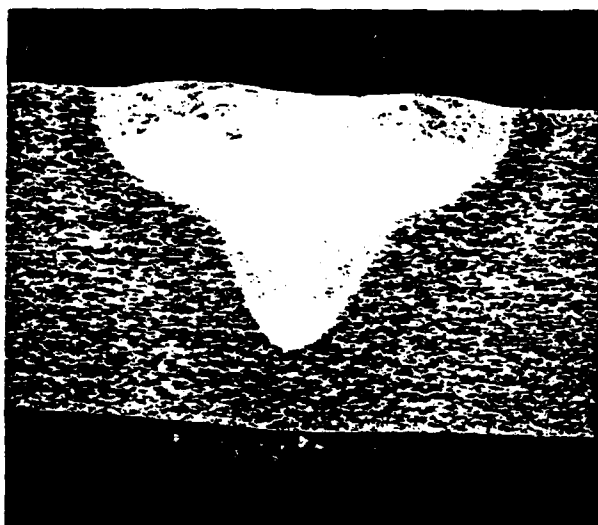




BEAM: Annular  $f/7$  MICOM Shield GAS FLOW RATE: 200 CFH  
 KW: 10 WELD SPEED: 20,30,40 FOCUS: Optimum MATERIAL: 1/2" 2219



BEAM: Annular  $f/7$  SHIELD: Conventional GAS FLOW RATE: 150 CFH  
 KW: 10 WELD SPEED: 20,30,40 FOCUS: Optimum MATERIAL: 1/2" 2219



BEAM: Annular f/18      MICOM Shield      GAS FLOW RATE: 200 CFH  
 KW: 10      WELD SPEED: 30, 40      FOCUS: Optimum      MATERIAL: 3/8" 2219

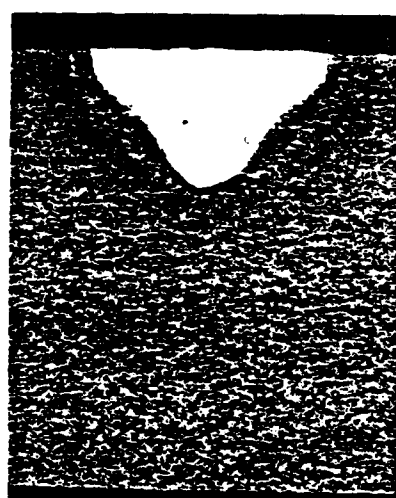
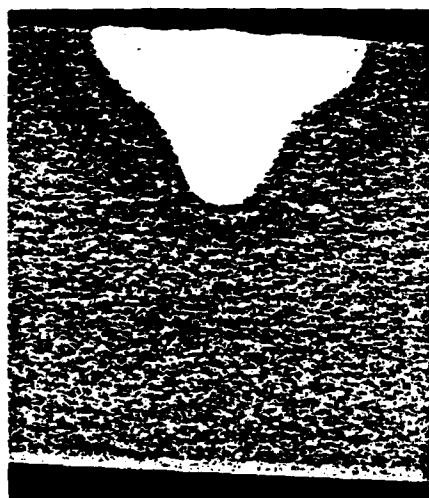
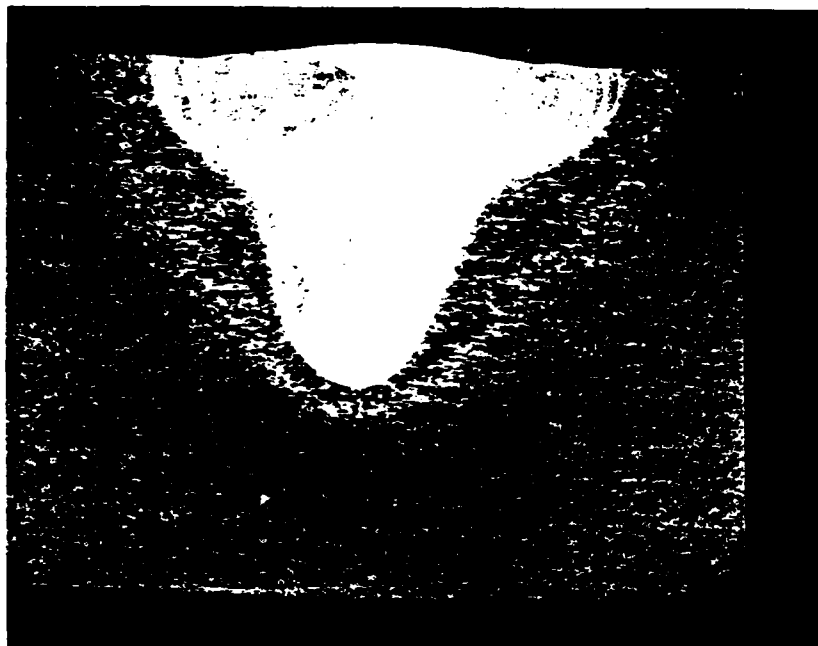
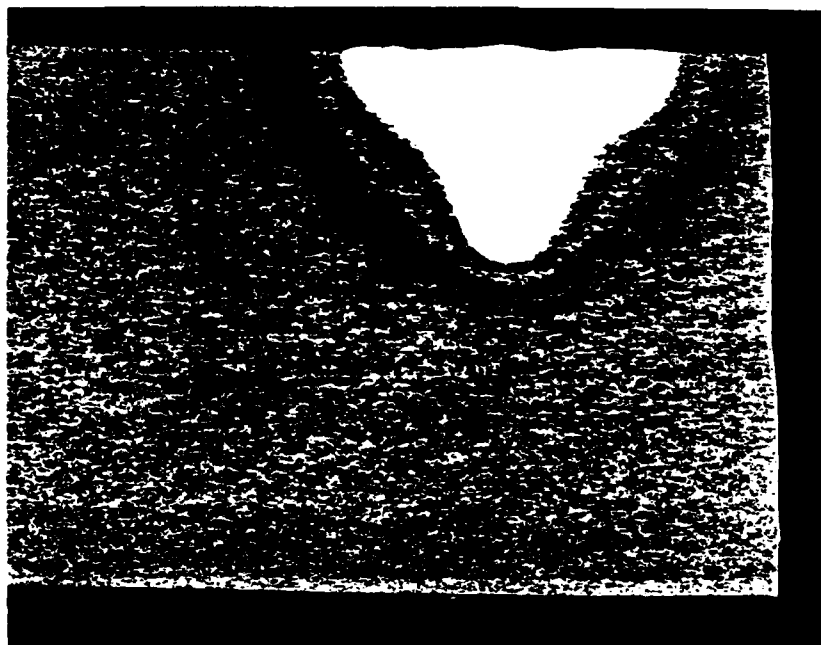


Figure 6. Macrosections of bead on aluminum plate laser welds. The F-7 sharp focus lens apparently negates the effect of the MICOM shield. Mag 6X.

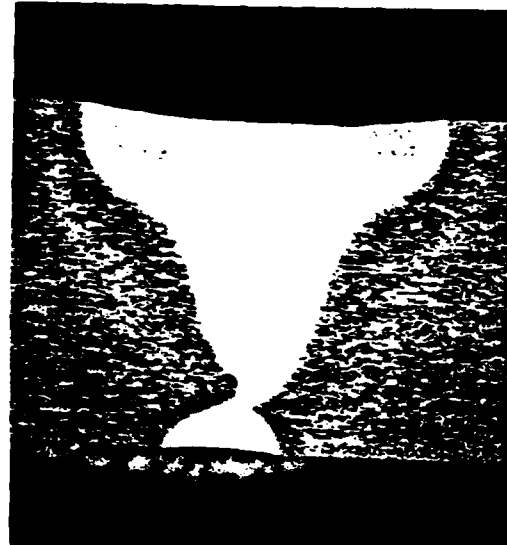
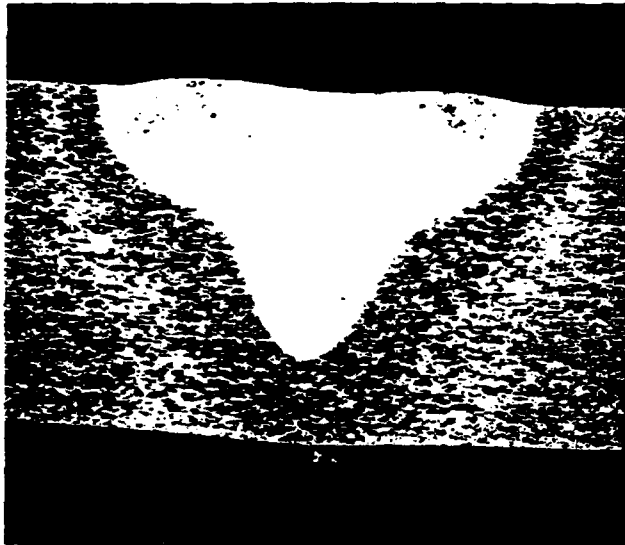


BEAM: Annular f/18      MICOM Shield      GAS FLOW RATE: 200 CFH  
 KW: 10      WELD SPEED: 30 IPM      FOCUS: Optimum      MATERIAL: 1/2" 2219

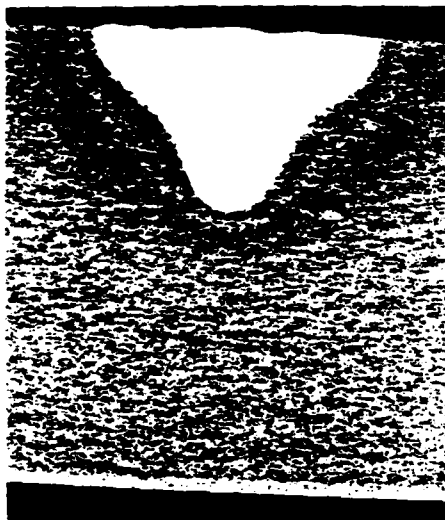


BEAM: Annular f/18      SHIELD: Conventional      GAS FLOW RATE: 150 CFH  
 KW: 10      WELD SPEED: 30 IPM      FOCUS: Optimum      MATERIAL: 1/2" 2219

Figure 7. Macrosections of bead on aluminum plate laser welds showing the effect of shielding techniques on weld heat input and bead shape. Mag 6X

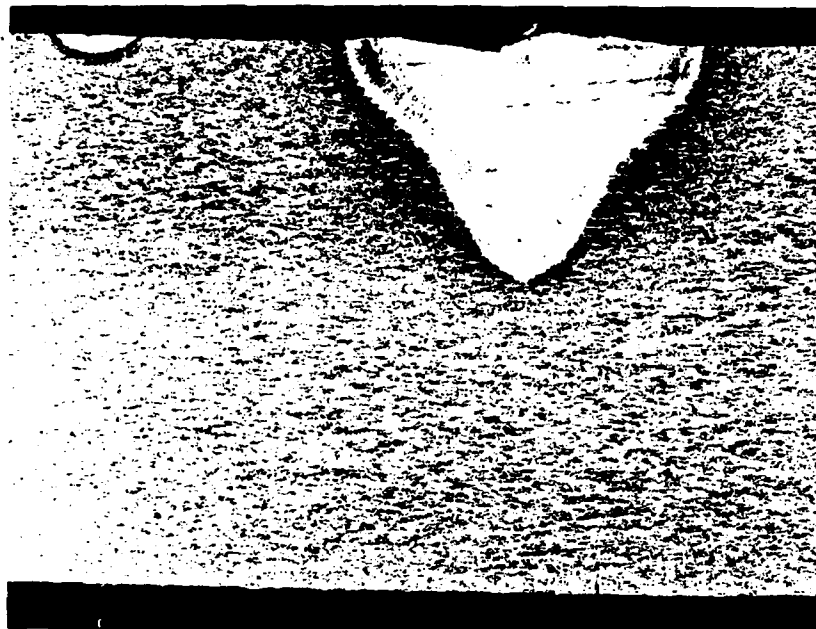


BEAM: Annular f/18      MICOM Shield      GAS FLOW RATE: 200 CFH  
 KW: 10      WELD SPEED: 30, 40      FOCUS: Optimum      MATERIAL: 3/8" 2219

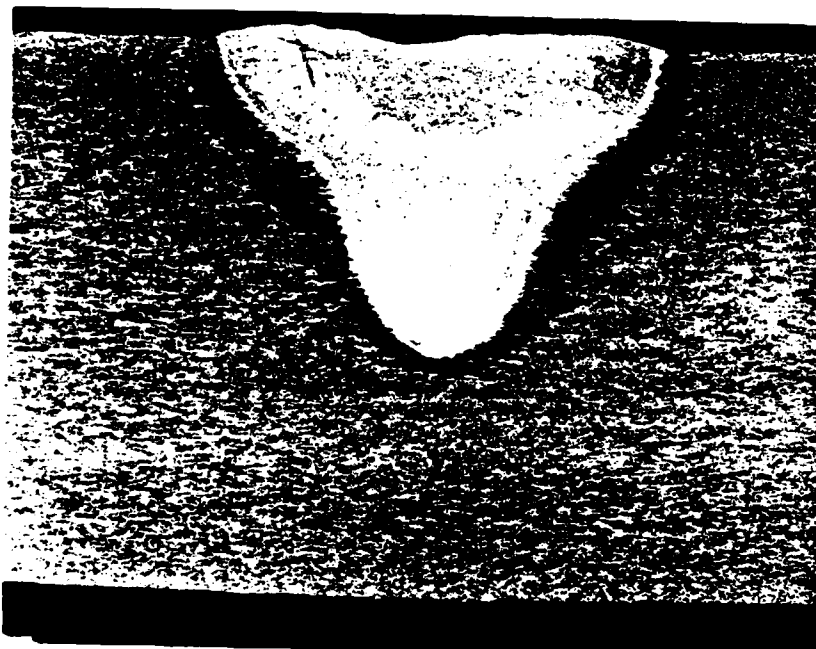


BEAM: Annular f/18      SHIELD: Conventional      GAS FLOW RATE: 200 CFH  
 KW: 10      WELD SPEED: 30,40      FOCUS: Optimum      MATERIAL: 1/2" 2219

Figure 8. Macrosections of bead on aluminum plate laser welds showing the effect of travel speed and shielding on weld heat input and bead shape. Mag 6X.



BEAM: Annular f/18 SHIELD: Conventional GAS FLOW RATE: 150 CFH  
 KW: 10 WELD SPEED: 40 IPM FOCUS: Optimum MATERIAL: 2219



BEAM: Annular f/18 MICOM Shield GAS FLOW RATE: 150 CFH  
 KW: 10 WELD SPEED: 40 IPM FOCUS: Optimum MATERIAL: 2219

Figure 8A. Macrosections of bead on aluminum plate laser welds showing the effect of travel speed on weld heat input and bead shape. Mag. 6X.



BEAM: Annular f/18 SHIELD: Conventional GAS FLOW RATE: 150 CFH  
 KW: 10 WELD SPEED: 30 IPM FOCUS: Optimum MATERIAL: 2219



BEAM: Annular f/18 MICOM Shield GAS FLOW RATE: 150 CFH  
 KW: 10 WELD SPEED: 30 IPM FOCUS: Optimum MATERIAL: 2219

Figure 8B. Macrosections of bead on aluminum plate laser welds showing the effect of travel speed on weld heat input and bead shape. Mag. 6X.

weld quality since it is a long established practice that optimum weld joint preparation requires removal of foreign materials (dirt, grease, and other impurities) exposing only bare base metal to the welding arc. However, for the purpose of study, these tests show that anodized aluminum responds significantly better to laser beam coupling than a bare aluminum surface.

#### E. Summary

A welding shield (MICOM shield) developed at Redstone Arsenal increased the weld heat input significantly over a conventional shield. In fact, under some conditions using the f/18 lens, the increase exceeded the conventional by a factor of two. The shield, however, did not prove effective with the f/7 lens. The crescent beam and the one-sided annular beam produced a deeper penetration and greater heat input than the pure annular beam; however, at the expense of increased porosity levels. The pure annular beam produced the best weld surface appearance and the lowest porosity of the three beam shapes evaluated. Welds made with the pure annular beam resembled a TIG weld in both surface appearance and cross section.

The rougher the bead appearance, the higher the porosity level, with the f/7 lens producing the roughest bead. Both bead appearance and porosity level are probably directly related to the degree of weld puddle turbulence; the more concentrated the beam, as with the f/7 lens, the more the puddle turbulence. Weld penetration and bead shape were essentially the same within a thickness range of 3/8 in. to 1/1 in. There was no apparent difference in weld bead shape and size between the various types of aluminum alloy evaluated.

Minor changes in focal length had no significant effect on weld geometry when using the f/18 lens; however, the f/7 lens was found to be more critical in focal distance (to workpiece). Raising the MICOM shield 1/2 in. above the workpiece greatly reduced the heat input into the workpiece. This is at least partially due to the helium jet in the shield being less effective in removing the plasma in the raised position. Increasing the helium flow rate from 50 to 150 CFM significantly improved weld energy input. This and raising the MICOM shield point toward the importance of removing the plasma. Minimum porosity levels were apparent at welding speeds of 30-35 ipm. Less porosity occurred with the f/18 lens and the pure annular beam which represented the least energy concentration spot size, then with other lens and beam configurations.

Cracking in the weld bead was more prevalent in small weld beads where the condition of freezing of the molten puddle was fastest. This condition is similar to the cracking occurring at the starting and stopping points of the conventional arc welding process when not properly performed. Anodized aluminum provide a much better laser beam coupling than bare aluminum, but this coupling media is impractical in that the media itself impairs weld quality. The use of the MICOM shield can enhance welding of aluminum by providing more heat energy into the workpiece thereby increasing laser welding efficiency and/or increasing laser weld capacity. Additional work is currently needed to refine the laser welding process and the MICOM welding shield.

#### F. Conclusions

Parameters for laser welding of aluminum were optimized to the extent possible in this program. It is believed that laser welding of aluminum can be

Figure 14A shows this effect of weld travel and shielding gas flow directions.

#### 8. Effects of MICOM Shield Position

As a comparison of the basic travel direction photo in Figure 14A with Figure 15 shows, raising the shield one/half inch above the optimum level also had an adverse effect on the weld bead.

#### D. Summarized Bar Chart

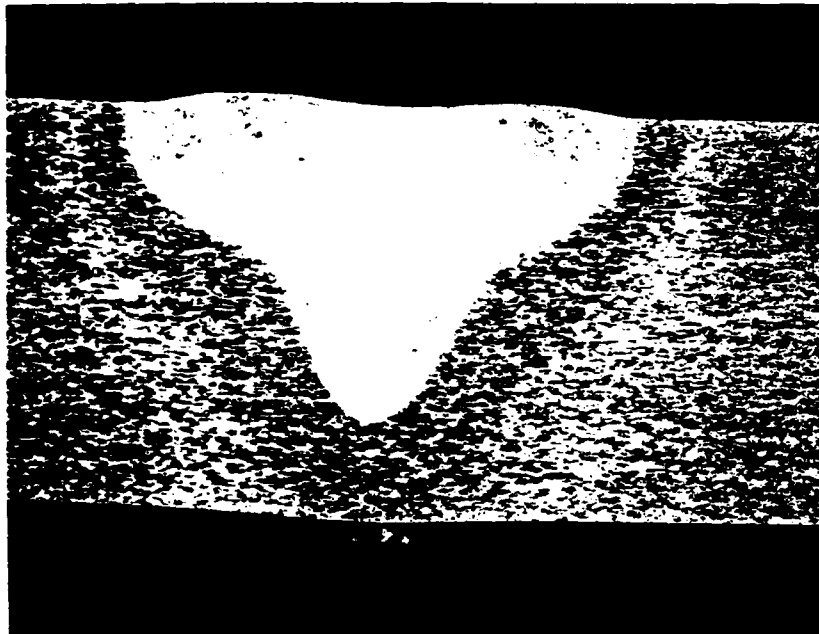
The effect of all the variables on melt area (a function of heat input) is summarized in Figure 21. What is immediately obvious is the distinct superiority of the MICOM shield in every case except where the f/7 lens was used (bars 37 through 46). The shield was generally most effective with an f/18 lens and a pure annular beam, showing the largest percentage increase of melt area over conventional shielding. However, based on efficiency per unit of laser beam power the condition which produces the greatest melt area was the f/18 one-sided annular beam used with the MICOM shield (bars 1, 15, 17, and 18). Bar No. 20 (largest melt area) represents a 20% lower beam power at half the speed, or a net increase in weld energy input of 60%, so that based on efficiency, the yield is low.

The effect of gas flow is illustrated in bars 12 through 15, and the effect of shield position in bar 16. Higher concentrated energy yields better coupling, higher heat input, and consequently more melt area. Compare similar parameter bars of the one-sided annular beam and crescent beam with the uniform annular beam (bars 15, 17, 18, 21, 25, with 30, 33, and 6, 10, 19, with 31, 35). The f/18 lens provides increased coupling and consequently melt area than the f/7 lens when using the MICOM shield. Compare bar 33 vs 39 and 43, bar 32 vs 43, bars 28 and 32 vs 39 and 42, and bars 30 vs 41 and 43. The reverse seems to be true when using the conventional shield; compare 38 and 45 vs 29 and 34. Raising the position of the shield above the workpiece 1/2" higher than normal reduces the effect of the MICOM shield; compare bar 18 with bar 16. This is probably due to the fact that plasma formed above the weld is more effectively blown away with the shield lowered. The shield in the raised position reveals the reflective effect of the shield. In this position less plasma is being blown away than with the conventional gas jet shield; yet the weld nugget is larger than the comparable conventional gas shielded weld nugget. This is probably attributable to the reflective effect of the shield. (Compare bar 16 with bar 19.) Gas flow rate affects the size of the weld nugget. (Compare bars 12, 13, 14, and 15; and 17 and 18.) The use of various types of aluminum alloys does not appear to alter the weld nugget size. The effect of welding speed and heat input is displayed by bars 17, 18 vs 20. For an increase of approximately 50% heat input brought about by a reduction in speed and power the total melt area change is relatively minor for a one-sided annular beam. With a crescent beam, the effect is more pronounced (bar 21 vs 27). Reproducibility is shown by bar 28 vs 32; and 32 vs 33, which also illustrate the effect of thickness.

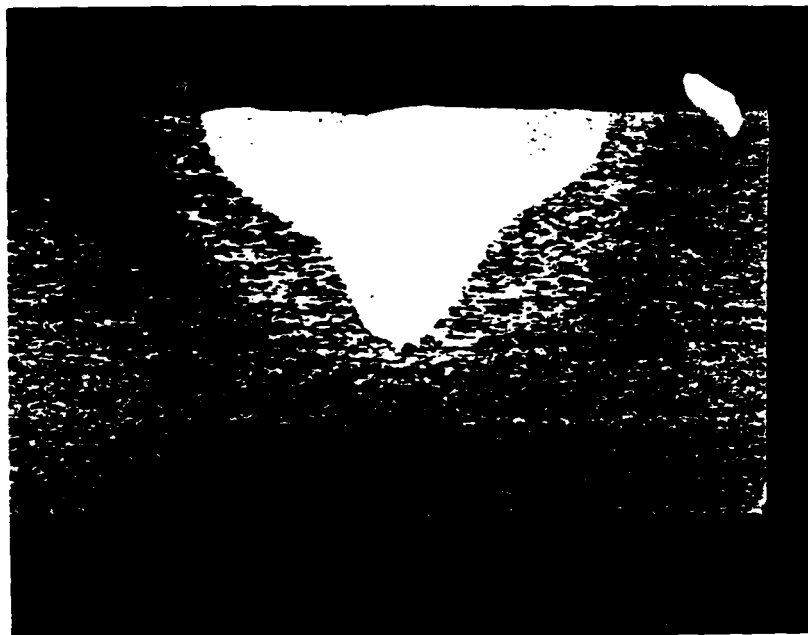
#### Effect of Anodized Coatings

Figures 22 and 23 illustrate the effect of clad, and light anodized aluminum on laser beam coupling. Macrographs in Figure 23 show excessive porosity which is probably a result of the anodic coating. Coatings inherently deteriorate



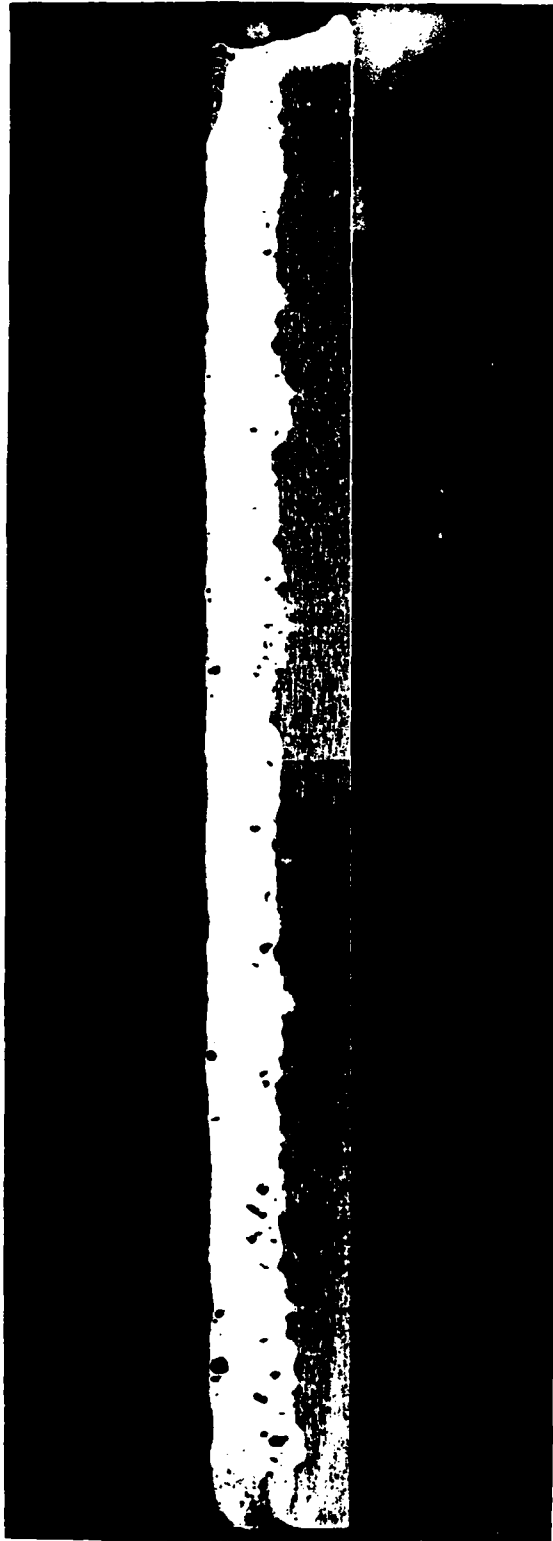


BEAM: Annular f/18 SHIELD: MICOM Shield GAS FLOW RATE: 200 CFH  
 KW: 10 WELD SPEED: 30 IPM FOCUS: Optimum MATERIAL: 3/8" 2219



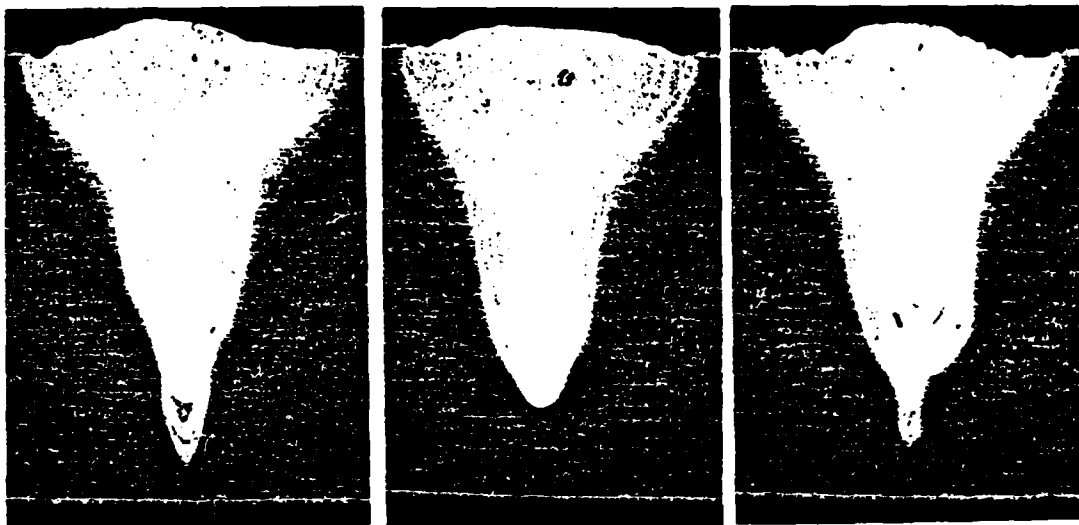
BEAM: Annular f/18 SHIELD: MICOM Shield GAS FLOW RATE: 200 CFH  
 KW: 10 WELD SPEED: 40 IPM FOCUS: Optimum MATERIAL: 3/8" 2219

Figure 20. Laser welded aluminum bead on plate showing the effect of travel speed on weld penetration. Mag. 6X.

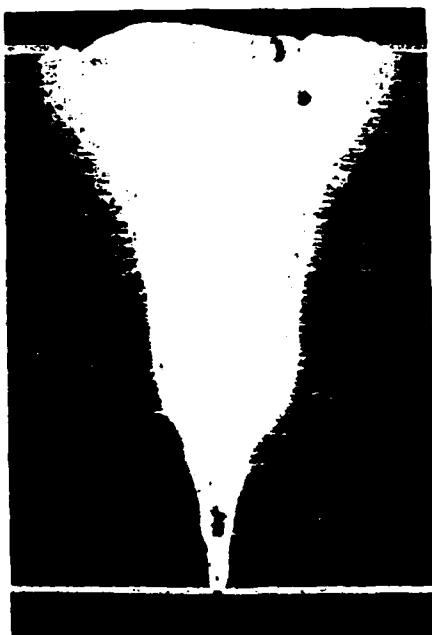


BEAM: One-sided Annular  $f/18$  SHIELD: Conventional GAS FLOW RATE: 150 CFH  
KW: 8 WELD SPEED: 40 FOCUS: Optimum to  $+1/2$ " MATERIAL:  $1/2$ " CLAD 7075

Figure 19. Longitudinal macrosection of laser welded aluminum bead on plate showing effect of varying lens to workpiece distance. Mag 1.6X.



B  
K



BEAM: f/18 One-sided Annular MICOM Shield GAS FLOW RATE: 150 CFH  
KW: 8 WELD SPEED: 40 FOCUS: Optimum + 3/8", 5/8" MATERIAL: 1/2" CLAD 7075

Figure 18. Laser welded aluminum bead on plate welds showing the effect of focal length on weld penetration and bead shape. Mag 6X.

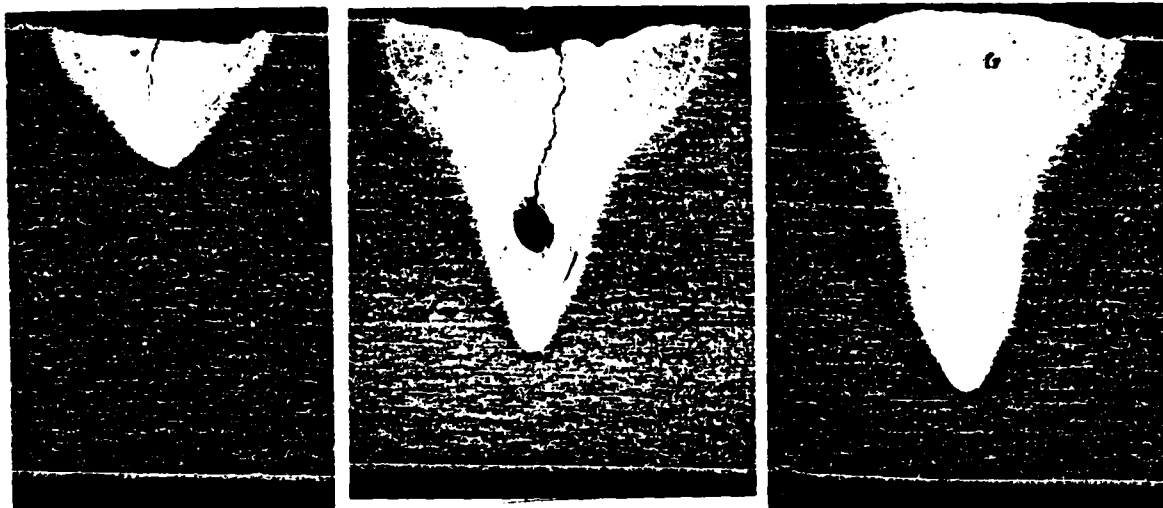


Figure 16. Laser welded aluminum bead on plate showing effect of power levels on weld bead penetration. Mag 6X.

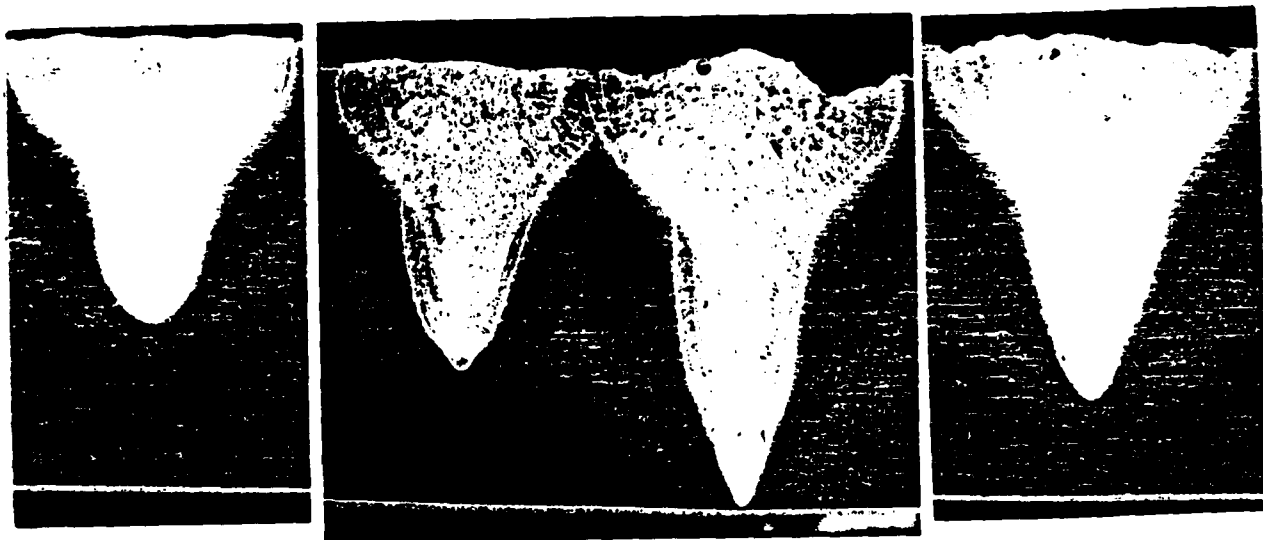
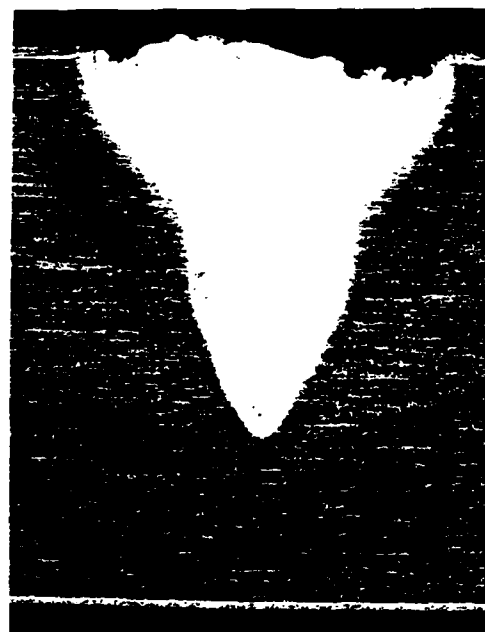
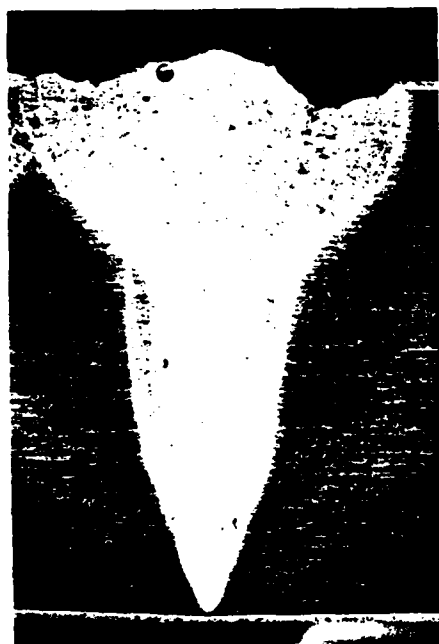
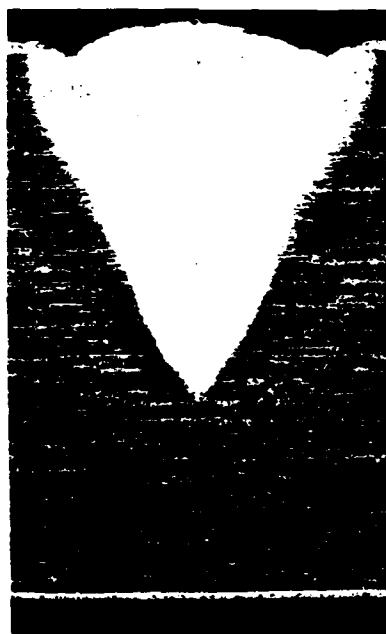


Figure 17. Laser welded aluminum bead on plate showing effect of shielding gas flow rate on weld penetration and bead shape. Mag. 6X.

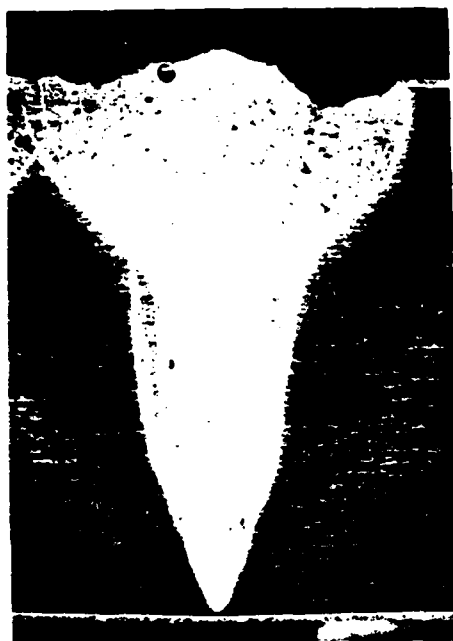


BEAM: F-18 One-sided Annular MICOM Shield      Opposite Travel Direction  
 Basic Travel Direction      GAS FLOW RATE: 200 CFH  
 KW: 8 WELD SPEED: 40 IPM FOCUS: Optimum      MATERIAL: 1/2" CLAD 7075  
 Figure 14A. Macrosections of aluminum bead on plate welds showing  
 effect of weld direction on bead shape. Magnification 6X.



BEAM: f/18 One-sided Annular MICOM Shield      GAS FLOW RATE: 200 CFH  
 KW: 8 WELD SPEED: 40 FOCUS: Optimum      MATERIAL: 1/2" CLAD 7075

Figure 15. Macrosection of aluminum bead on plate welds showing  
 effect of raising the shield 1/2 inch above optimum level.  
 Compare with top left. Mag. 6X

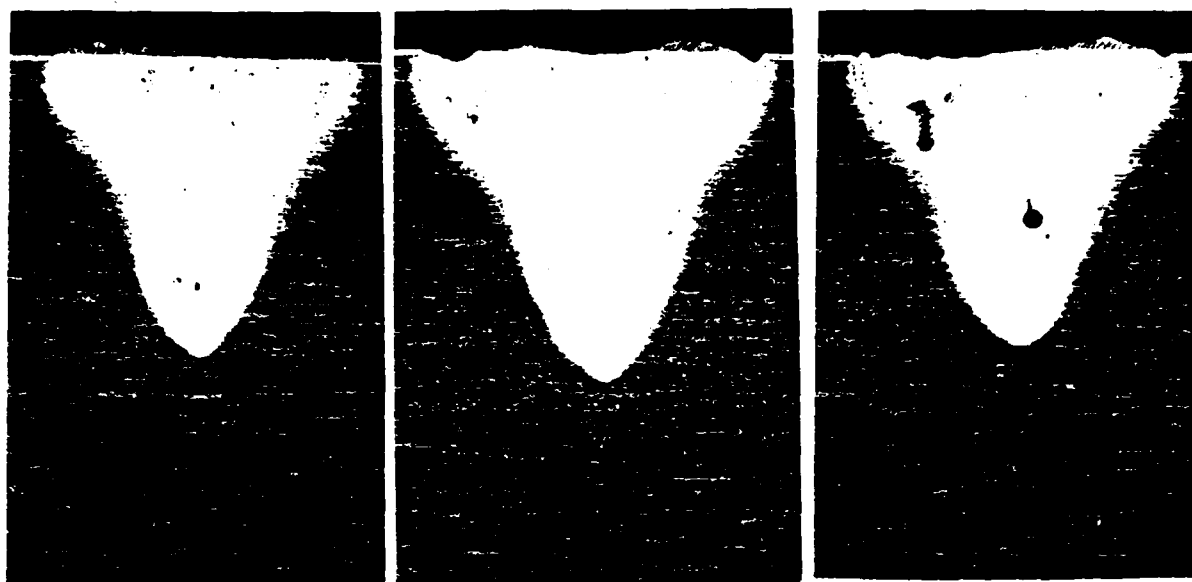


BEAM: f/18 One-sided Annular MICOM Shield GAS FLOW RATE: 200 CFH  
 KW: 8 WELD SPEED: 40 IPM FOCUS: Optimum MATERIAL: 1/2" 7075 CLAD(left)  
 1/2" 5052(right)



BEAM: f/18 One-sided Annular MICOM Shield GAS FLOW RATE: 200  
 KW: 6.5 WELD SPEED: 20 IPM FOCUS: Optimum MATERIAL: 1/2" 5052

Figure 14. Macrosections of aluminum bead on plate welds showing the effect of material types on weld penetration and bead shape. Mag. 6X



BEAM: f/18 One-sided Annular SHIELD: Conventional GAS FLOW RATE: 150  
 KW: 8 WELD SPEED: 40 IPM FOCUS: Optimum + MATERIAL: 1/2" CLAD 7075  
 1/8, 1/4, 5/8



BEAM: f/18 One-sided Annular SHIELD: Conventional GAS FLOW RATE: 150  
 KW: 8 WELD SPEED: 40 IPM FOCUS: Optimum + MATERIAL: 1/2" CLAD 7075  
 3/4, 7/8

Figure 13. Macrosections of aluminum bead on plate welds showing the effect of focal length on heat input. Mag. 6X.

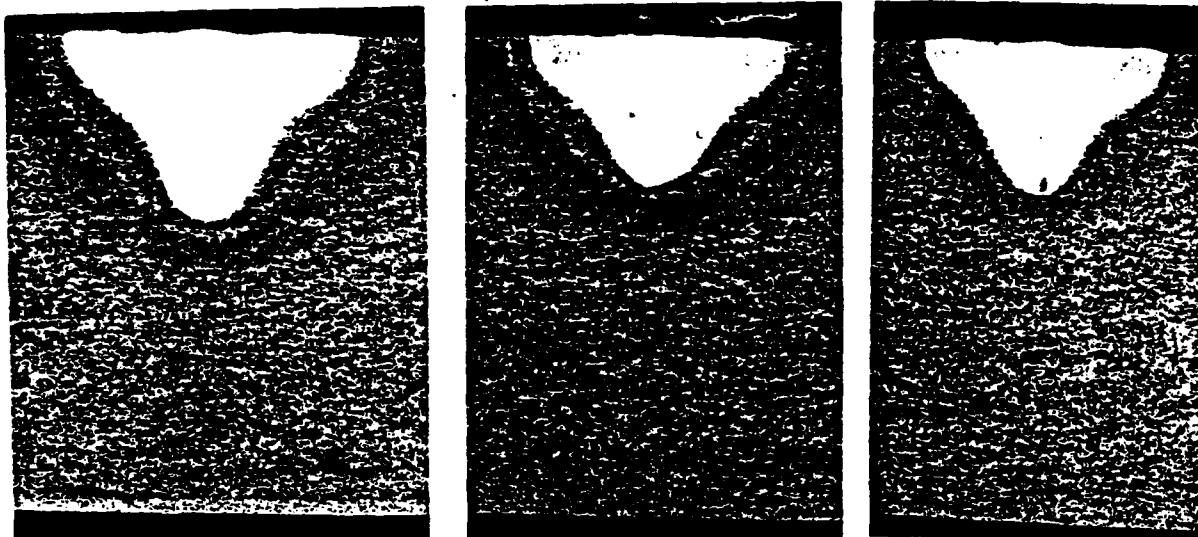


Figure 11. Macrosections of aluminum bead on plate laser welds showing the effect of speed on weld heat input. Mag. 6X.

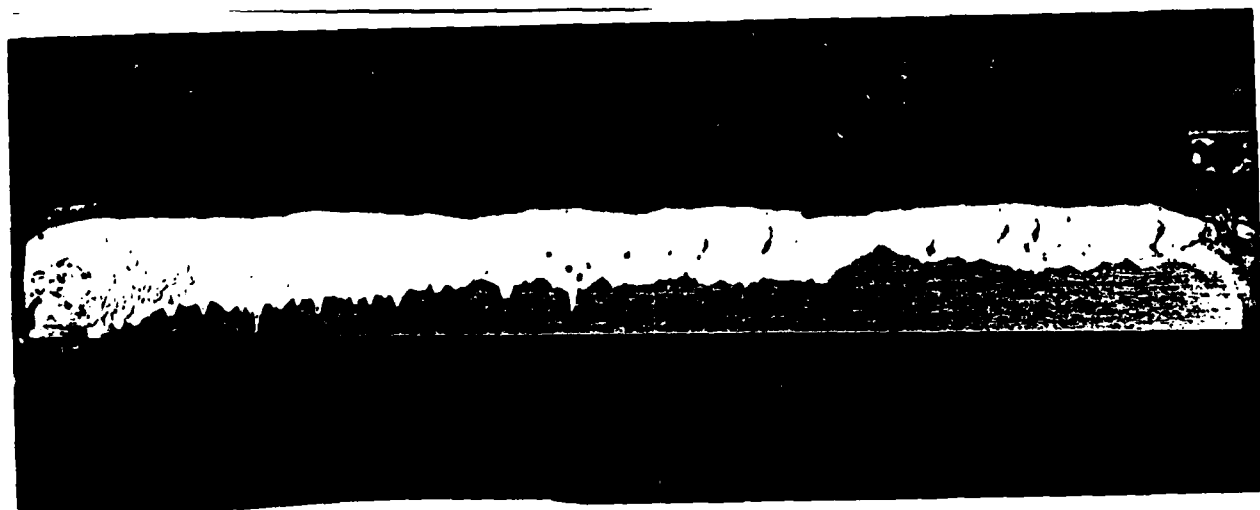
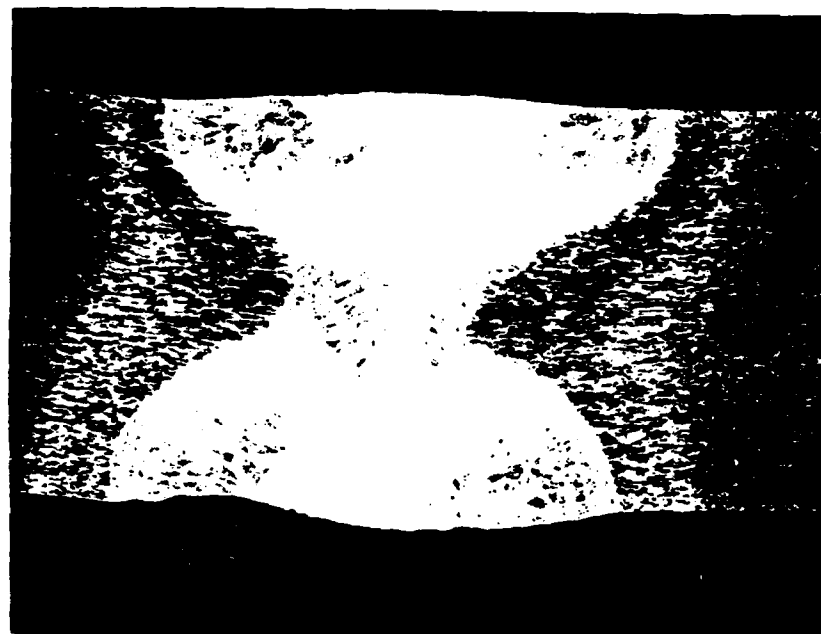
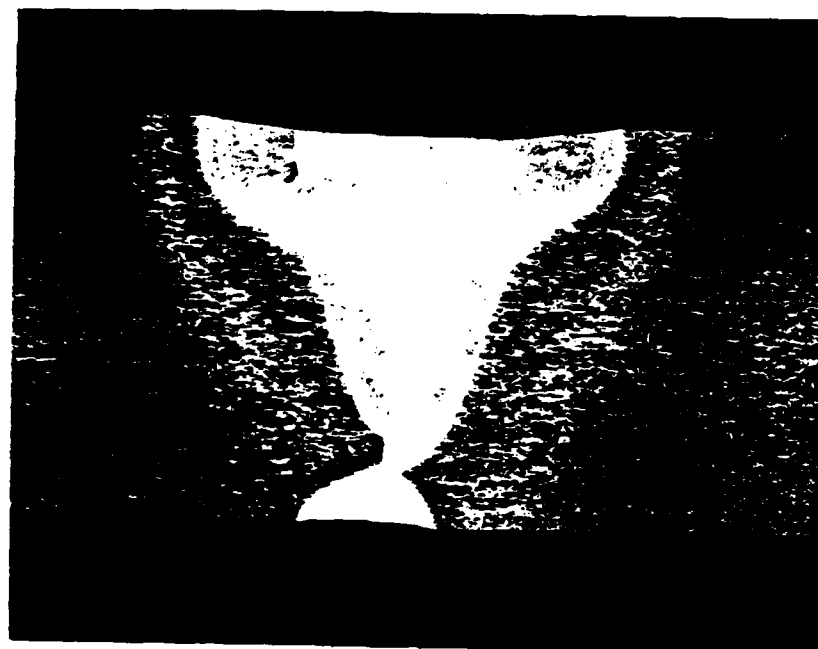


Figure 12. Longitudinally cut macrosections of aluminum bead on plate laser welds showing effect of speed on weld penetration. Note that porosity is minimal at apx 30 IPM. Non-uniform penetration is due partly to the shifting of the weld puddle. Mag. 1.6X.





BEAM: Annular f/18      MICOM Shield   GAS FLOW RATE: 150 CFH  
 KW: 10   WELD SPEED: 30   FOCUS: Optimum   MATERIAL: 3/8" 2219



BEAM: Annular f/18      MICOM Shield   GAS FLOW RATE: 150 CFH  
 KW: 10   WELD SPEED: 40   FOCUS: Optimum   MATERIAL: 3/8" 2219

Figure 10. Macrosections of aluminum laser welds.  
 Top 2-pass butt weld; Bottom 2 pass bead on plate.  
 Mag 6X

experience with this alloy has shown that frequent macro-cracking occurs when welding this alloy using conventional welding processes.

## 2. Travel Speed

The effect of weld speed is illustrated in Figures 8, 11, 12, and 20. Figure 12 is a longitudinal cut weld which was made by adjusting speed of travel during the weld run. The variation in penetration is due at least partly to an irregular displacement of the weld bead root from side to side during welding.

## 3. Shielding Gas

Effects of shielding gas mixtures and flow rates are shown respectively in Figures 9 and 17. A 200 cfm flow rate is apparently best. This can only be explained by the probability that more of the plasma above the weld puddle is being blown away clearing the path for the beam to reach the workpiece. Figure 10 illustrates weld passes made from either side. The top illustration is an actual butt weld. Note at this point that the welds made using the f/18 lens and annular beam produce welds similar in bead shape and appearance to welds made by the automatic GTAW process.

## 4. Lens-to-Work Distance

The effect of lens to workpiece distance is illustrated in Figures 13, 18, and 19. An increase of 4/8 in. with the f/18 lens appears to be the critical point which affects weld size. This is an advantage in production in that minor variations in height of the workpiece can be tolerated.

## 5. Effect of Alloy Types

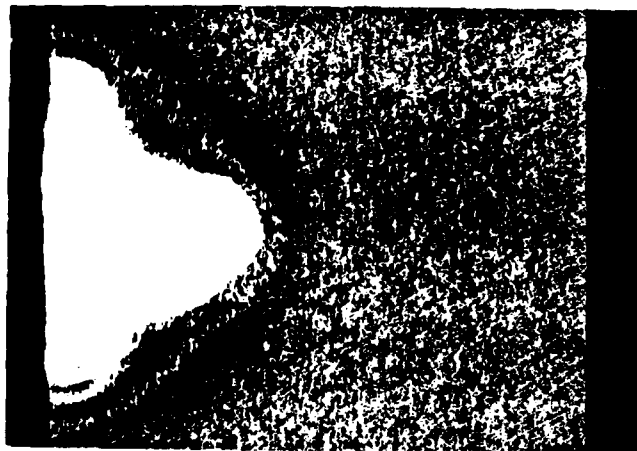
As shown in Figure 14, the effect of varying alloy types was not detectable.

## 6. Effect of Weld Energy

Effect of change in weld energy is also illustrated in Figure 14. A power level of 8 kw at 40 ipm produced deeper penetration than a power level of 6.5 kw at 20 ipm, though the melt area was greater with the latter. This is not surprising since the greater heat input in the latter case (due to the slower speed) is expected to produce more melt area. For a constant speed, the depth of penetration is a function of beam power, assuming all other parameters are held constant (Figure 16). Cracking tendency of 7075 aluminum is a problem when welding this alloy under conventional welding conditions, but the situation is aggravated under faster freezing conditions as evidenced by improper starts and stops when welding with a conventional MIG or TIG process. Figure 16 left and center illustrates cracking due to fast freezing conditions. The center bead probably cracked due to the porosity indicated by the large cavity, which is conducive to cracking and aggravated by its location where initial freezing occurs.

## 7. Interactive Effect of Weld Travel Direction and Shielding Gas Flow Direction

The basic travel direction, in which the weld work piece moves in the opposite direction to the shielding gas jet flow, produces a deeper weld bead than is obtained when the work piece moves in the same direction as the jet flow.



200 He, 0 Ar

BEAM: Annular f/7

KW: 10

SHIELD: MICOM Shield

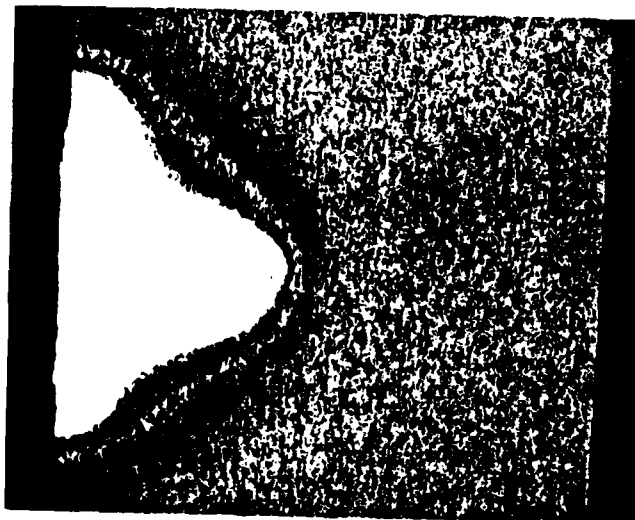
WELD SPEED: 40



150 He, 50 Ar

GAS FLOW RATE: 200:150:180 Ar 0:50:20

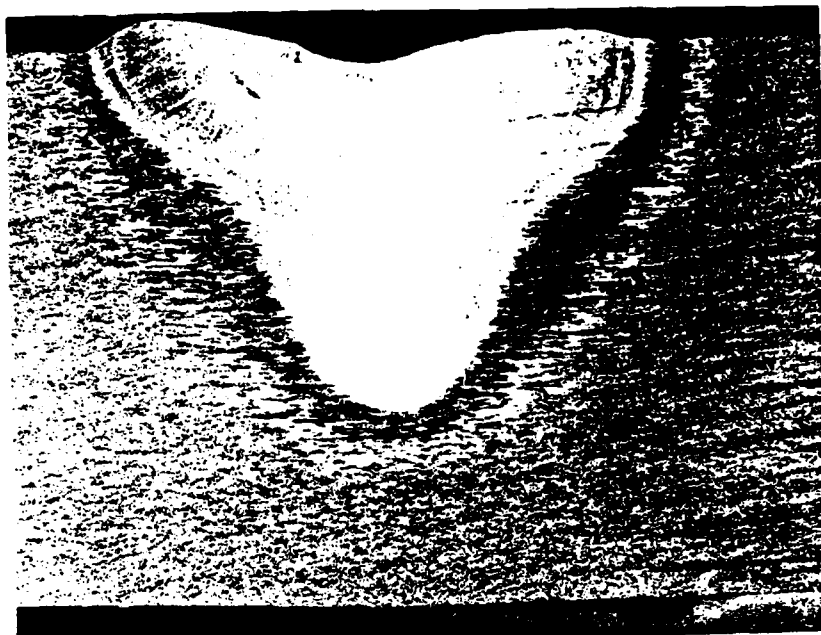
FOCUS: Optimum



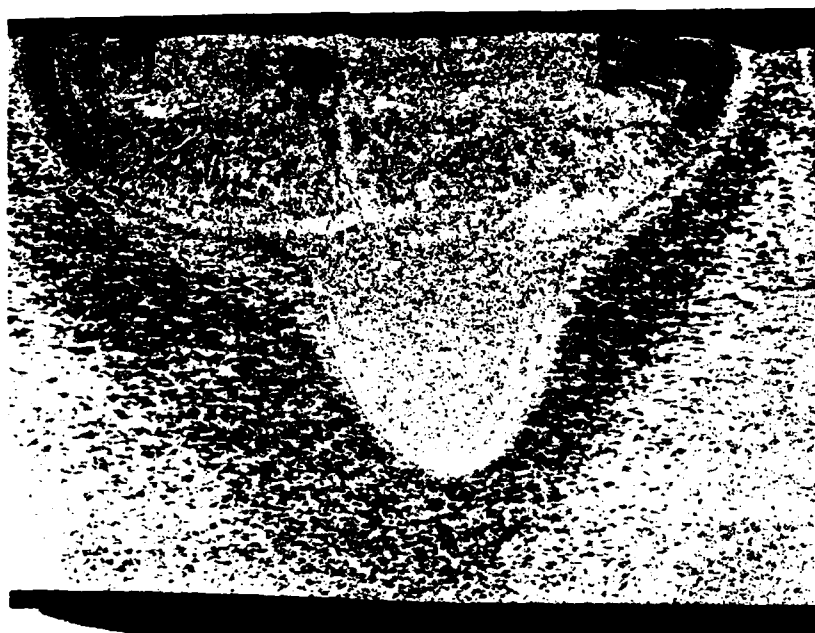
180 He, 20 Ar

MATERIAL 1/2" 2219

Figure 9. Macrosections of bead on aluminum plate laser welds showing the effect of helium and Ar gas mixture proportions on weld heat input and bead shape. Mag 6X.



BEAM: Annular f/18 SHIELD: Conventional GAS FLOW RATE: 150 CFH  
 KW: 10 WELD SPEED: 20 IPM FOCUS: Optimum MATERIAL: 2219



BEAM: Annular F-18 SHIELD: MICOM SHIELD GAS FLOW RATE: 150 CFH  
 KW: 10 WELD SPEED: 20 IPM FOCUS: Optimum MATERIAL: 2219

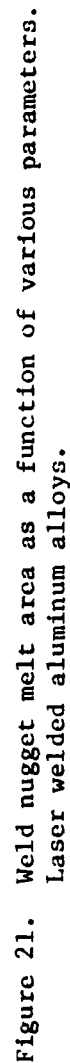
Figure 8C. Macrosections of bead on aluminum plate laser welds showing the effect of travel speed on weld heat input and bead shape. Mag. 6X.

a reliable and productive process. Although porosity was still prevalent in aluminum weldments, tensile tests indicated an acceptable strength level achievable (compares with the TIG process). Further development work is needed to additionally refine the process, both from the standpoint of improved weld bead shape and internal quality. This may possible be achieved by experimenting with travel speed, weld groove configurations, angle of beam to work incidence, twin beam technique or other techniques.

The development of an improved welding shield is a significant contribution of this program effort. Again, additional development is needed to optimize weld quality. This may best be pursued through changes in cavity geometry. The obstructive reflectance characteristic of aluminum which has previously deterred its weldability with a laser was at least partially countered by improved optimization of welding parameters and through the development of a reflective shield.

#### G. Recommendations

In order to perfect the laser welding of aluminum process, a follow-up study of the mechanics of the process itself should be made. The behavior of the beam as it strikes the workpiece, the formation of the plasma and its dispersal or removal, the weld puddle behavior, should all be studied in detail, possibly through high speed photography. Observations should be made under varying conditions, such as varying gas shielding flow rates, bead on plates vs square butt and a range of V-groove angle configurations, different laser beam configurations and focal lengths, off focus positions, welding speeds, angle of beam to workpiece off the conventional 90° position, etc. It is believed that if the turbulence of the puddle could be eliminated, weld quality would be enhanced. Welding in the keyhole mode bears this out.



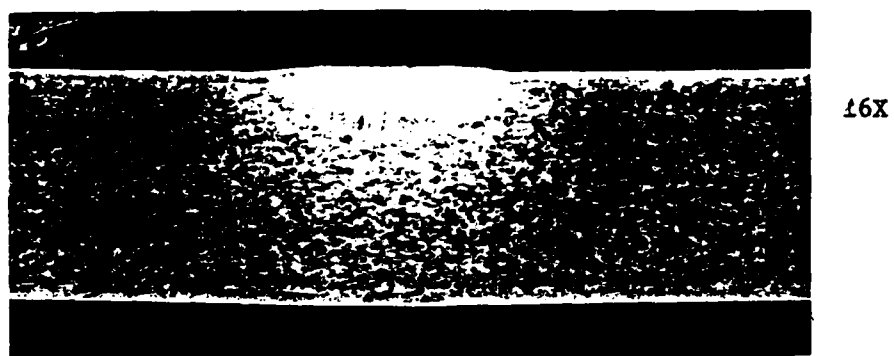
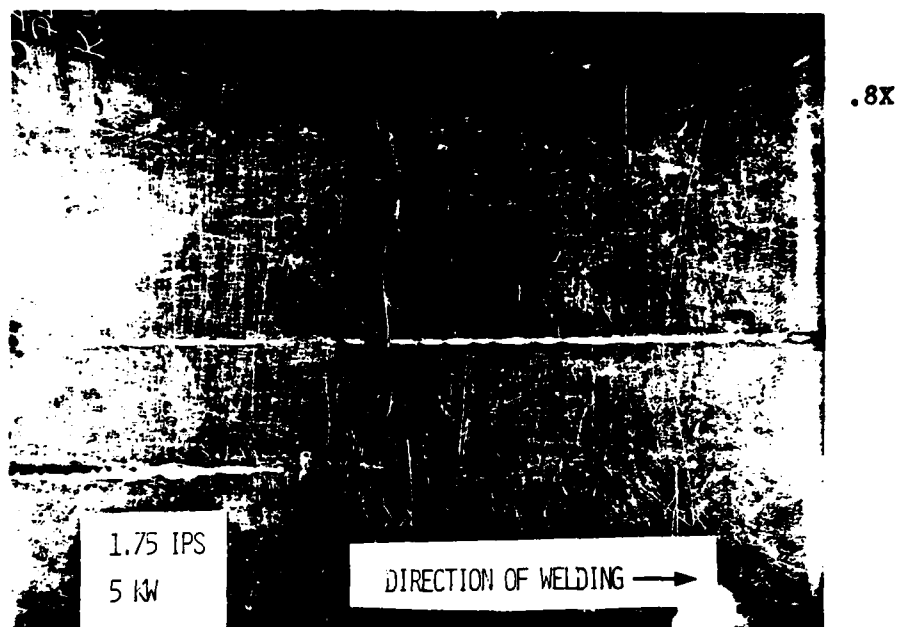
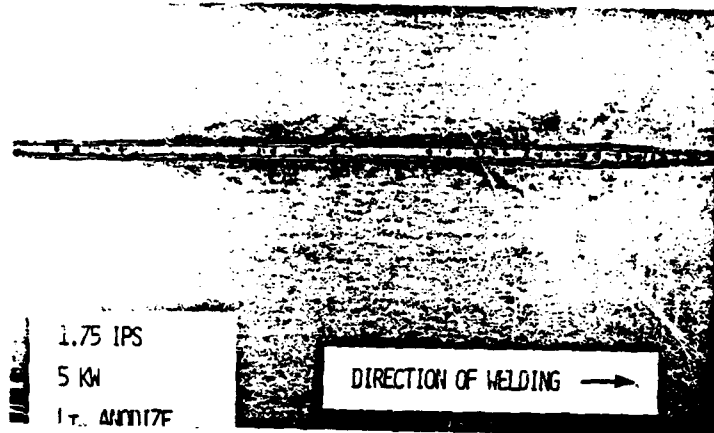
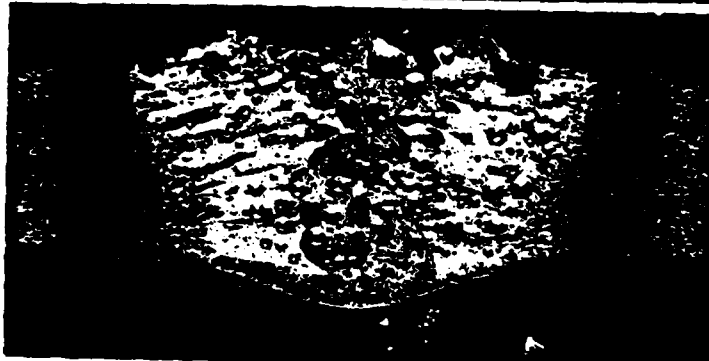


Figure 22. .080 inch thick clad aluminum laser weld pass,  
105 IPM 5 KW.

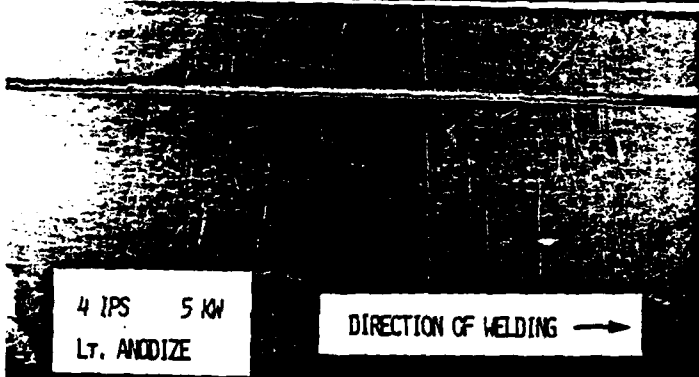


.8X

Light anodized .080 in. thick  
aluminum sheet laser weld pass  
105 IPM 5 KW

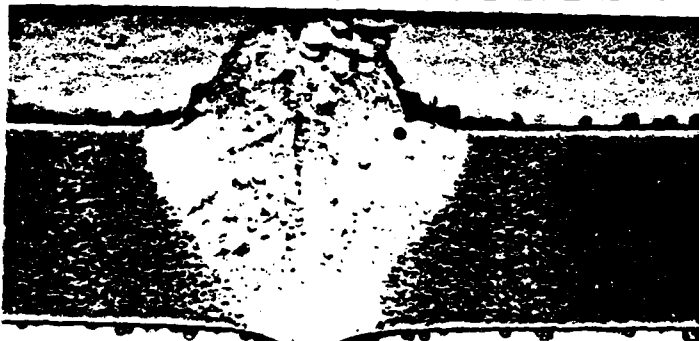


16X



.8X

Light anodized .080 inch thick  
aluminum sheet laser weld pass  
240 IPM 5 KW



16X



## APPENDIX

I.	INTRODUCTION . . . . .	86
II.	LASER WELDING SYSTEM . . . . .	86
	A. Equipment. . . . .	86
	B. Automation of Laser Welding Operation. . . . .	108
	C. Operation & Integration of System. . . . .	108
	D. Welding System Operation . . . . .	108
III.	EQUIPMENT DEVELOPMENT. . . . .	124
	A. Power Control. . . . .	124
	B. Automatic Laser Control. . . . .	124
	C. Mirror Alignment . . . . .	128
	D. Gas Shielding . . . . .	131
	E. Welding Table Stability. . . . .	131

## APPENDIX

### THE MICOM 50 KILOWATT LASER WELDING SYSTEM

#### I. INTRODUCTION

The laser adapted for this laser welding project was a 50 kw peak output CO<sub>2</sub> laser device designed and developed as a prototype mobile weapon test system. Converting this laser for welding involved optics design, initial testing to establish operating characteristics, equipment redesign and development to increase output power stability to achieve consistent weld quality, and automation of control functions to reduce manpower requirements for welding operations. The total laser welding system consists of the high power CO<sub>2</sub> laser and the following subsystems: vacuum, gas, cooling, power, controls, and welding accessories. The interconnection of the system is shown in Figure 1, and the equipment layout is shown in Figure 2.

#### II. LASER WELDING SYSTEM

##### A. Equipment

**High Power Laser** - The high power laser (HPL) shown in Figure 3 is a continuous wave, CO<sub>2</sub> laser which radiates in the far infrared at a wavelength of 10.6 microns. The transverse flow laser features mutually perpendicular gas flow, electrical discharge, and optical axis. This design shortens the dwell time of the lasing gas in the optical cavity, providing the conditions necessary for higher energy density. The HPL utilizes the ionizer-sustainer concept. Lasing is initiated by a low power, broad beam ionizer that irradiates the optical cavity. The main, or sustainer, electrical power is delivered to the conducting gas, resulting in a uniform, controllable discharge.

**Vacuum** - The vacuum system consists of a roughing pump (Figure 4) and a turbomolecular pump, which is a 16 stage ion pump that operates at 16,000 rpm capable of achieving  $10^{-9}$  torr in the E-beam cavity. When the laser is operating, the E-beam conduction reduces the vacuum level in the E-beam cavity during lasing operations. When the E-beam vacuum drops to  $4 \times 10^{-5}$  torr lasing operation must cease to prevent high voltage arcing.

**Gas System** - The gas system consists of a supply of carbon dioxide (CO<sub>2</sub>), carbon monoxide (CO), nitrogen (N<sub>2</sub>), and helium (He), (Figure 5). The gases are blended and circulated through the laser sustainer cavity with a Roots blower. The gases are then vented into a 55 gallon barrel to extract glycol before escaping into the atmosphere. The laser has the capability of operating with a closed gas system, but it has not been used in that manner during welding operation. Laser gas is usually supplied in large volume because of the quantities used during operations. The present configuration uses a semi-trailer of carbon monoxide connected to an electrically operated control valve. The carbon dioxide, helium, and nitrogen shown in Figure 5 were available from a trailer, but are now supplied by connecting several large gas bottles to a plenum. Ten bottles of each are connected to a plenum and then pressure regulated prior to connecting to the mixing station shown in Figure 6. At the mixing station all four gases are fed through pressure regulators with input and output pressures monitored before passing through individual flow meters. After passing through the flow meters, the gases pass into a mixing tank where they blend to become

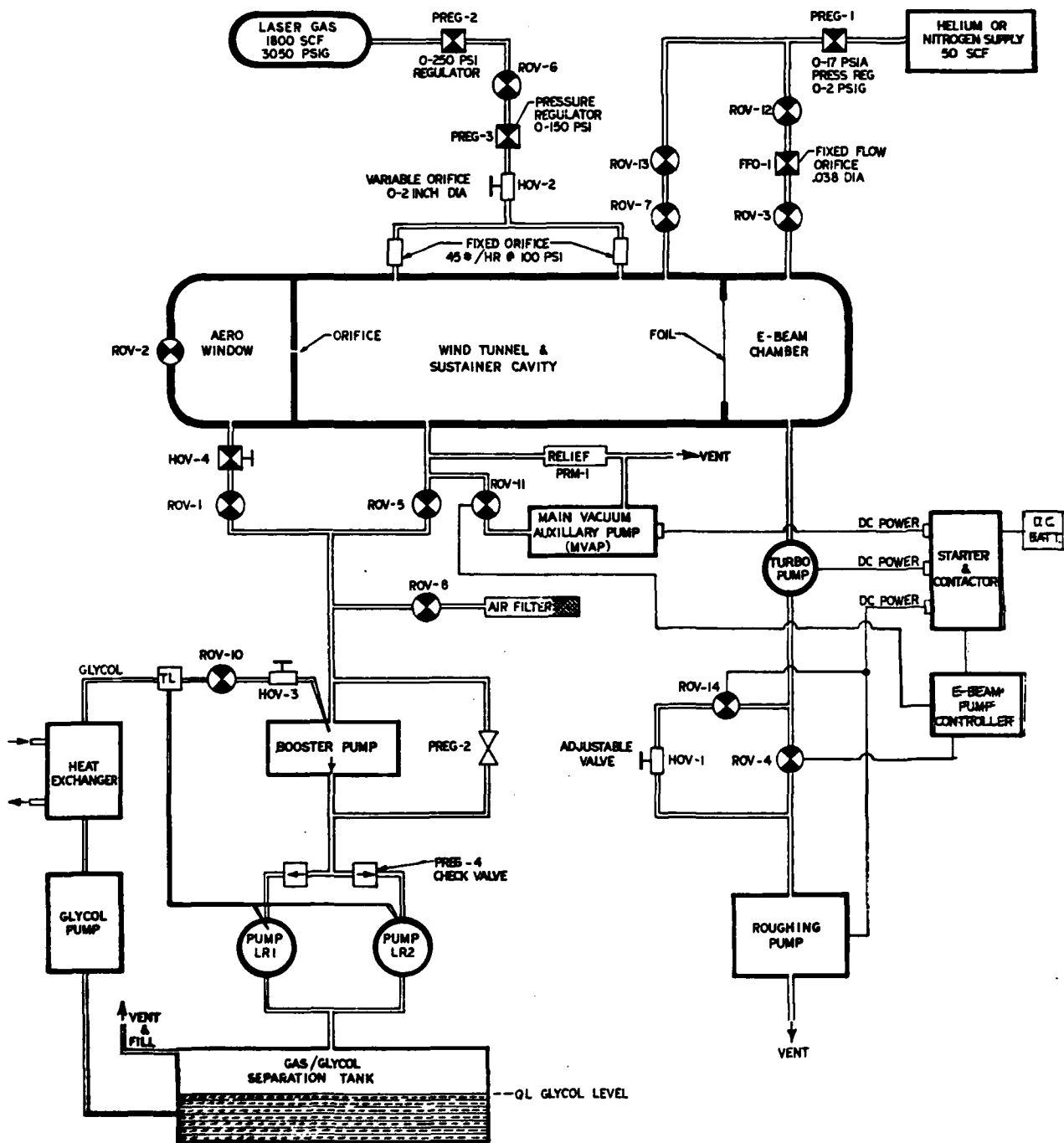


Figure 1. Laser system interconnect diagram

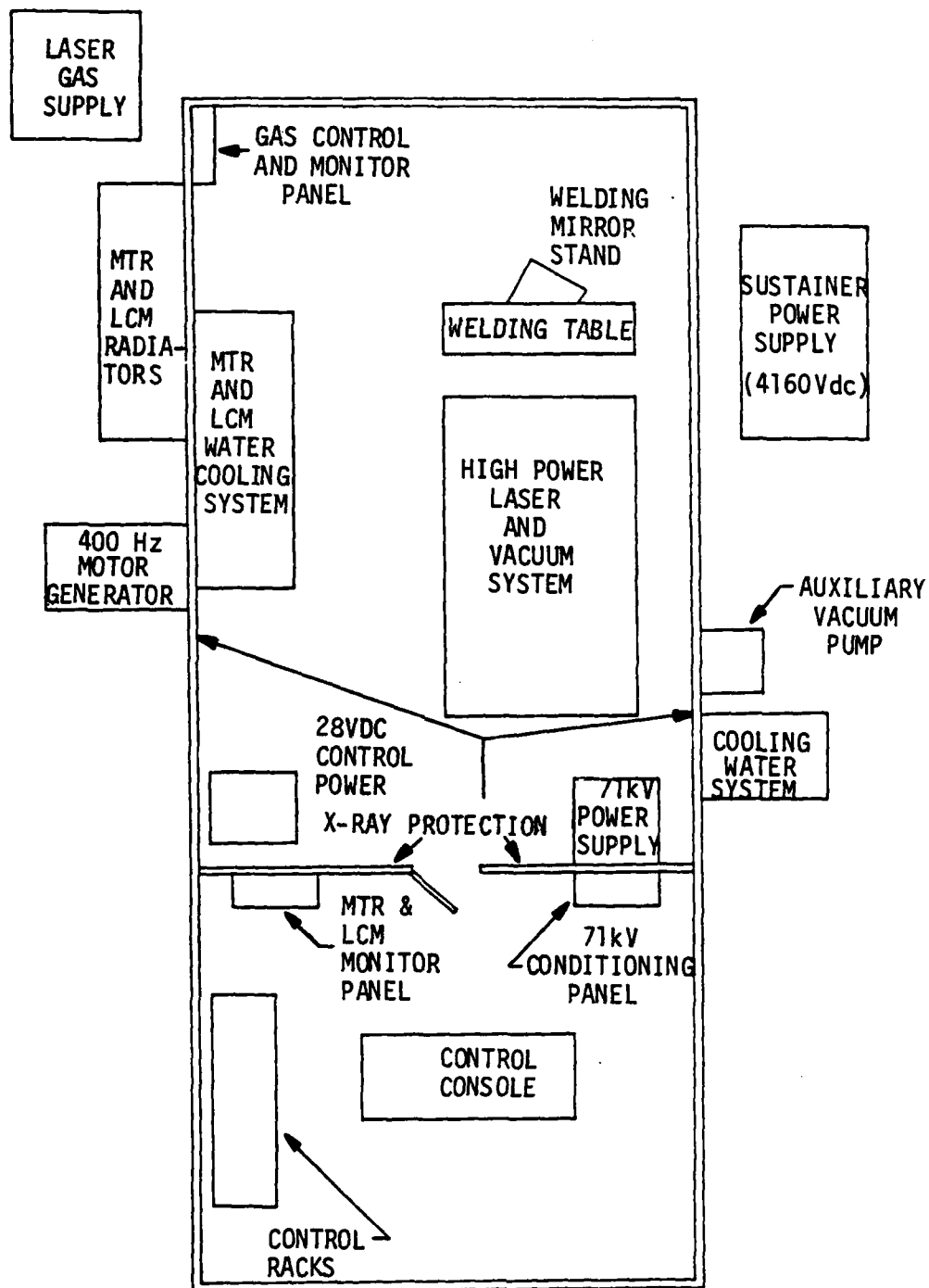


Figure 2. Equipment layout

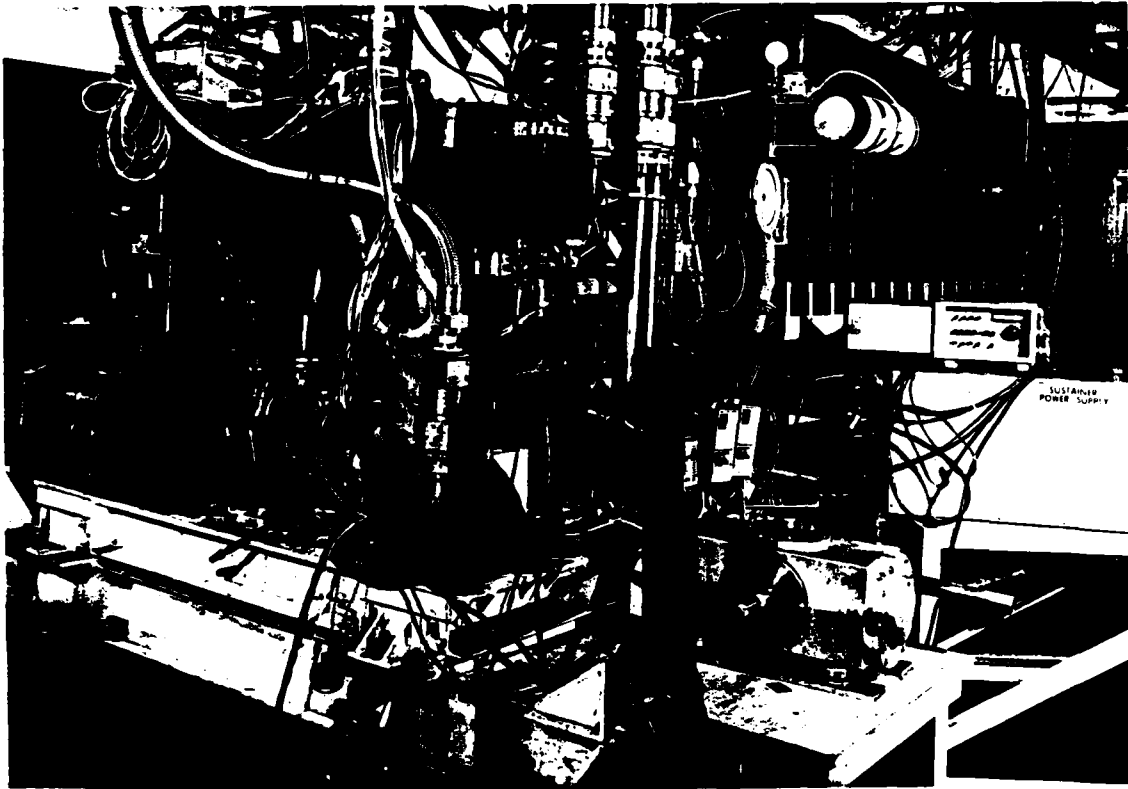


Figure 3. Laser - Aerowindow view

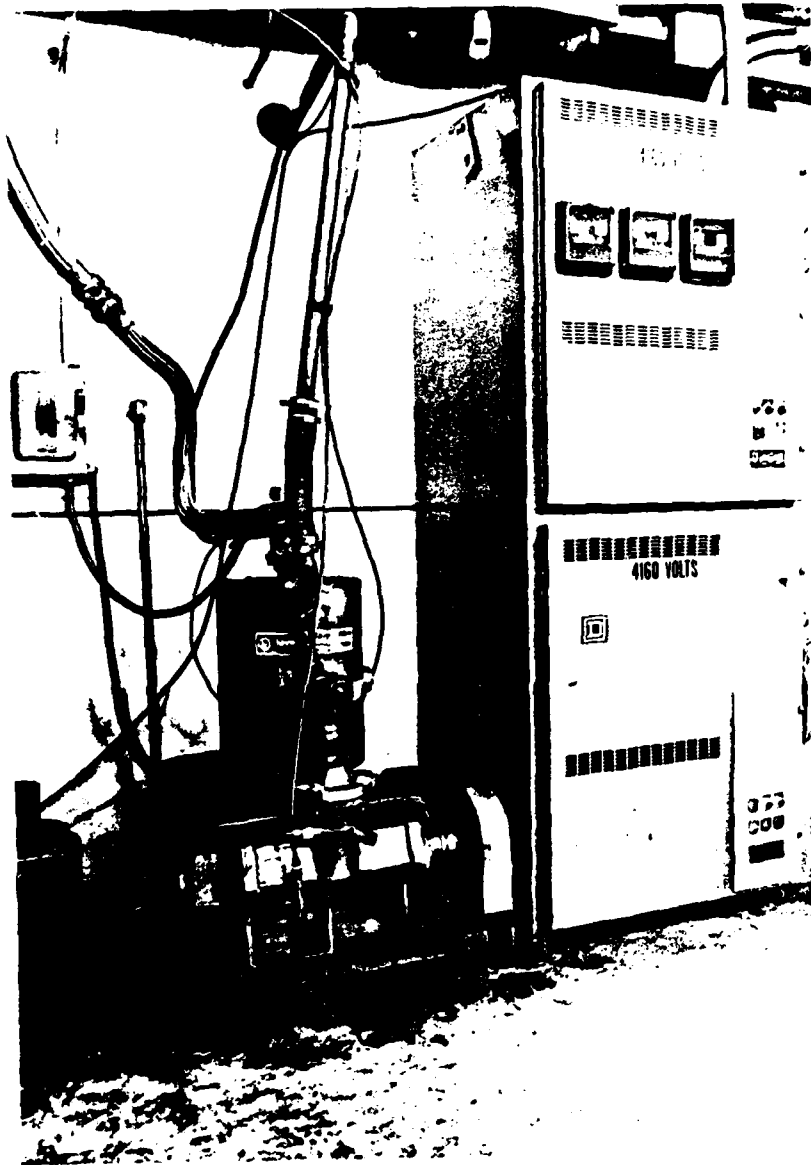


Figure 4. Kinney pump and 4160 Vdc power panel

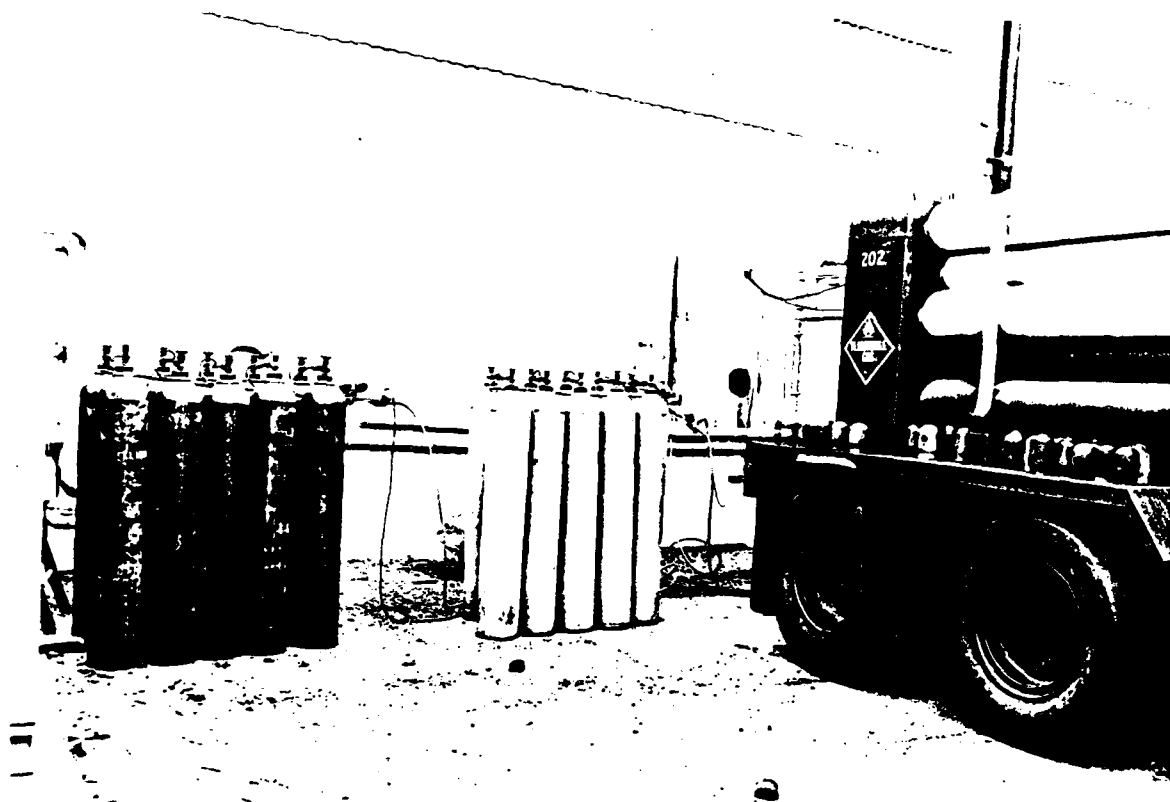


Figure 5. Gas supply setup

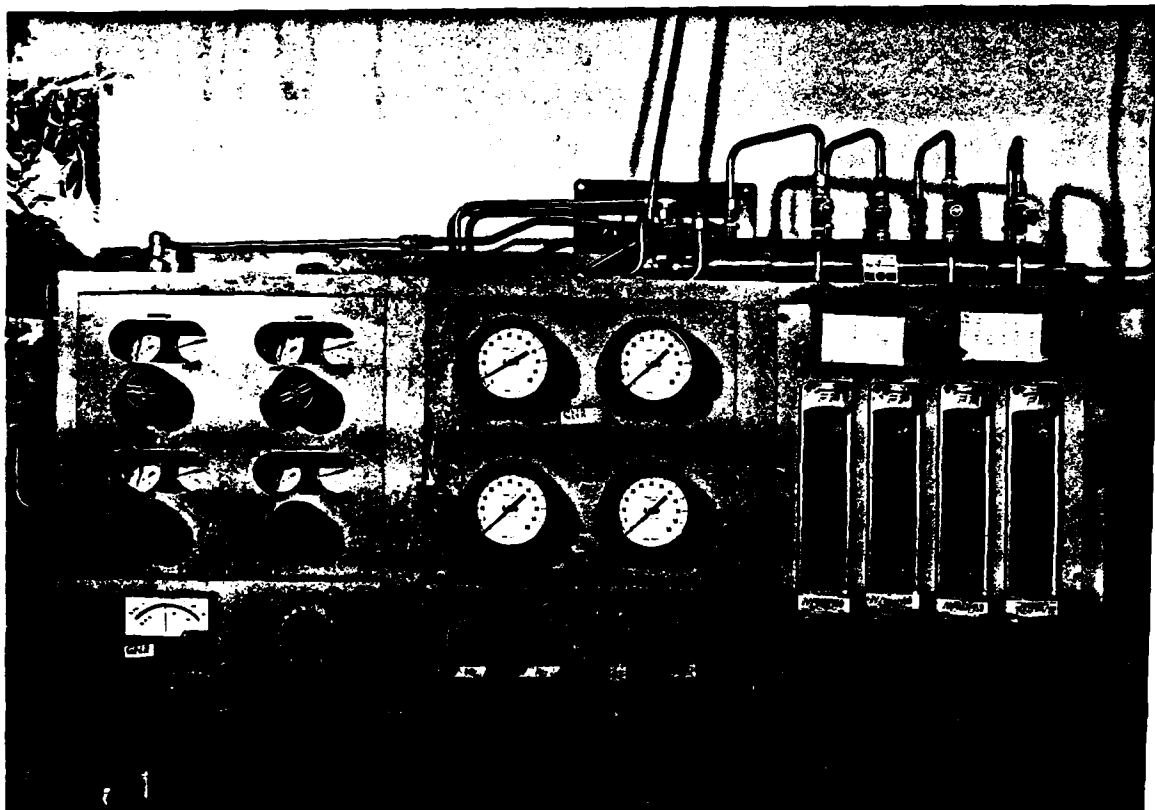


Figure 6. Gas control panel



the laser gas. The flow meters are adjusted for the following flow rates in cubic feet per minute: CO<sub>2</sub>, 130; CO, 130; He, 777; and N<sub>2</sub>, 518. These flow rates give a mixture of CO<sub>2</sub>, CO, N<sub>2</sub>, and He in a ratio of 1:1:4:6 respectively. This mixture is pumped through a line to the sustainer cavity by the Roots blower. The gas mixtures flow through the sustainer cavity when the gas valves at the supplies are energized and the Roots blower is operating. The operating cost of gas is approximately \$150 per hour which provides about 6 minutes of lasing. Therefore, the gas should not remain flowing if an interval of 5 minutes or more exists between runs.

**Cooling System** - The water cooling system is composed of two circulating systems: The Laser Cooling Module (LCM) and the Mirror Temperature Regulating Module (MTRM). The MTRM cools the output mirror, feedback mirror, and focusing mirror located in the sustainer cavity. The LCM cools the sustainer cathode and anode, aerowindow, and the heat exchangers on the laser. The cooling water is demineralized with a Culligan water conditioner system. A supply tank is associated with the purification system to hold a supply of the demineralized water. The quality level is monitored by a Culligan megohm/cm meter that has a sensor in the water line going to the E-beam filaments. The resistivity of the water must be high to prevent arcing of the high voltage to the water line. All water connections for cooling the E-beam filament supports are grounded to protect against arcing problems. Arcing within the E-beam cavity to the copper cooling line will cause a rupture of the line and a loss of coolant within the cavity.

**Control System** - The control system shown in Figures 7 through 12 monitors and sequences all laser operations. The design of the system has sufficient automation to permit one man operation. Most control functions are centered at a control console with the welding activity being monitored by closed circuit television.

During a controlled operation, the 400 Hz power is activated first so that the necessary pumps can operate when activated by the control console. Cooling functions are activated next, and flow rates and temperatures of coolants are monitored before proceeding to set up the laser. The vacuum system is converted over from standby equipment to on-line equipment as the next control function. While the vacuum system is stabilizing, a feedback mirror system is activated to accurately control output power for consistent weld penetration.

The laser gas is turned on by the operator at the control console when the sustainer cavity inlet pressure is below 4 torr. While the gas is stabilizing, the 4160 Vdc power supply is energized at the source but not turned on at the control console. The gas flow rates are given a final check and all personnel in the laser area move to the control console area.

The 71,000 Vdc power supply is activated at the console to permit the E-beam cavity to generate a cloud of electrons when the lasing mode is activated, then the 4160 Vdc is activated to prepare the sustainer cavity for lasing. All pre-preparation control steps are completed. With the desired power level set at the console, the laser can be switched on and off by manual control or with remote control established at the welding table. If an automated welding test is desired, the welding table has the necessary controls such that once it is put in motion, it can turn on the laser and shield gas and terminate the test at a preset location.

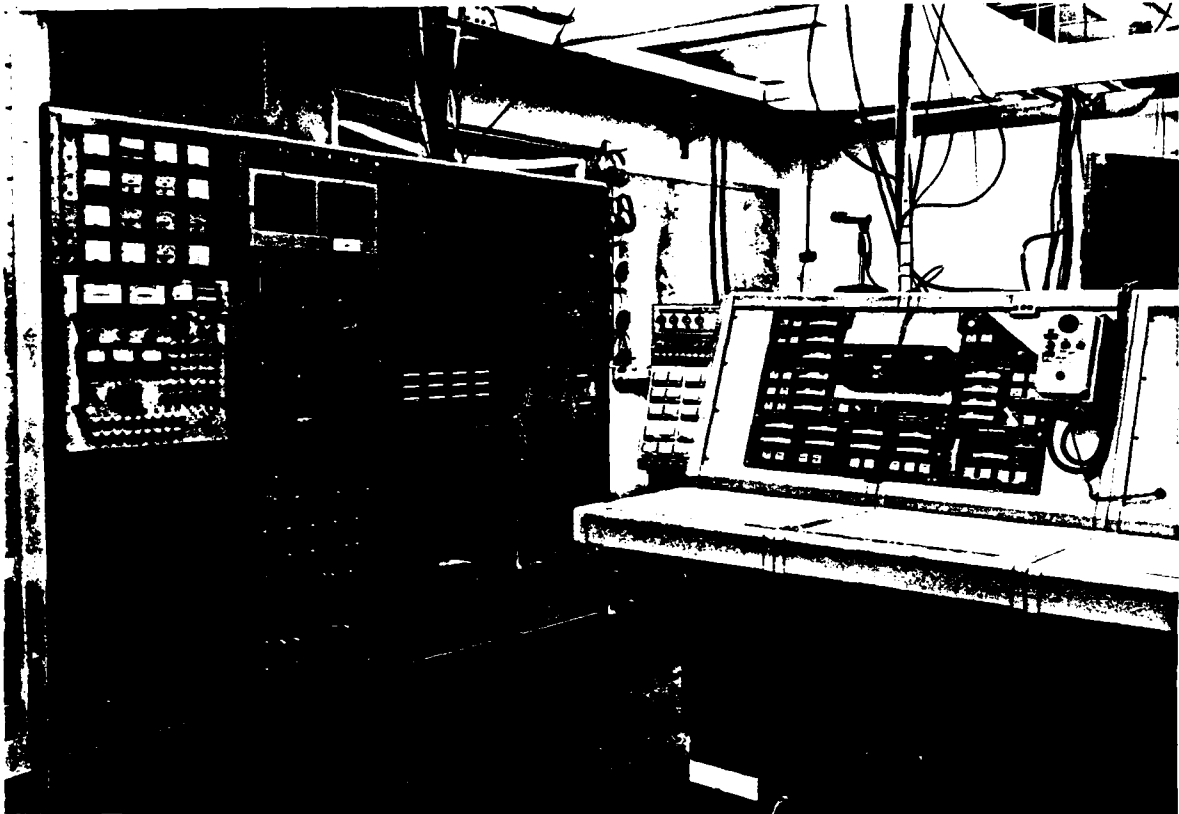


Figure 7. Control system

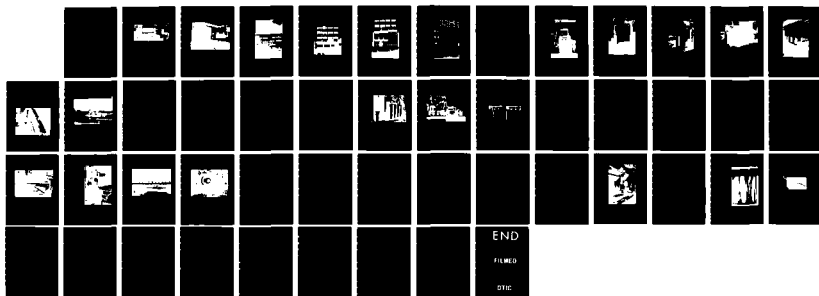
AD-A158 082 MANUFACTURING METHODS AND TECHNOLOGY APPLICATION OF HIGH ENERGY LASER WEL. (U) ARMY MISSILE COMMAND 2/2

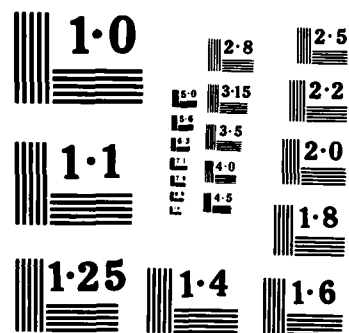
NL

UNCLASSIFIED

J V MELONAS  
F/G 20/5

**UNCLASSIFIED**





NATIONAL BUREAU OF STANDARDS  
MICROCOPY RESOLUTION TEST CHART

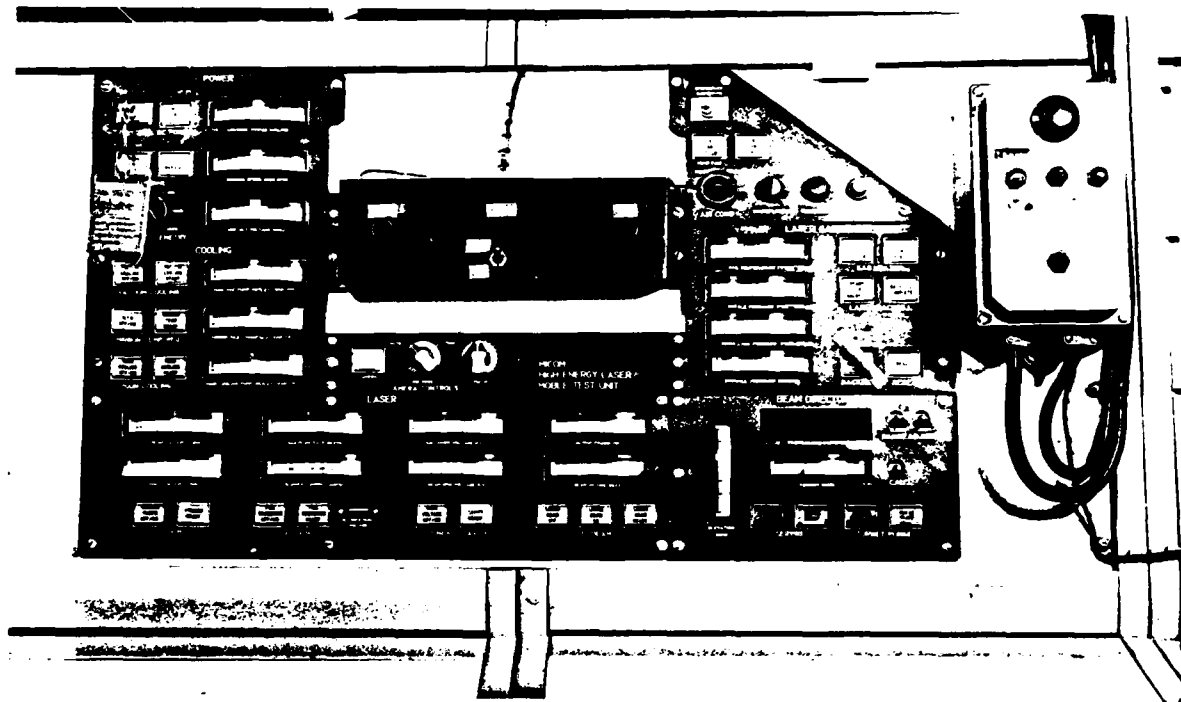


Figure 8. Control console panel

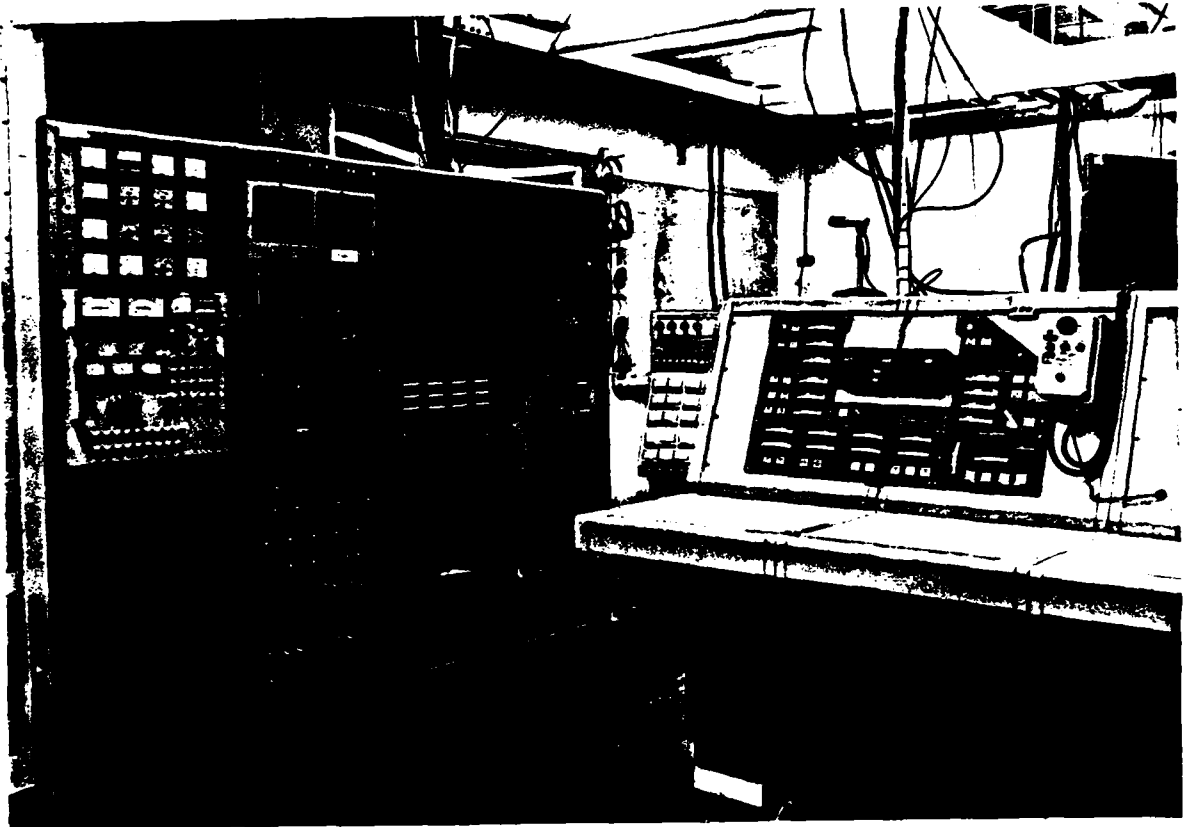


Figure 7. Control system

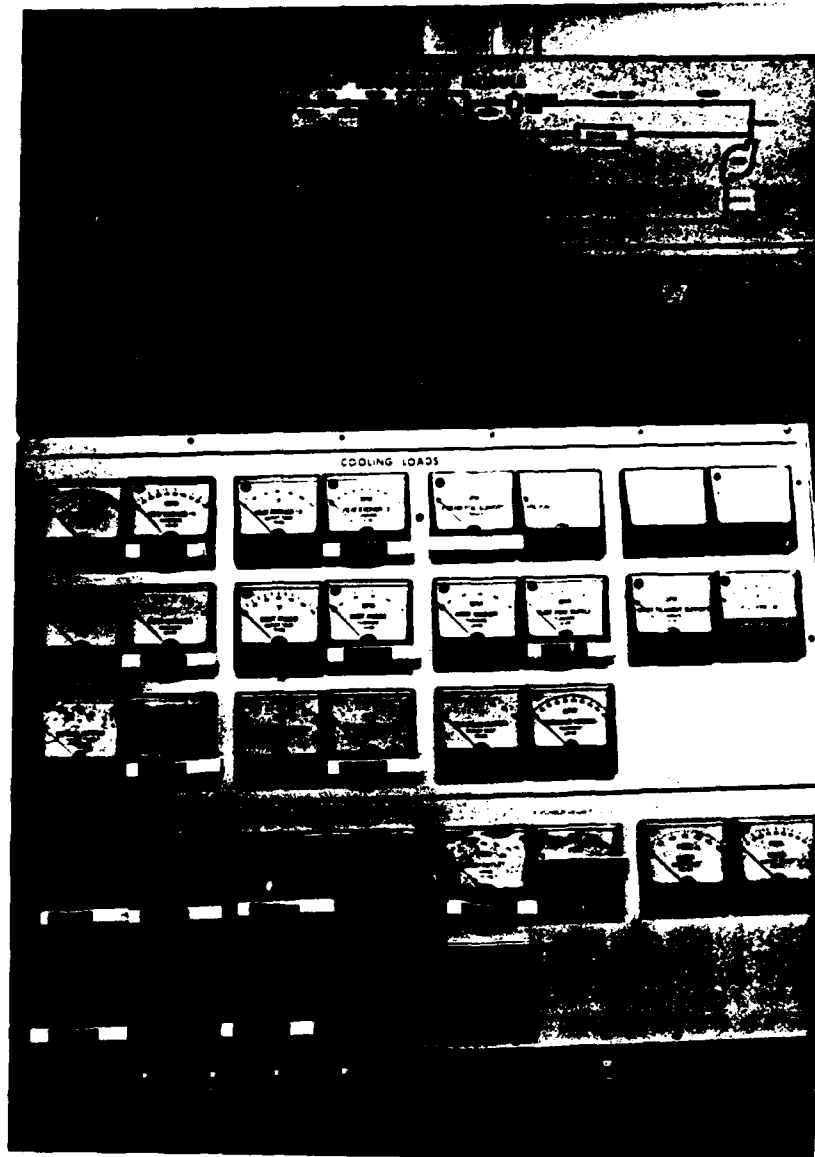


Figure 9. Coolant monitoring panel



Figure 10. Vacuum monitoring panel



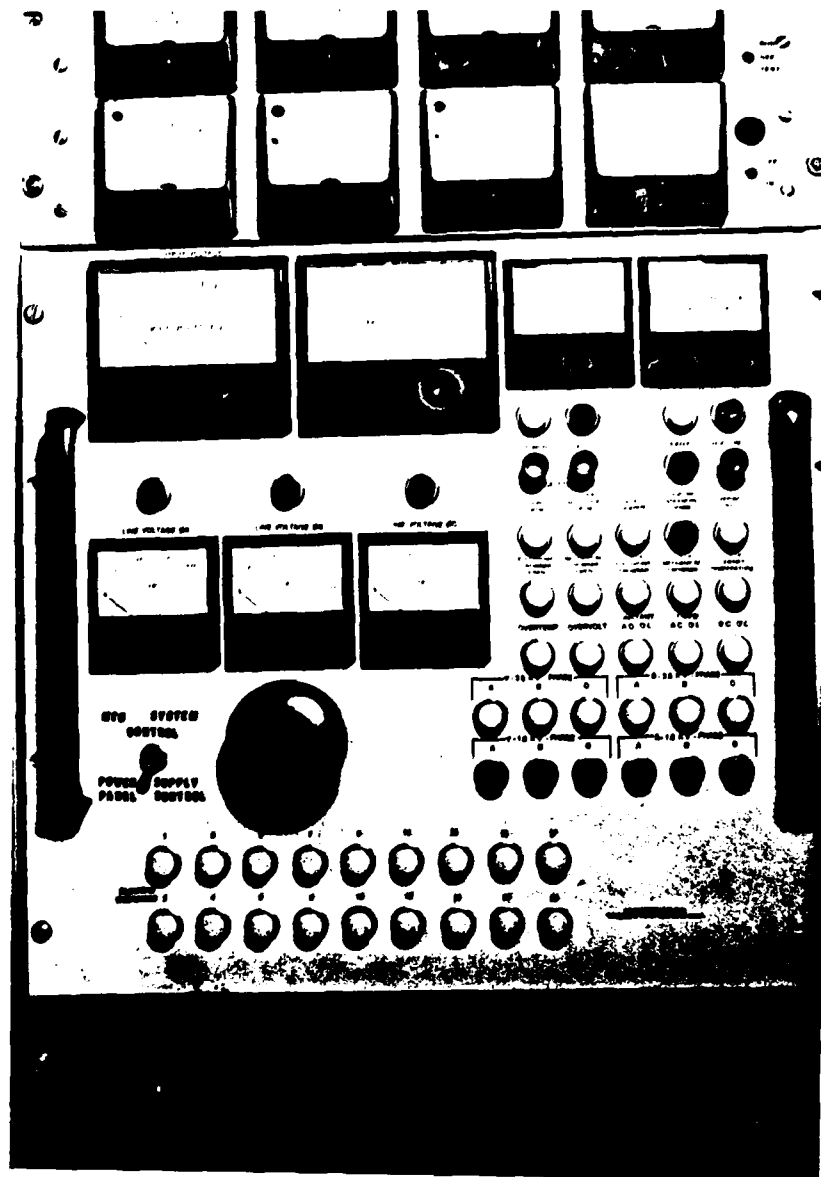


Figure 11. Sustainer power supply



Precaution should be taken to remove the high voltages after a welding operation. After witnessing the welding operation on closed circuit television, the operator usually needs to make a new set-up or discontinue operation. It is essential that the laser and both high voltage power supplies be off prior to entering the laser room. As an additional precaution, the filaments to the E-beam cavity should also be off. When the last weld is completed, the laser shut-down procedures must be followed. Basically, the turn-on procedure is performed in reverse. The gas to the laser is turned off and permitted to pump down. When the inlet pressure to the sustainer cavity is below 4 torr, the vacuum pumps can be switched over to auxiliary, and the main vacuum pump is shut down. As the sustainer cavity is evacuated of gas, the blower shuts down automatically and then all cooling can be turned off. If further testing is to be completed during the day, the remaining controls can be left on. Emergency switches exist on the control panels when time is not permitted for sequential shut-down to take place. This switch should only be used in a real emergency.

**Power System** - Incoming commercial power is 110/208 Vac, 60 Hz and 4160 Vac, 60 Hz. The laser requires 28 Vdc; 208 Vac, 400 Hz; 110/208 Vac, 60 Hz; 4160 Vdc; and 71,000 Vdc. The 28 Vdc power is used for control power and instrumentation. Monitoring equipment such as water purity meters and vacuum gauges requires 110 Vac, 670 Hz. The motors associated with cooling and gas circulation require 208 Vdc, 400 Hz power. The high voltage power supplies also require 208 Vac, 400 Hz and 4160 Vac, 67 Hz. The 71,000 Vdc power supply shown in Figures 13 and 14 is driven from the 400 Hz generator or a turbine driven generator (see Figures 15 and 16) while the higher powered 4160 Vdc power supply (see Figures 4 and 17) is driven from the 4160 Vac line. The high voltage power supplies are not brought on-line until all system check outs are completed. The two high voltage power supplies are sequenced on to obtain the lasing action. The laser area is cleared of all personnel and the access doors are locked before either power supply is activated. The 4160 volt, 100 ampere sustainer power supply is activated first. If this power supply arcs through the gas mixture in the sustainer cavity, a brief lasing action can take place. Extreme precautions must be taken after this power supply is activated. Next, the 71 kv power supply is activated. No lasing action takes place until the E-beam cavity begins conduction unless an arc occurs in the E-beam. Again, a brief lasing action can take place. With normal operation, lasing will not occur until the grid bias of the E-beam cavity is raised above cut-off. The E-beam is held at cut-off with -1500 volts grid bias. The bias is variable to -800 volts where maximum conduction of the E-beam takes place. Most laser output power demands are in the 5 kw to 30 kw range.

**Welding Table** - The laser beam is stationary; therefore, the workpieces to be welded have to be moved on a welding table shown in Figures 18 and 19. A fixture with the capability listed below was modified and adapted for the application.

- Remote-controlled, variable-speed electric motor drive (in both forward and reverse direction).
- Speeds variable from 30 to 300 inches per minute.
- Total travel 40 inches.
- Maximum length of weld 40 inches.
- Movement perpendicular and in line with laser beam.
- Mounting provisions to rotate workpiece 0 to 90°.
- Gas shield to prevent oxidation of workpiece during welding process.

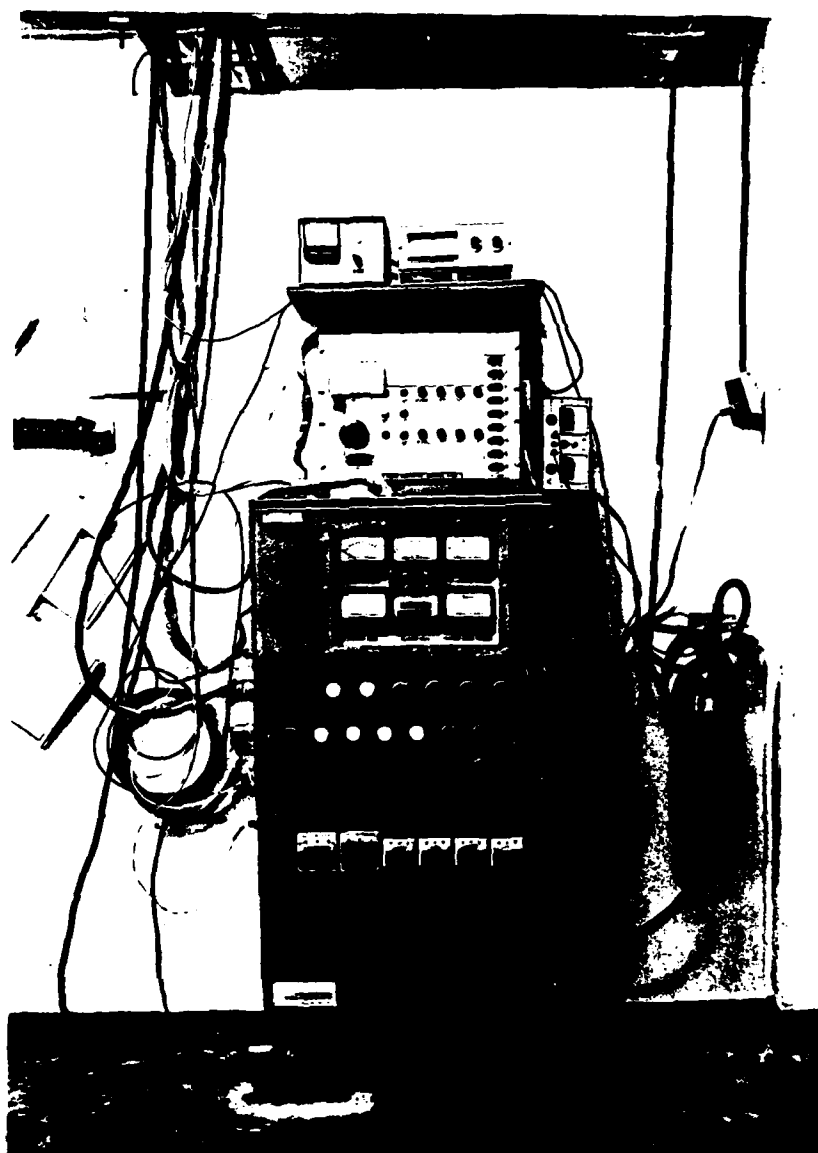


Figure 13. 71 kV control panel

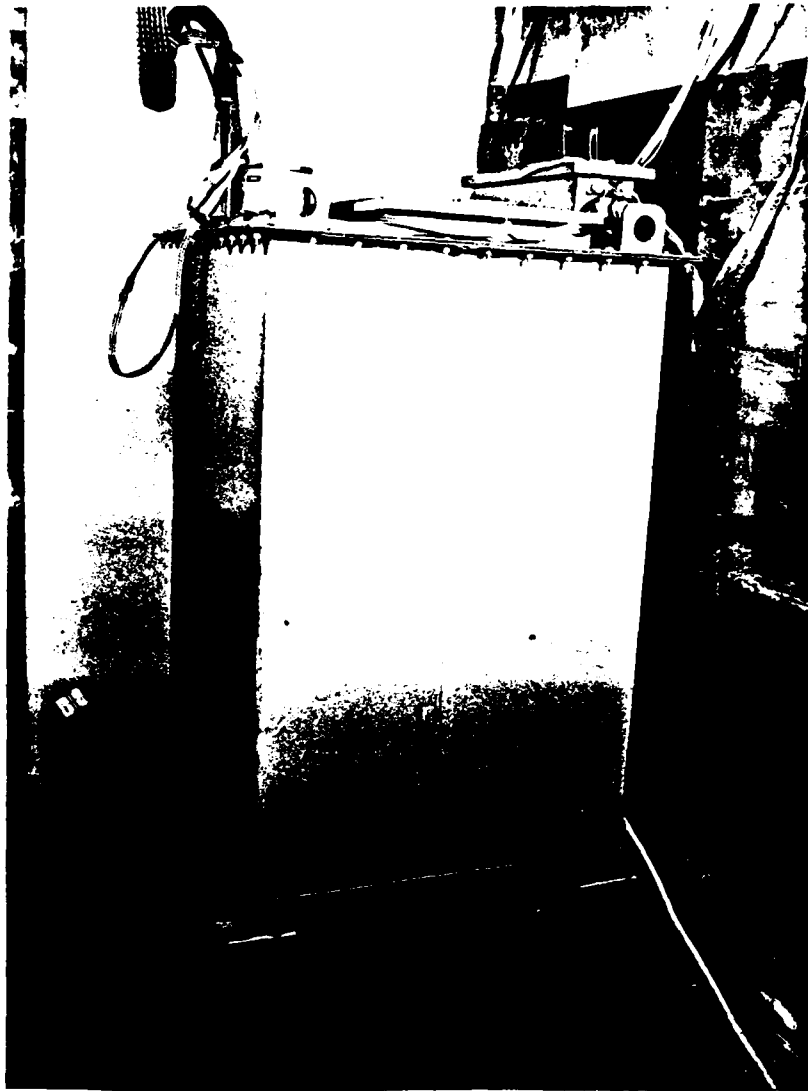


Figure 14. 71 kV power supply

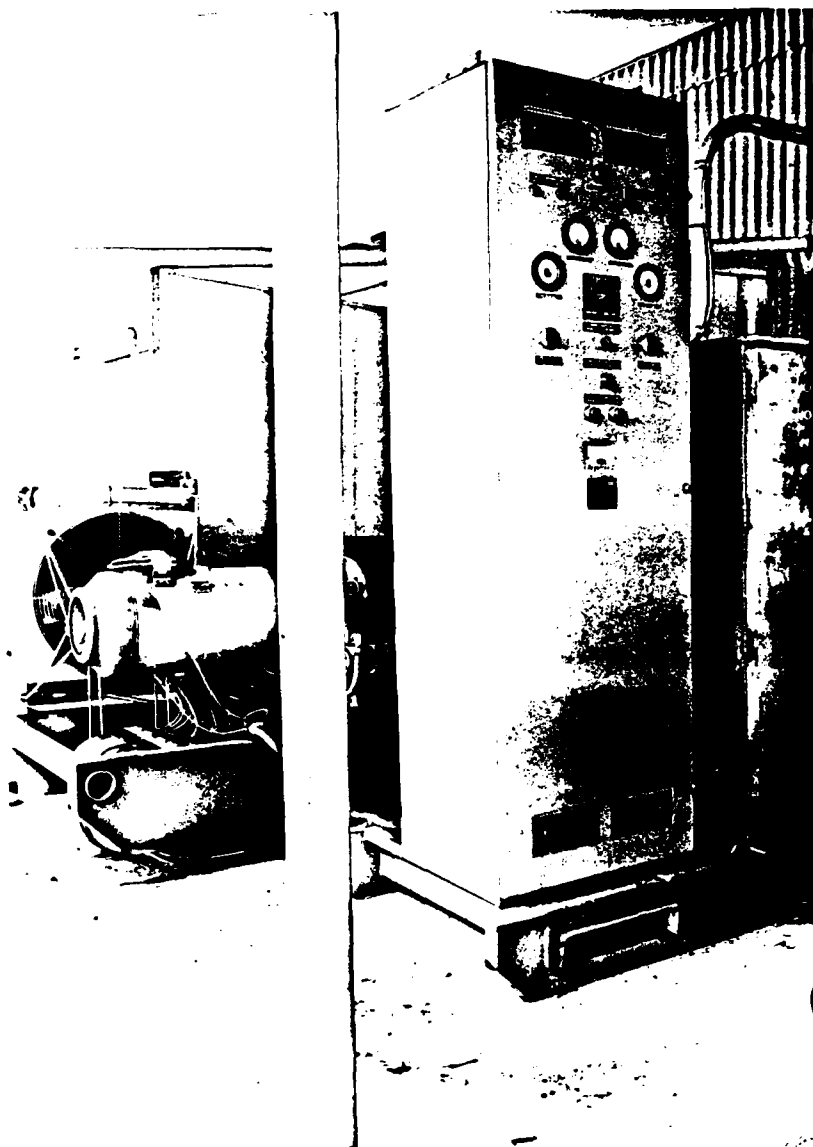


Figure 15. 400 Hz motor-generator

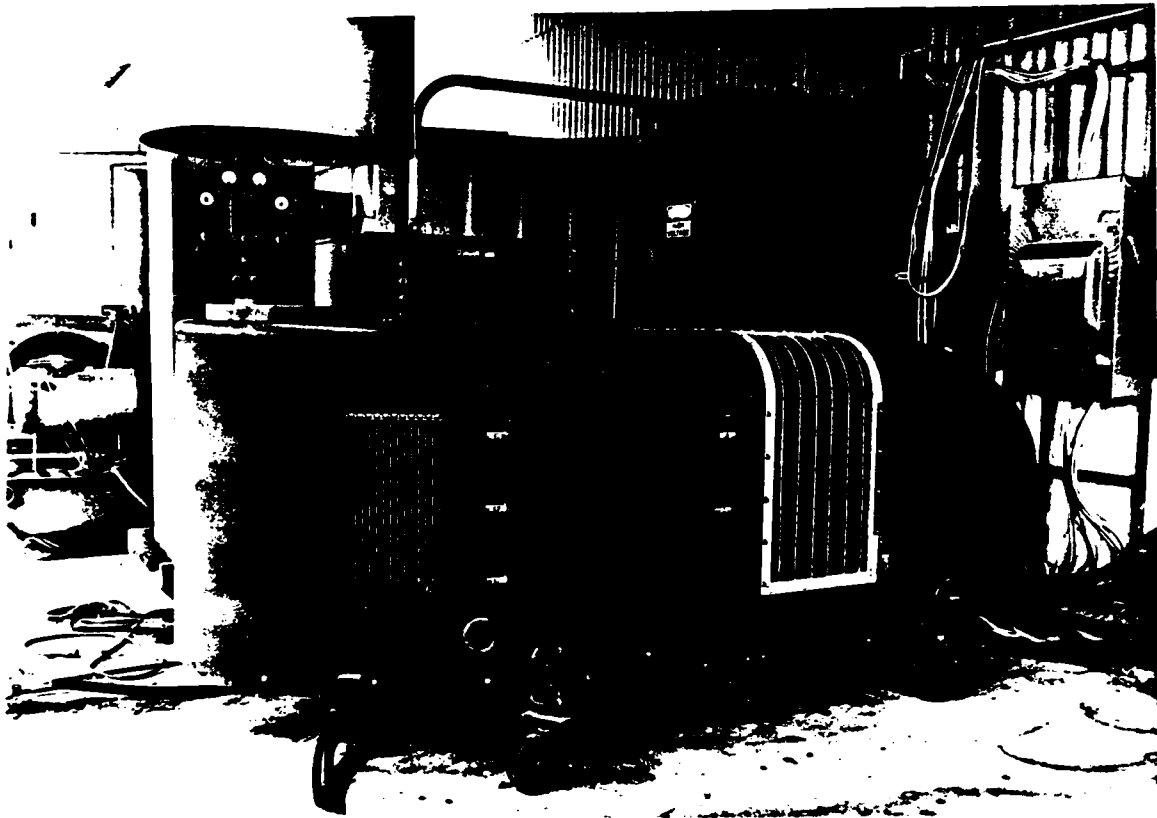


Figure 16. Turbine driven generator



Figure 17. 4160 Vdc power supply



## II. TEST

### A. Control Room

1. E-BEAM PRIMARY POWER: ON
2. BACKFILL RESET switch: RESET
3. H.V.: ON
4. SUSTAINER CAVITY: HIGH VOLTAGE ON
5. GRID ENABLE light: "On"
6. Check voltages as they come up
7. Set ramp level potentiometer to 0
8. Conduct test using E-BEAM LASER BEAM ON and LASER BEAM OFF switches.

D. Control Room

1. Check E-beam cooling water quality
2. E-BEAM PRIMARY POWER: OFF
3. Cooling instrumentation power: "On"
4. MTU DISPLAY DRIVER: SYSTEM POWER ON
5. Check radiation badges and hearing protection
6. DC POWER: CONTROL POWER ON
7. Warning lights: "On"
8. VACUUM COOLING: VACUUM COOLING ON
9. MIRROR TEMPERATURE REGULATOR: MTR ON
10. Check pressures and flows of:
  - (a) LCM cooling
  - (b) MTRM cooling
11. MAIN COOLING: MAIN COOLING ON

E. Laser Room

1. Detector power: "On"
2. Reticle retracted and rubber plug removed
3. Kinney pump valve: Closed

F. Control Room

1. Power to chopper: "On"
2. Vacuum: VACUUM PUMPS ON
3. Check status board for "start"
4. Check ROV5 position
5. Check sustainer cavity pressures
6. After sustainer cavity pressure has reached less than 4 torr:
  - (a) FILL SEQUENCE: FILL SEQUENCE ON
  - (b) GAS SOLENOID: ON
7. Check that sustainer cavity pressures rise and blowers start.

G. Laser Room

1. Check and adjust gas flows and pressures :  
(All four gages set at 50 PSI)
2. Clear conference room and laser room of all people
3. Close door and lock

H. Inside Location

1. 4160 "Main Power": "On"
2. LAB SPS switch: RESET and then ON

TABLE I. LASER WELDER OPERATION CHECK LIST

I. PRETEST

A. Outside Location

1. Turn on gases:

- (a) Helium
- (b) Nitrogen
- (c) Carbon Monoxide
- (d) Carbon Dioxide

2. Check fenced area clear and gate closed

3. Open door for cooling fans

4. Turn on 400-Hz supply:

- (a) MASTER SWITCH: ON
- (b) Wait for OIL PRESSURE light: NO GO to go off
- (c) LOCAL START switch: Push on
- (d) Inside ("Generator") switch: ON
- (e) Set FREQUENCY ADJUST control to 400 Hz
- (f) OUTPUT CONTACTOR: Push close

B. Inside Location

1. Cooling Water: "On" and flowing

2. 208 volt supply: "On"

C. Laser Room

1. West doors closed and locked

2. Conference room clear

3. MTRM pressure check: 30 PSI

4. LCM pressure check: 35 PSI

5. CO monitor check: "On" and functioning

6. All MTU ac (400 Hz) circuit breakers: "On"

7. Experimental setup check:

- (a) Equipment in place
- (b) Backstop in place
- (c) By-product exhaust system functioning

8. Glycol: Check level

NOTE: After foil change, check the following after step 8:

- (a) Proper J26 connector
- (b) MTU/dc power connector on simulator

9. Aft lead shield in place

resume after the vacuum system has recovered; usually within 3 to 5 minutes. When a test is completed, the laser should be turned off along with the 71 kV power and the 4160 Vdc power. If a delay is expected, the gas should be shut down also. (Do not reapply gas for a minimum of 5 minutes. The blower motors can overheat if started too frequently.) When the test is completed, the laser can be further shut down by changing to the standby vacuum system and turning off the coolant systems.

Table I lists sequential procedure with the necessary check points used to activate the HPL welder and monitor system status while bringing the HPL welder on-line. E-beam cavity controls and interconnections are shown in Figures 26 through 29.

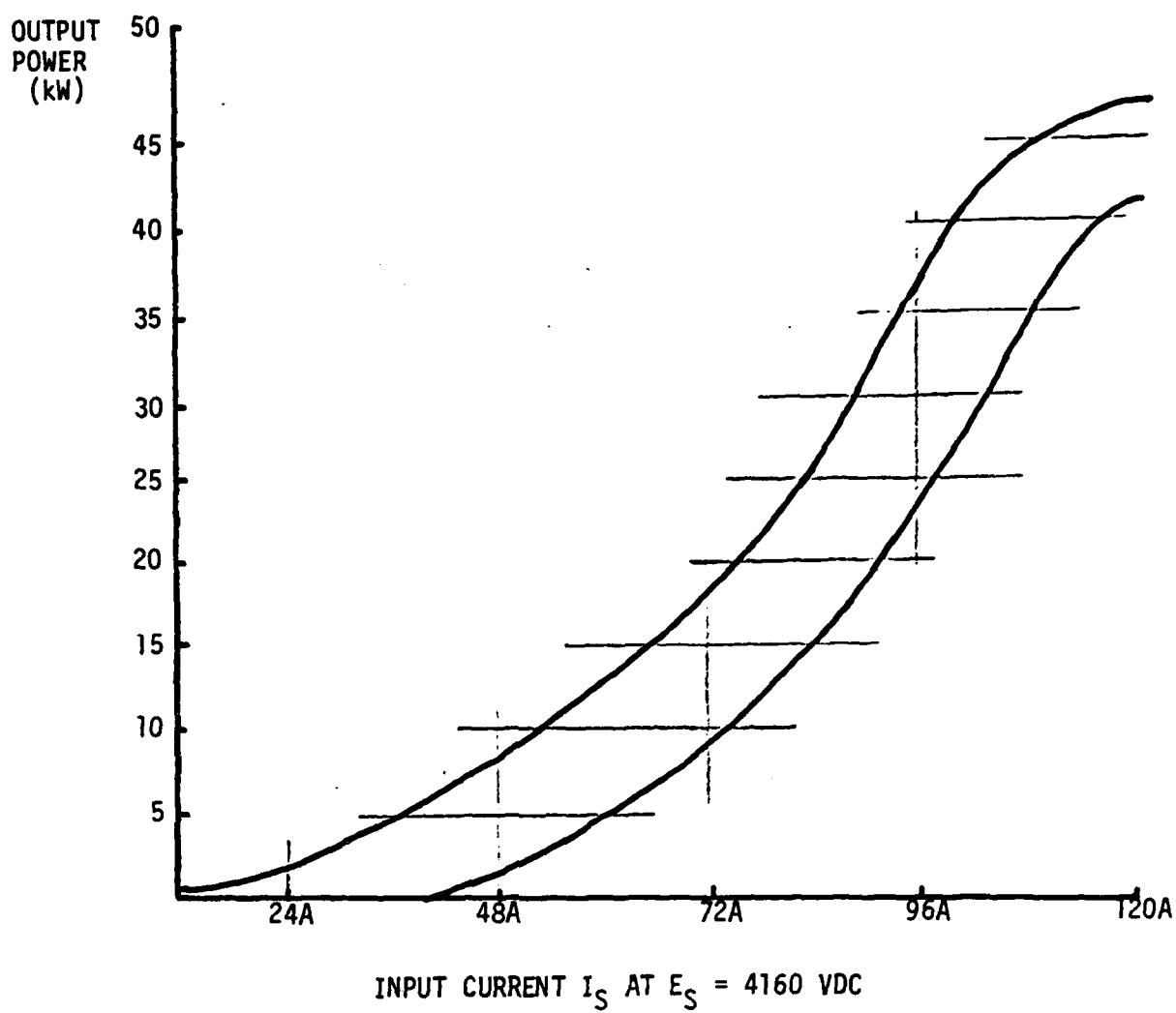


Figure 25. Laser output power curve

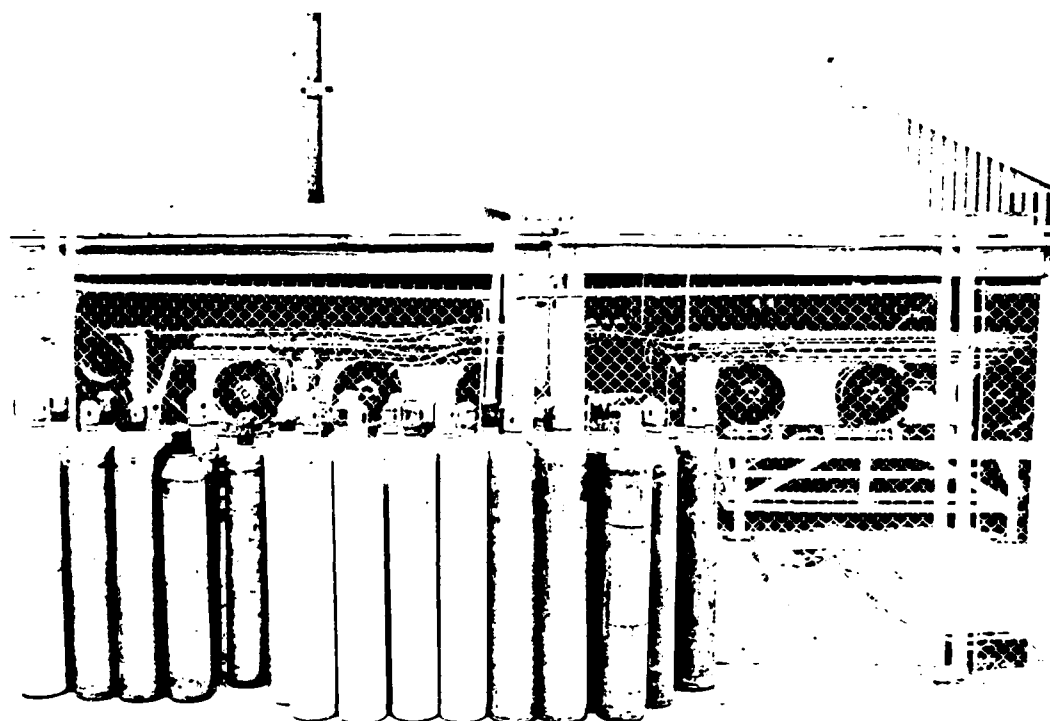


Figure 24. LCM and MTRM cooling system radiators

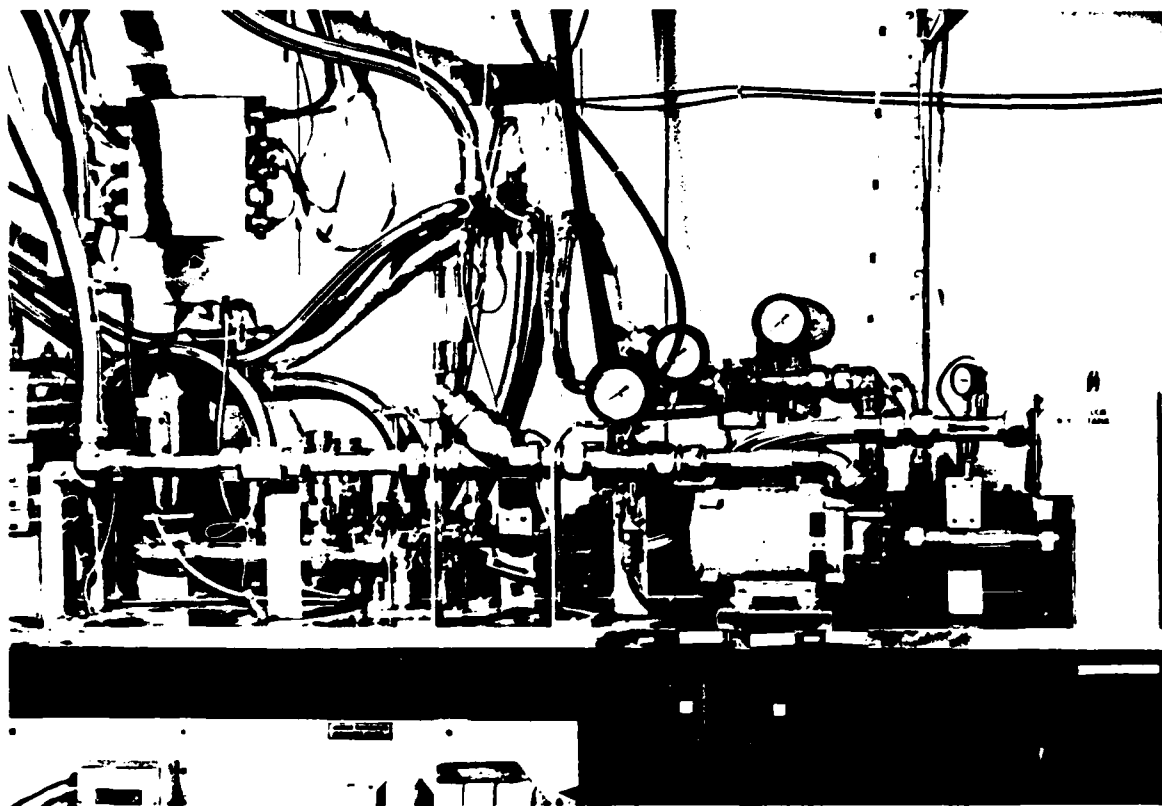


Figure 23. LCM and MTRM water circulating system

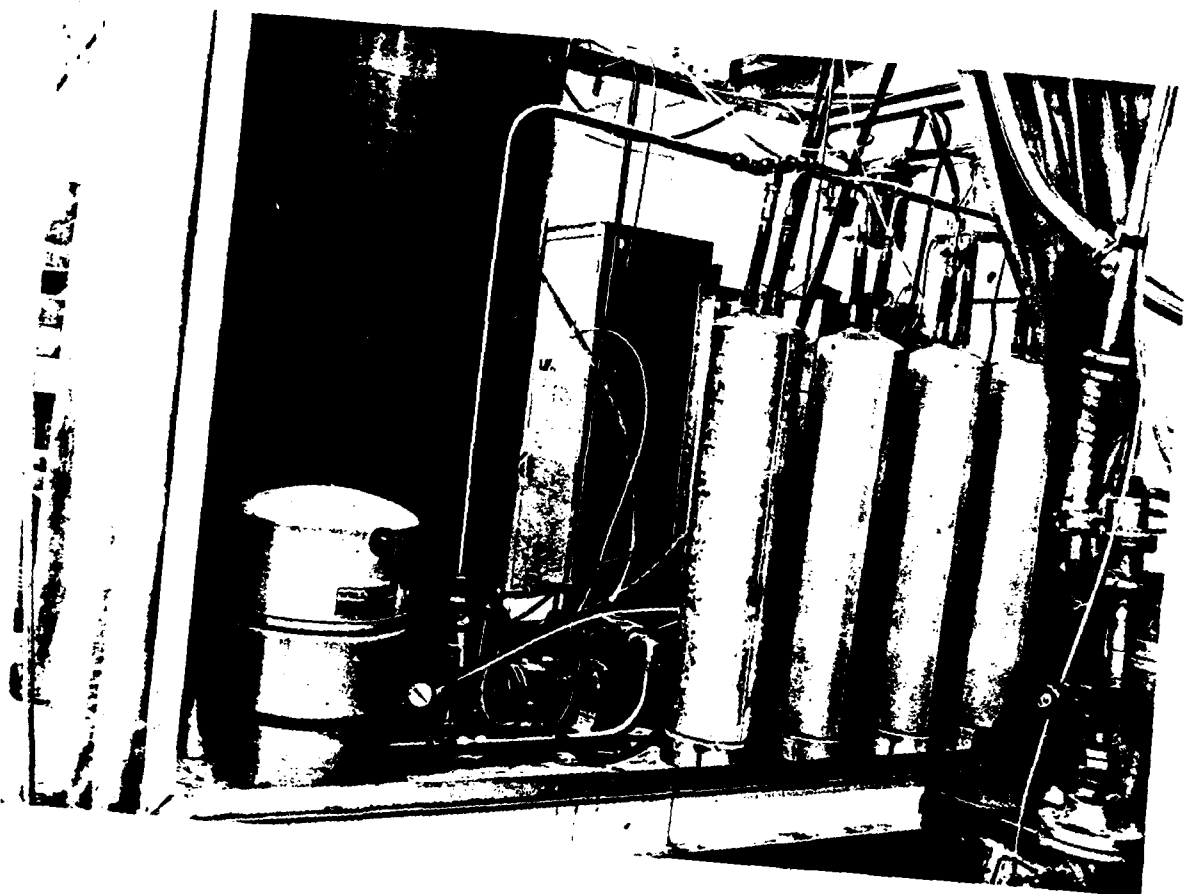


Figure 22. Deionized water system



Constant attention must be directed to safety of eyes, hearing, radiation, poisonous gas, hazardous voltage, and laser beam control. Personnel operating the equipment must be qualified in first aid. A minimum of two operators must be in attendance, and both must have first aid training.

An operator in training must be under the immediate direction of a regular HPL operator. All laser control functions must become automatic to the operator before the operator can be responsible for the laser operation.

Before initiating any laser functions, the welding table and welding samples should be positioned for welding. The weldable material is placed on the welding table, and the metal joint must be aligned to intersect the laser beam. Sequencing switches on the welding table must be positioned to start the lasing action an inch ahead of the welding sample. The laser will impact scrap material prior to coming in contact with the welding sample. Welding speed is set at the control console according to the speed control to the chart shown in Figure 21.

With the welding table arrangement completed, the laser can be powered for use. Initially, the preliminary checks include turning on the deionizing water system which provides coolant to the laser E-beam filaments and provides a supply of deionized water for replenishing the LCM and MTRM closed cycle systems (Figures 22 through 24). Static pressures for the LCM and MTRM must be 30 psi and 35 psi respectively. The allowable tolerance is plus or minus 1 psi. The pressure can be increased by adding the pressurized deionized water directly into the cooling system through the fitting provided. An overpressure can be bled off by the special bleed valves provided.

Activation of the laser is initiated by turning on the LCM and MTRM coolant circulation systems. Check on the coolant systems are made by monitoring the coolant instrumentation panel. Each meter has a warning level indicator to attract the observer to malfunctioning units. Malfunctions within the cooling system would terminate a test until replacement of the faulty component. The laser vacuum system is activated after turning off the standby vacuum system. Instrumentation in the control area will sequence vacuum pumps to achieve the necessary vacuum. Meters on the instrumentation panel indicate when stabilization is reached. The functions to this point may be energized indefinitely provided hearing protection is worn by all personnel in the immediate area.

The gas flow to the laser and the application of high voltage are the next functions energized. The gas flow rates must be checked when activated to confirm proper laser gas mixture. Personnel must monitor gas flow and then exit from the laser area before energizing any high voltage. The test must be ready to run because operating expense is heavy while laser gas is flowing. An effort should be made to perform the lasing operation within a five minute operating period.

To obtain the lasing action, apply 4160 Vdc power to the sustainer cavity and then turn on the 71 kVdc E-beam power. Lasing will begin when grid bias to the E-beam is adjusted above cut-off. The magnitude of lasing energy is determined by monitoring sustainer current and reading the output power from the curve shown in Figure 25. The duration of the lasing test is limited by the sustained vacuum level in the E-beam cavity. When the pressure increases above  $4 \times 10^{-5}$  torr, the lasing test must be discontinued. Additional testing can

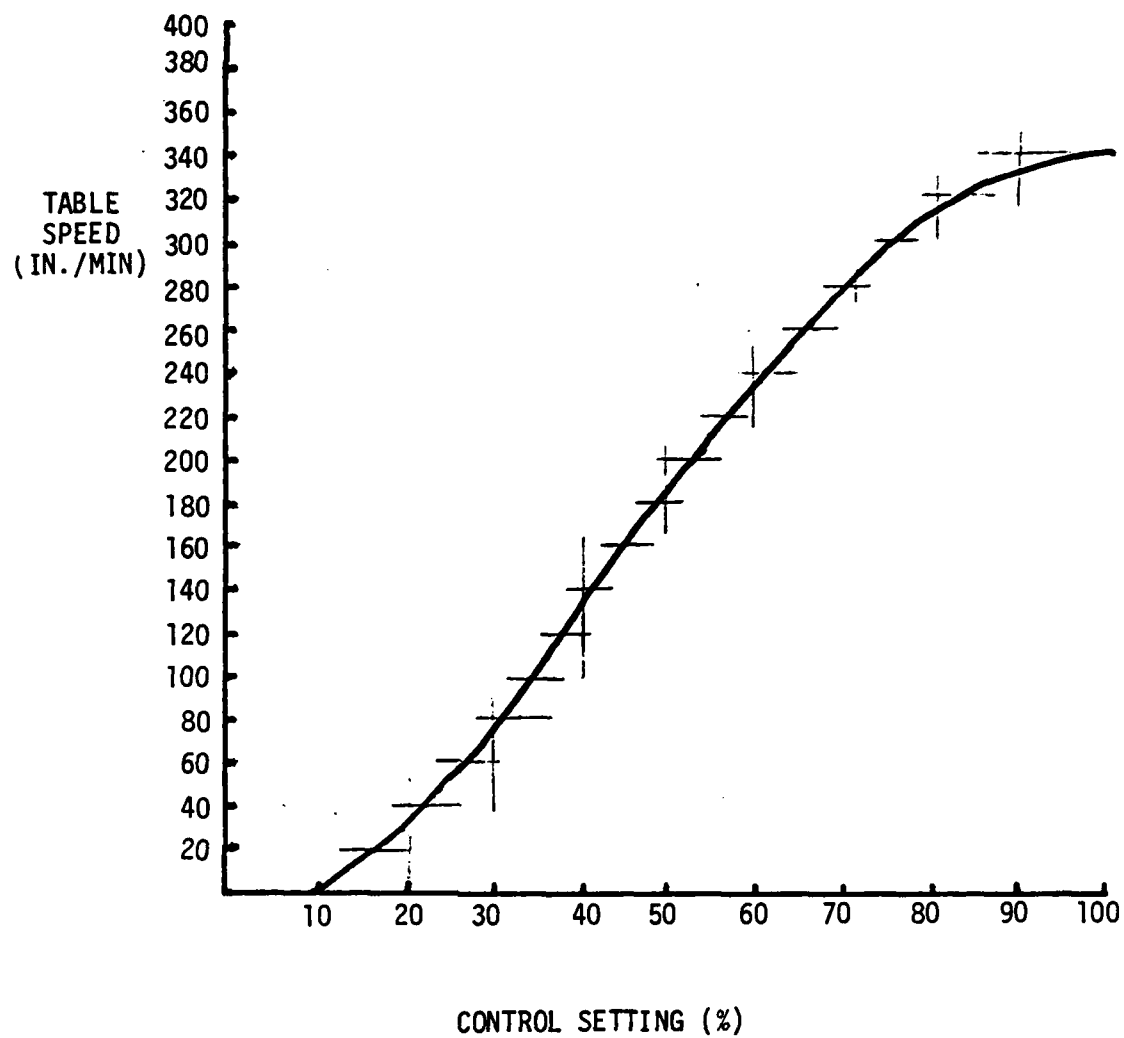


Figure 21. Speed control chart

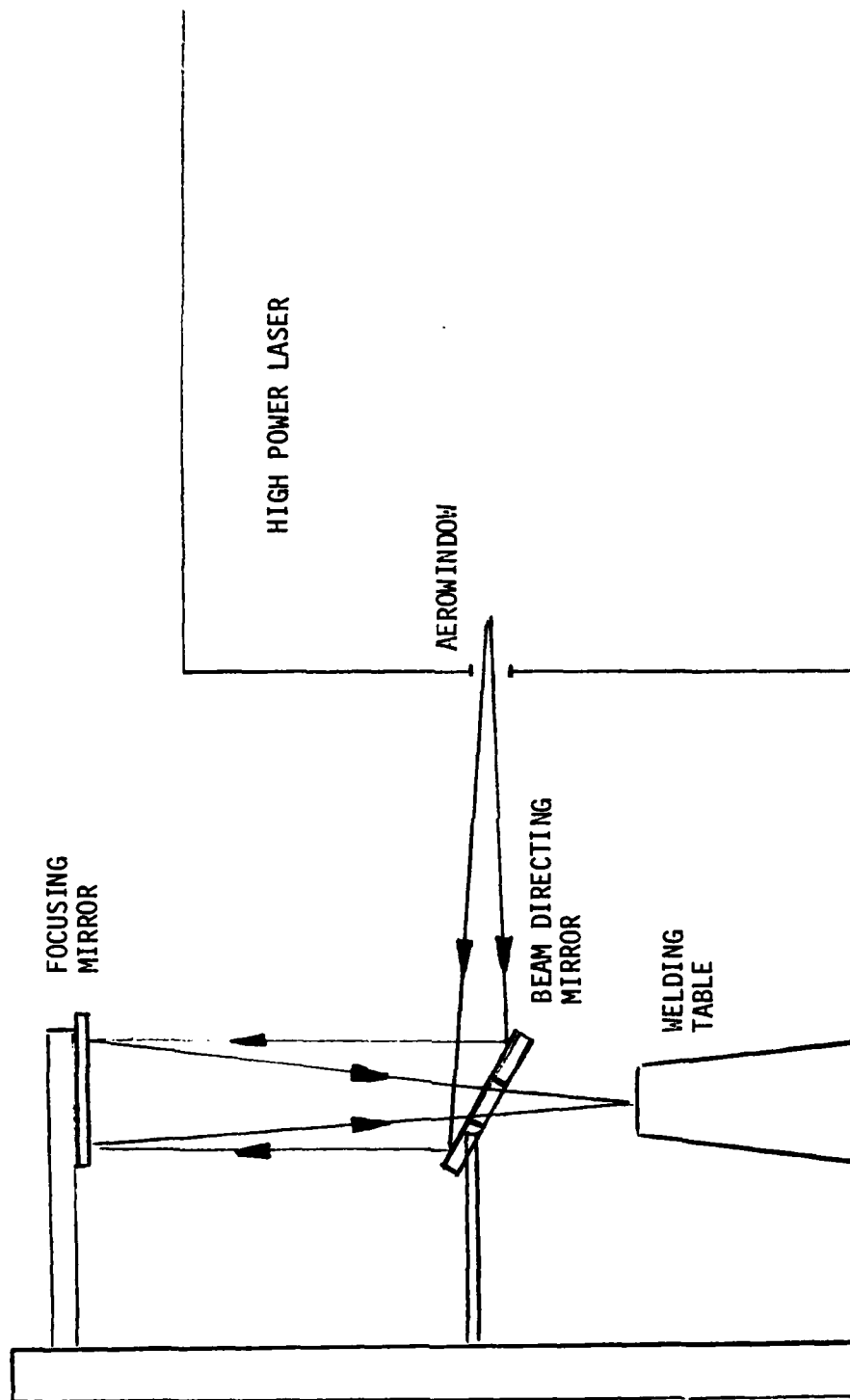


Figure 20. External optics system

## B. AUTOMATION OF LASER WELDING OPERATION

The purpose of automating the laser welding operation is to:

- Reduce the complexity and number of steps required in the welding operation.
- Reduce the number of operators required to perform laser welding.
- Reduce the use of shield gas prior to and after actual welding operation.
- Increase the safety, efficiency, and reliability of the laser welding operation.

Automation features include:

- Automatic termination of welding table travel in both directions (safety feature).
- Automatic start and stop of shield gas flow (reduces gas consumption).
- Automatic check of welding table speed. Laser is not turned on unless welding table speed is adequate. (Reduces possibility of poor welds.)
- Adjustable sequencing of shield gas flow, start, stop, and laser beam on and off modes.

## C. OPERATION AND INTEGRATION OF SYSTEM

The welding table automation control is mounted at the control console. Indicator lights energize to indicate table position and which function is occurring. When the table is moving toward the starting end, a light energizes as the table automatically stops at that end-of-travel. With the welding table properly set up with a weldable material, the laser is placed in operation and the welding table set into operation. All lasing action is controlled by the welding table. The table moves toward point of impact with the welding beam. The first check is to determine that proper speed is achieved. If speed is not proper, the laser will not be energized. A speed light on the control panel indicates when proper speed is achieved, then the shield gas and laser action are turned on just prior to the workpiece reaching the point of impact. As the workpiece leaves the laser beam area, the shield gas and laser beam are shut off. The workpiece proceeds to the end-of-travel and stops. Additional details of welding table operation are provided in Section III.

An external optics system is required to orient and focus the laser beam onto the weldable workpiece (Figure 20). The laser beam exits the laser cavity at the aerowindow, traveling parallel to the floor. The beam strikes a gold-plated copper mirror at a 45° angle. The beam is annular shape at this point and about 4 in. in diameter. The mirror is oval and larger than the laser beam, and also has a hole in the center that is smaller than the hole in the annular laser beam. All energy strikes the mirror and is deflected upward to a focusing mirror. This mirror reflects the beam downward through the hole in the 45° mirror and focuses the beam onto the workpiece for welding.

## D. WELDING SYSTEM OPERATION

The operation of the HPL consists of laser operating instructions that make the operator aware of required procedures that must be adhered to. The HPL is a dangerous device which requires a conscious effort by the operator to maintain a consistent safety standard. Familiarity causes laxity in control procedures.

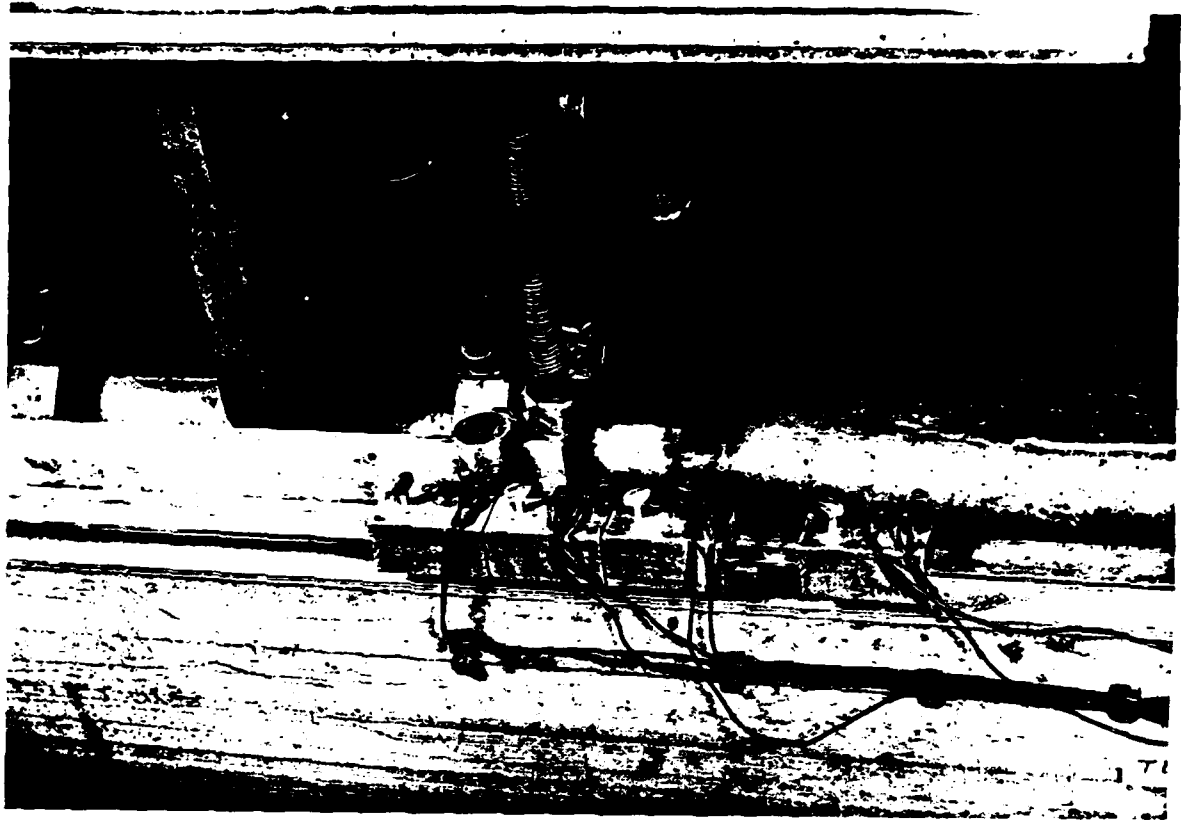


Figure 19. Welding table sequencer

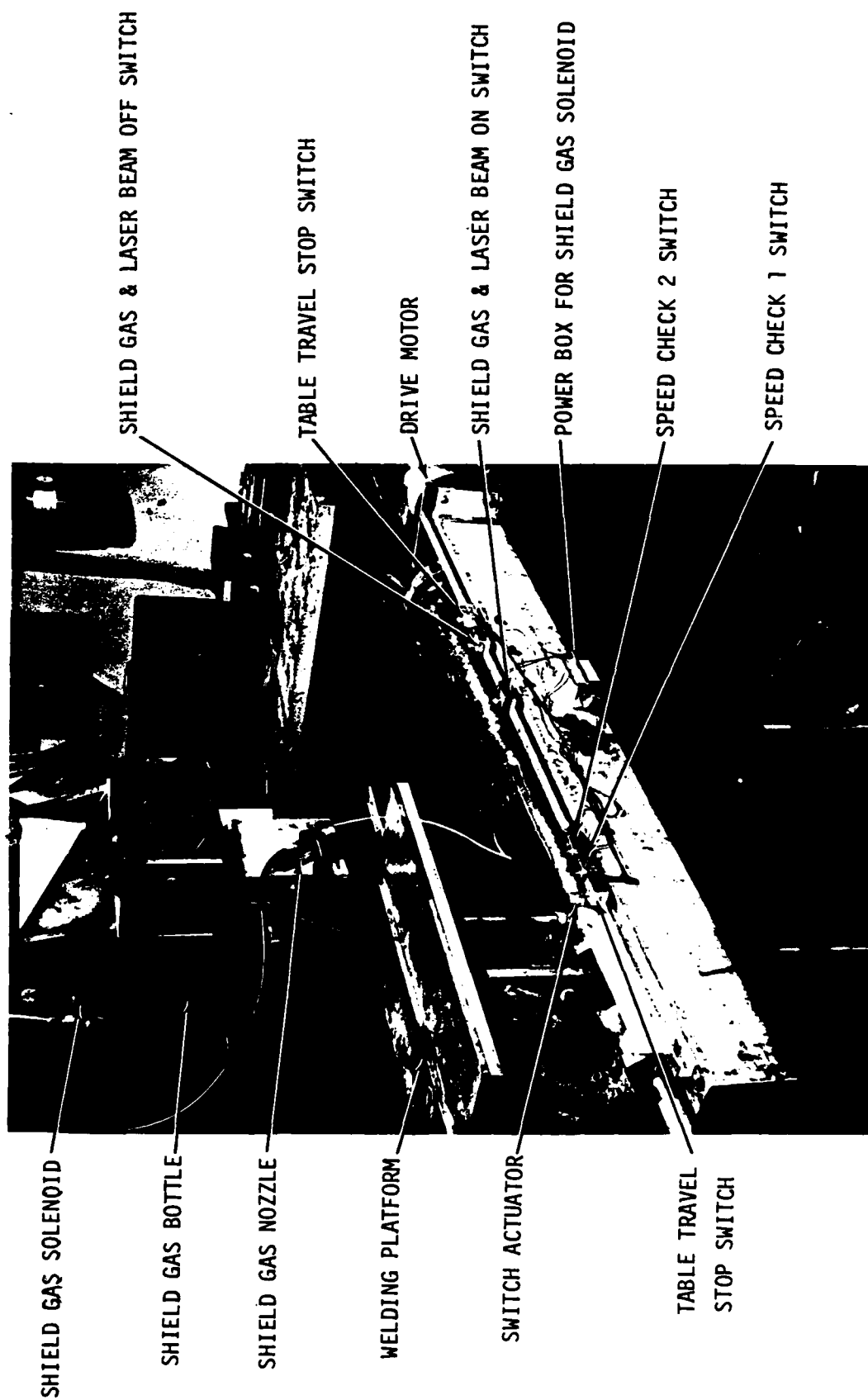


Figure 18. Welding table

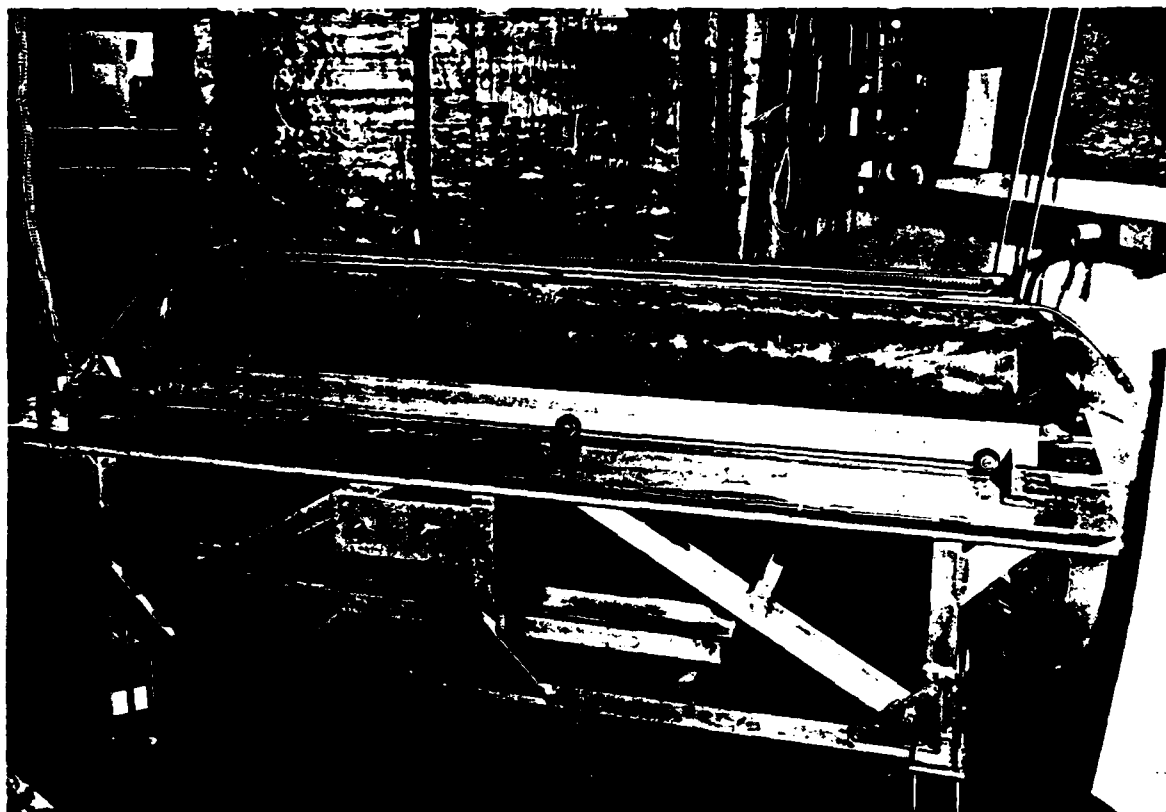


Figure 26. E-beam cavity on maintenance table

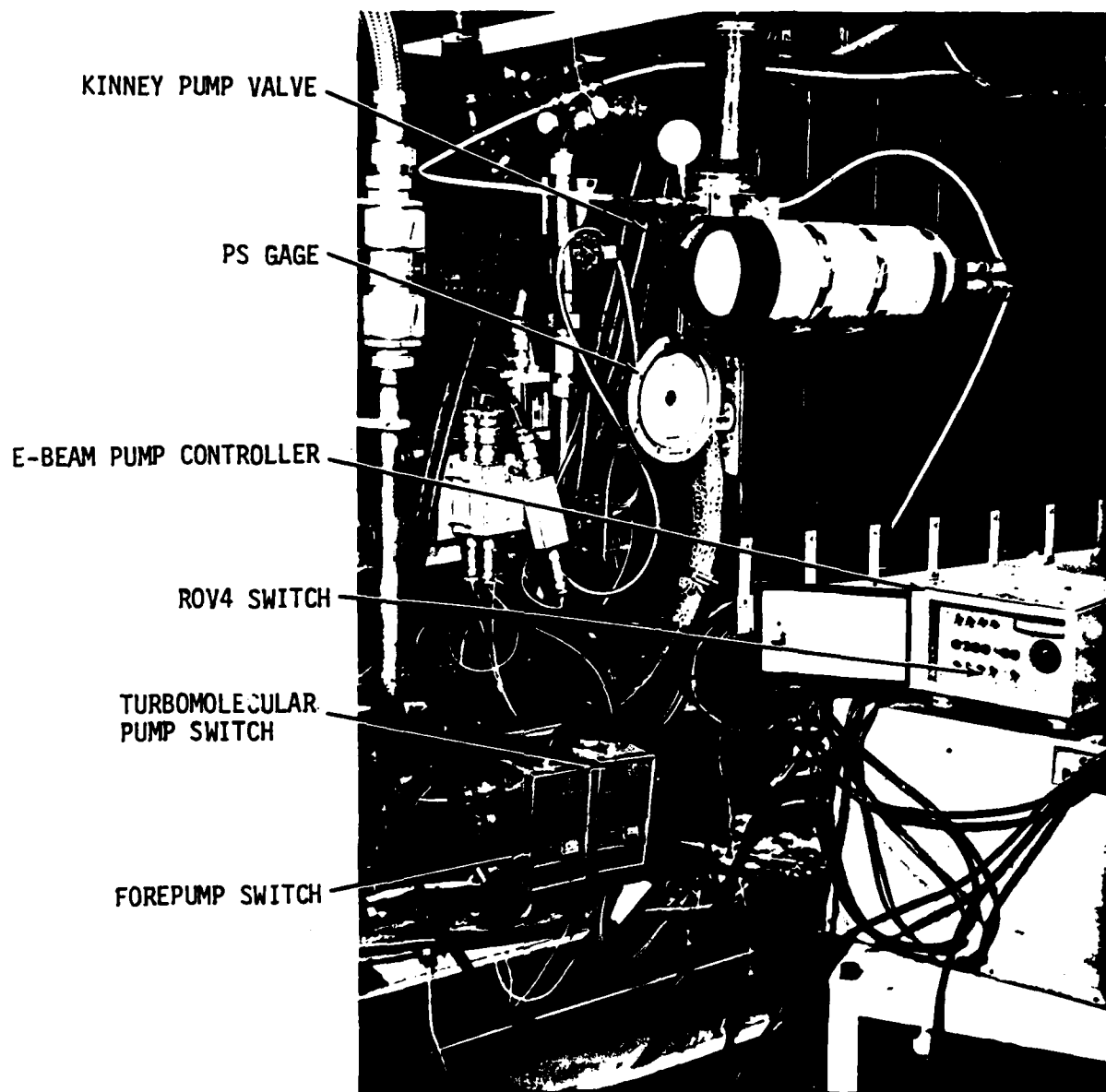


Figure 27. E-beam backfill controls



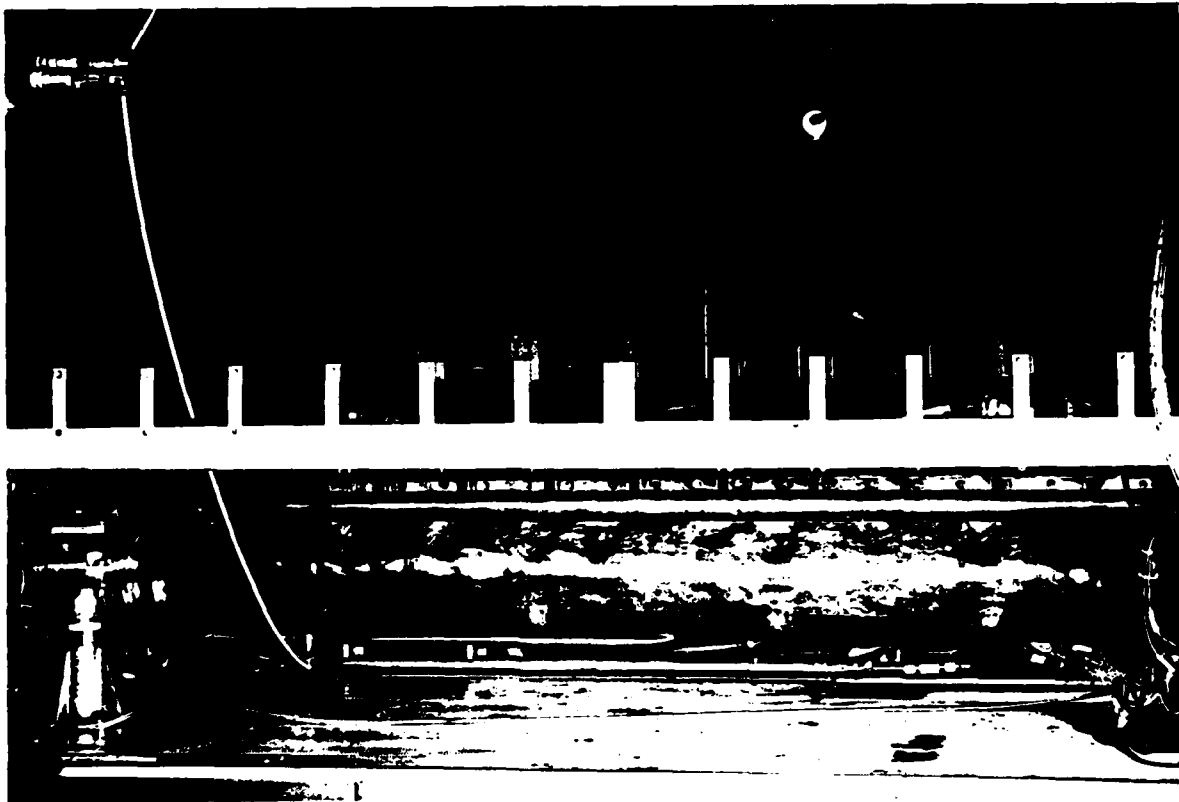


Figure 28. E-beam interconnections -  
Side view of E-beam cavity mounted in laser

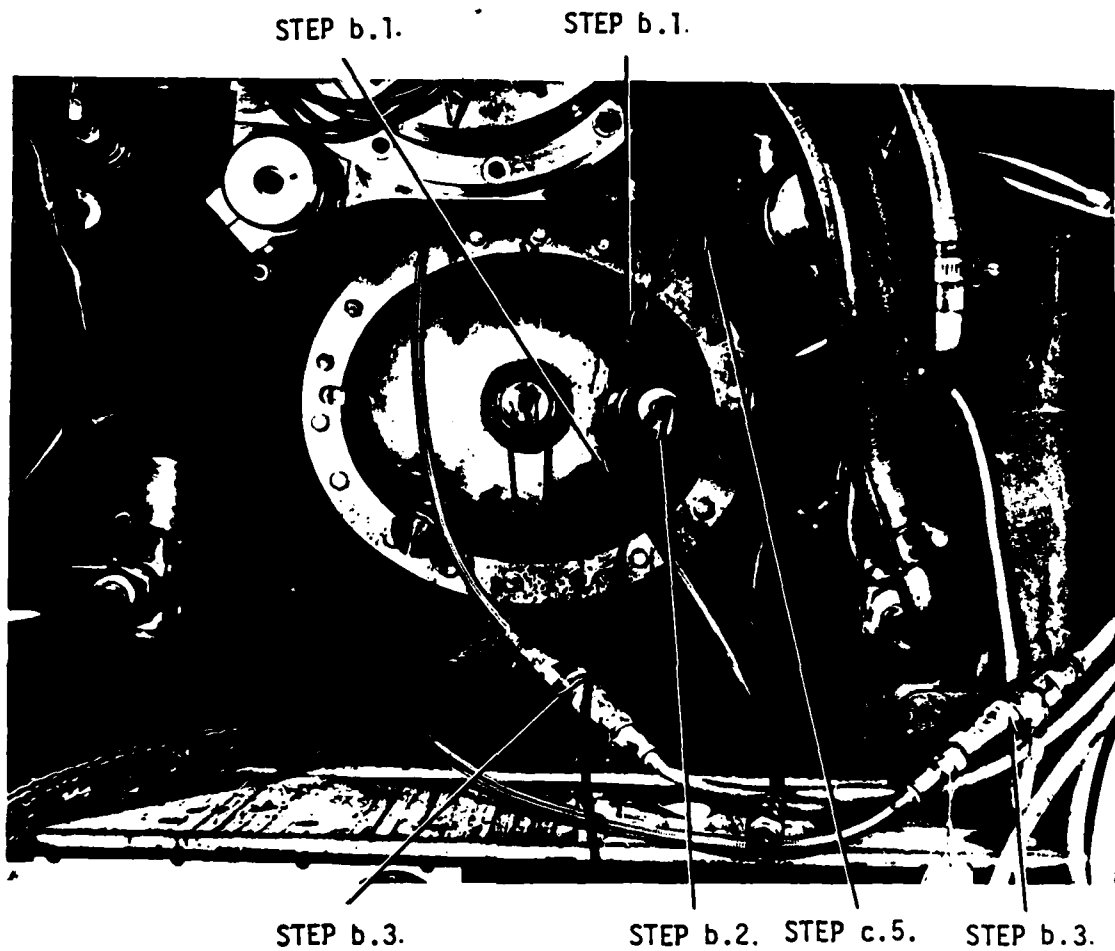


Figure 29. E-beam interconnections - Back end view

### III. EQUIPMENT DEVELOPMENT

#### A. Power Control

Early welding problems were known to be caused by an uncontrolled output power from the laser. High-speed oscillograph recordings were made of the output power as a function of time. When the laser was operated in the open loop, sustainer current, or E-beam current feedback control, the output power fluctuated or dropped as a function of time. Usually a significant drift in power was noted within 0.25 seconds. To stabilize the laser output power, an analysis was made of the laser control loop response. The system response to an error signal above 30 Hertz was noted to be attenuated appreciably.

To stabilize the laser output power, a sampling system monitors the laser output and makes corrections by feeding a signal into the E-beam power supply to correct power drift. The system operates using a rotating mirror that intersects the laser beam and reflects a portion of beam energy into a pyroelectric detector that converts the light pulse to an electrical signal (Figure 30). The amount of energy reaching the detector is attenuated and focused to condition a consistent feedback signal within the range of the pyroelectric detector sensitivity. An amplifier was designed to match the pyroelectric detector output and interface with the existing control system. Sufficient safety precautions were incorporated to prevent the loss of laser control. All power control modes were fed through the same amplifier box so that the method of control can be selected at the amplifier. A noticeable improvement in output power stability was noted with the power feedback design incorporated. The original design was with a single revolving mirror for feedback which permitted a substantial amount of ripple in the feedback signal. The feedback system was improved further by using a four-mirror feedback system to reduce the ripple effects.

A specification for power stability had power drift limits for welding established at  $\pm 10$  percent. Earlier methods of control had power drift of  $\pm 30$  percent. Final test data for the mirror feedback system was recorded on a Honeywell Model 1858 Visicorder. An analysis of the test data showed an overall stability of  $\pm 6$  percent. Welding samples shown in this report were made with the new power control system.

#### B. Automatic Laser Control

1. Welding Table - Since the laser beam position is stationary, the workpieces to be welded have to be moved through the beam. A fixture with the capabilities listed below was modified and adapted for the application. (See Figures 18 and 31).

- o Remote controlled, variable-speed electric motor drive (in both forward and reverse direction).
- o Speeds variable from 30 to 300 inches per minute.
- o Total travel 40 inches.
- o Maximum length of weld, 40 inches.
- o Movement perpendicular and in-line with laser beam.
- o Mounting provisions to rotate workpiece 0 to 90 degrees.
- o Gas shield to prevent oxidation of workpiece during welding process.

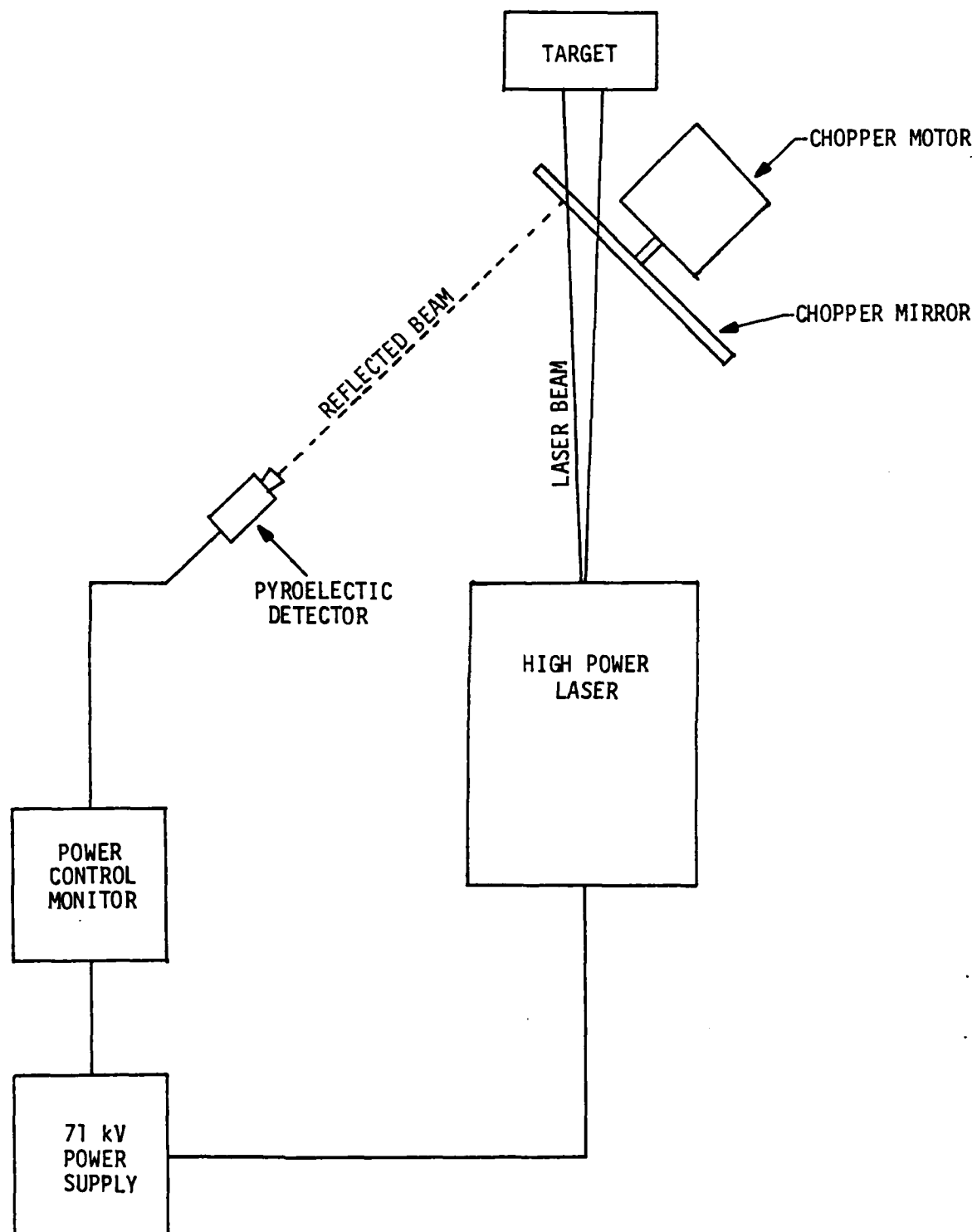


Figure 30. Power feedback loop

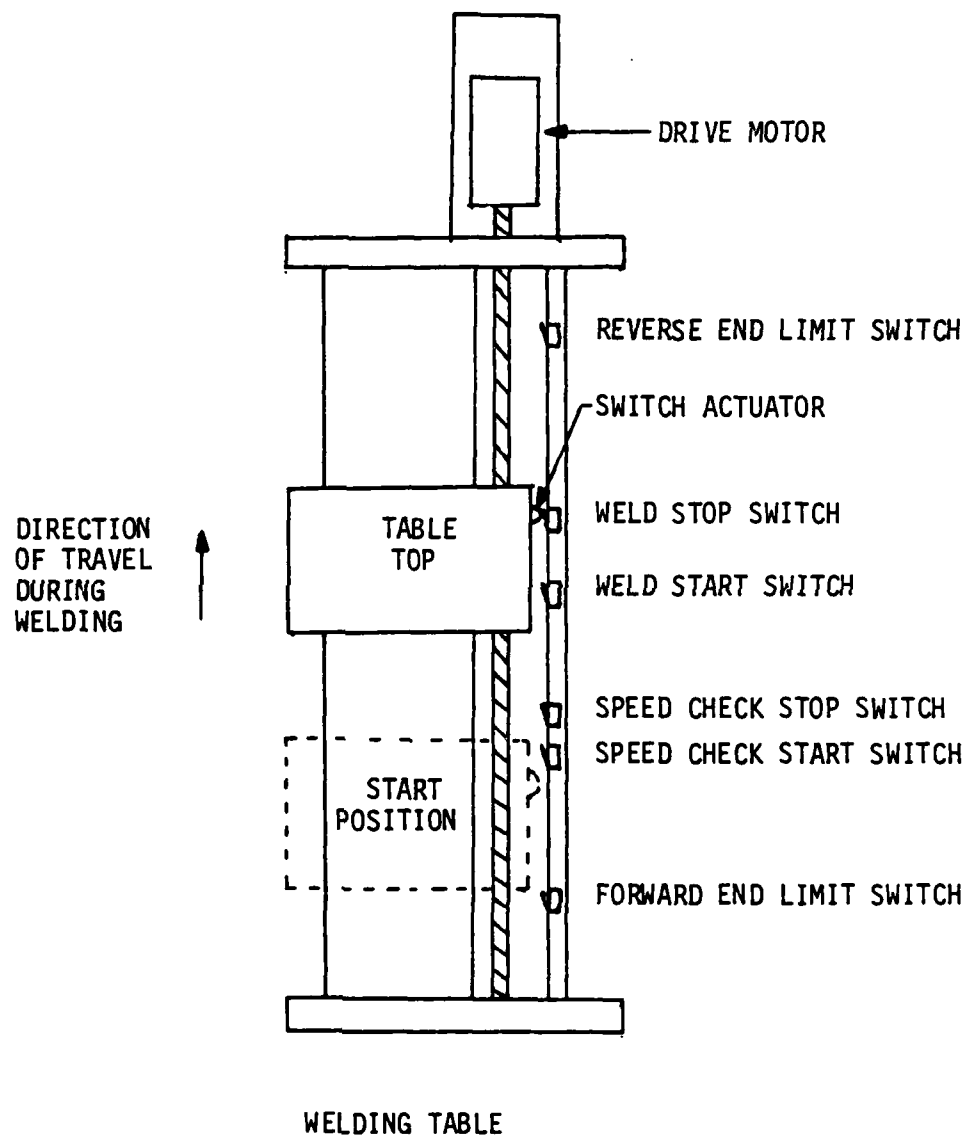


Figure 31. Welding table controls

2. Automation of Laser Welding Operation - The purpose of automating the laser welding operation is to:

- Reduce the complexity and number of steps required in the welding operation.
- Reduce the number of operators required to perform laser welding.
- Reduce the use of shield gas prior to and after actual welding operation.
- Increase the safety, efficiency, and reliability of the laser welding operation.

Automation of the laser welding operation features:

- Automatic termination of welding table travel in both directions directions (safety feature).
- Automatic start and stop of shield gas flow (reduces gas consumption.
- Automatic check of welding table speed. Laser is not turned on, unless welding table speed is adequate. (Reduces possibility of over-powered welds.)
- Adjustable sequencing of shield gas flow, start, stop, and laser beam on and off modes.

### 3. Description of Operation and Integration in the Laser Welding System

The laser welding system was modified to perform the welding operation with automatic sequencing. These modifications are an integral part of the laser welding system. However, they are integrated in such a manner as to permit manual operation without the need to disconnect or require any part of the system. The operator can override any command initiated by the automatic sequencing, should the need to do so occur.

The hardware for the automatic operation consists of microswitches and a switch actuator mounted on the welding table, a chassis containing the signal conditioning, relays and components for interfacing with the control console, a display panel, and an electrical cable connecting the microswitches with the components mounted in the chassis and display panel.

Location and function of the microswitches are illustrated in Figure 19. All microswitches are mounted on the stationary part of the welding table. Their position can be adjusted to accommodate the variable parameters for each specific welding test. The switches are actuated by the switch actuator mounted on the moving work platform of the welding table.

The two table travel stops switches, one mounted at either end of the welding table prevent the welding table from running into the end of the welding table frame. When the switch actuator is in contact with the table travel stop switch, the power to the electric drive motor is interrupted. The drive motor can be started and stopped or the direction of travel changed as long as the

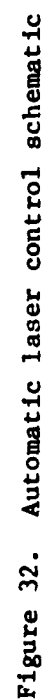
switch actuator is located between the two table travel stop switches. The drive motor control panel is located on the laser control console. Prior to the laser welding operation, the table is moved to the speed check 1 and speed check 2 switches are adjusted to correspond to the selected welding speed. When the table is in motion, the switch actuator will depress the speed check 1 switch first then the speed check 2 switch. The elapsed time between the activation of the two switches is electronically measured and compared to the desired value. This measurement is utilized by the electronic circuit to ensure that the welding table is moving at the correct speed before the laser beam and shield gas can be turned on. If the table is moving at the correct speed, the control circuit will permit the shield gas and laser beam to be activated when the shield gas and laser beam "on" switch is depressed by the switch actuator. The distance between the "on" and "off" switch is set to coincide with the length and location of the weld. The shield gas and laser beam are turned off when the switch actuator depresses the shield gas and laser beam "off" switch. Should the operator have cause to terminate the welding operation before the "off" switch is activated, he can do so by depressing the E-beam LASER BEAM OFF switch mounted on the laser control console panel. The table travel can be stopped by the operator at the motor control panel or it will be stopped automatically when the switch actuator depresses the table travel stop switch.

A monitoring panel, mounted on the control console, contains one switch and three indicator lights. The switch controls the mode of the laser welding operation, either automatic or manual. The status of the speed control and laser power is displayed by the indicator lights (see electrical schematics, Figure 32). When the speed light activates, the operator knows that everything is operational to that point. The operator then observes the welding operation on closed circuit television. When the operator observes the stop light, the equipment is deactivated so that personnel can enter the lasing area to check the weld activity.

### C. Mirror Alignment

Work was performed to improve handling of the laser beam after it leaves the laser on a path to the welding table. The laser beam deflection system is comprised of two gold plated copper mirrors supported by an I-beam and platform (see Figure 33). One mirror is a deflecting mirror and the other is a focusing mirror. The mirror orientation for laser output beam directing is positioned in front of the laser such that the laser beam will strike the first mirror and be deflected upward 90 degrees to strike a focusing mirror. The height of the focusing mirror is set so that when the beam is deflected back downward, it will pass through a hole in the deflecting mirror and come into focus just above the workpiece. More detail about the focusing is provided in the section on benchmark testing.

A vertical 7 foot structure supports the two mirrors. The structure was originally designed for a fixed welding position. With the structure in position and holding the mirrors, it was not possible to change position of the welding table because the mirror support obstructed the relocation of the welding table. To move the obstruction required a redesign for the mirror support. The new mirror support allows the mirror structure to be moved off axis by 45 degrees. The structure is now out of the way for rotating the welding table. This adjustment is necessary because of a non-symmetrical welding beam.





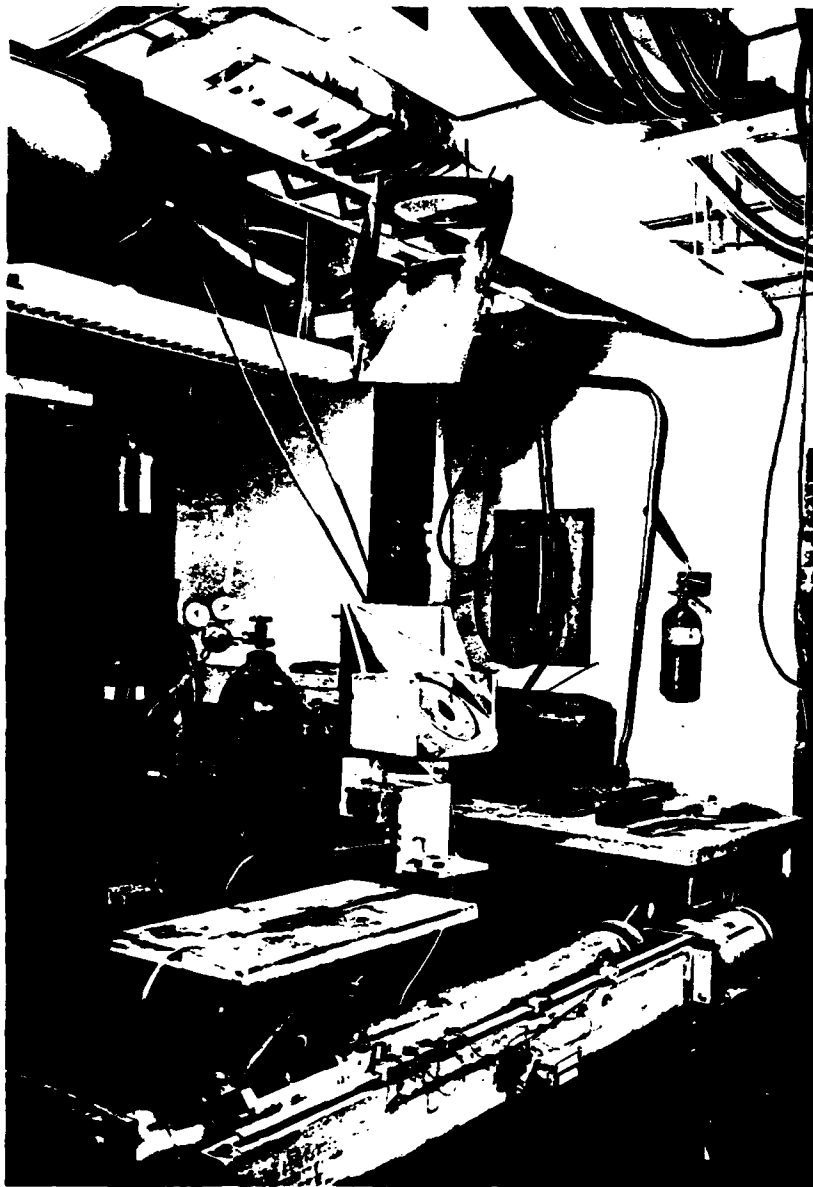


Figure 33. External mirror system

Laser beam quality tests of the high power laser showed that the beam is not focused to a concentric spot. The cross-section of the beam is somewhat oval shaped. The beam shape can be observed when burned into plexiglass. One such burn is shown in Figure 34. It can be clearly seen that the beam has two peaks of different intensities. This beam pattern is generated by the internal optics of the laser. Using proper alignment techniques, the output beam pattern has been adjusted for optimum obtainable shaping.

Because of the non-symmetrical laser welding beam, the workpiece has to move on an axis in line with the laser beam when a well defined narrow weld is desired. A broader beam is available by moving the workpiece perpendicular to the laser beam axis.

#### D. Gas Shielding


Laser welding was attempted for several weeks before any attempts were made to provide a gas shield. No benefit can be derived from discussing the many gas shield configurations that did not function properly. The major fault encountered was that the method of applying the gas shield to the weld would permit oxygen to be drawn in with the gas and not provide a good shield.

The present design for shielding the weld surface uses a two-piece shield design. A standard welding shield bar was inserted under the workpiece with the gas outlets from the shield bar increased by drilling an additional hole between each pair of holes on the shield bar. The shield bar was then plugged at one end, and gas was introduced into the opposite end. Shielding on top of the weldment was provided by a copper gas shield shown in Figure 35. The bottom view points out the features of the shield. Two lines are connected to a source of helium through a flow meter. The top line connects helium to the top of the shield plate and forces helium through the series of holes around the circumference of the laser beam inlet to the workpiece. The second gas inlet forces helium against the plasma, clearing it from the weld area. The spherical cavity is utilized to redirect reflected laser energy back to the workpiece. Reflective metals such as aluminum can be welded to approximately twice the penetration depth at a given weld rate and power level utilizing this spherical reflector feature, or the weld rate can be increased for a given weld depth. Positioning the gas shield above the weldment requires that the clearance not exceed 1/2 inch.

The only maintenance required for the gas shield is cleaning the reflective surface using a piece of cloth saturated with alcohol.

#### E. Welding Table Stability

A major effort was made to stabilize the laser output to achieve weld consistency. Equally important is the constancy of welding table speed. Speed checks on the welding table determined that table speed was not constant over any part of the table travel. Two problems existed that affected table speed. The welding table travels on a tubular steel bed with an attached guide to prevent a rocking motion. The steel bed had deep nicks that affected friction of table movement. The table is powered by a dc motor which inherently changes speed with load. After cleaning and



DOUBLE MODE  
OPERATION

Figure 34. Laser beam pattern

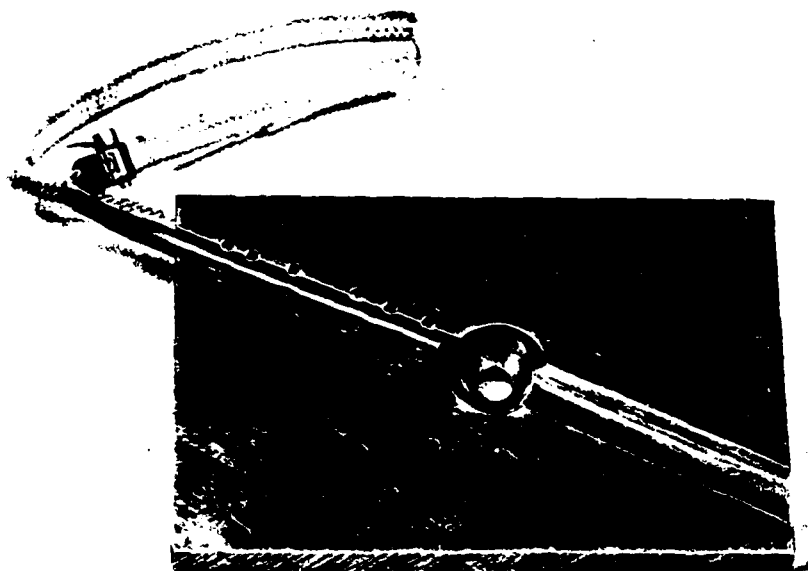


Figure 35. Gas welding shield

deburring the welding table bed, one additional problem existed. The carriage for the welding table is moved from one end to the other with a continuous worm gear about 8 feet long. This gear had been damaged at sometime and this resulted in a whiplash action that provided a jerking motion to the welding table. The gear was sent to a shop for straightening. During disassembly, the bearings for the worm gear were found to be bad and were replaced. A speed check circuit was originally added to the automatic laser control because the carriage problem gave speed variations of 2:1. The speed variation is no longer present, but the speed control does continuously monitor for speed variations.

# DISTRIBUTION

No. Copies

HQ, DARCOM  
US Army Materiel Development and Readiness Command  
ATTN: DRCMT  
5001 Eisenhower Avenue  
Alexandria, VA 22333

1

Commander  
US Army Aviation R&D Command  
ATTN: DRDAV-EGX, Mr. Dan Haugan  
4300 Goodfellow Blvd.  
St. Louis, MO 63120

1

Commander  
US Army Communications Electronics Command  
ATTN: DRSEL-POD-P-G,  
Messers Feddeler/Esposito/Resnic  
Fort Monmouth, NJ 07703

3

Commander US Army Communications &  
Electronics Command  
ATTN: DRSEL-LE-R, Mr. Leon Field  
Fort Monmouth, NJ 07703

1

Commander  
US Army Missile Command  
ATTN: DRSMI-RST  
Redstone Arsenal, AL 35898

5

Commander  
US Army Tank-Automotive Command  
ATTN: DRSTA-RCKM, Dr. J. Chevalier  
Warren, MI 48090

1

Commander  
US Army Armament Materiel Readiness Command  
ATTN: DRSAR-IRI-A, Mr. Dennis Dunlap  
Rock Island Arsenal, IL 61299

1

Commander  
US Army Armament R&D Command  
ATTN: DRSAR-PMP-P, Mr. Donald Fischer  
Dover, NJ 07801

1

Commander  
US Army Troop Support &  
Aviation Materiel Readiness Command  
ATTN: DRSTS-PLE, Mr. Don Doll  
4300 Goodfellow Blvd.  
St. Louis, MO 63120

1

Commander  
US Army Mobility Equipment R&D Command  
ATTN: DRDME-UE, Mr. R. Goehner  
Fort Belvoir, VA 22060

1

Commander US Army Armament R&D Command ATTN: DRDAR-SCM-P Dover, NJ 07801	1
Commander US Army Materials & Mechanics Research Center ATTN: DRXMR-ER, Mr. Roger Gagne Watertown, MA 02172	1
Air Force Materials Laboratory ATTN: AFML/LTM, Mr. H. A. Johnson Wright Patterson AFB, OH 45433	1
Commander US Army Armament R&D Command ATTN: SARWV-RS-AE, Mr. Len Luizzi Watervliet, NY 12189	1
Commander US Army Tank-Automotive R&D Command ATTN: DRSTA-RKA, Mr. Sam Goodman Warren, MI 48090	1
Commander US Army Armament R&D Command ATTN: DRDAR-LCU-M, Mr. Robert Coyle Dover, NJ 07801	1
Commander US Army Armament Readiness Command ATTN: DRSAR-IRW, Mr. Gerald Hall Rock Island, IL 61299	1
Naval Surface Weapons Center Code DC-30, Dr. John R. Thompson Dahlgren, VA 22448	1
Naval Ordnance Station Code 85, Mr. Richard Grollo Louisville, Ky 40214	1
Naval Ship Engineering Center Philadelphia Division Code 6721C, Mr. Joseph M. Bloomer Philadelphia, Pa 19112	1
David Taylor Naval Ship R&D Center Code 282, Mr. Joseph R. Crisci Annapolis, MD 21402	1
Naval Air Systems Command Code 52031D, Mr. William T. Highberger Washington, DC 20361	1

DCSRDS ATTN: DAMA-WSM-A, Mr. John Doyle Room 3B485, The Pentagon Washington, DC 20310	1
DCSRDA ATTN: DAMA-WSW, LTC Raymond Roskowski Room 3D455, The Pentagon Washington, DC 20310	1
DCSRDA ATTN: DAMA-CSC-BU, MAJ Paul Harvey Room 3D440, The Pentagon Washington, DC 20310	1
DCSRDA ATTN: DAMA-CSS-P, LTC L. R. Hawkins Room 3D416, The Pentagon Washington, DC 20310	1
DCSRDA ATTN: DAMA-CSS-P, LTC P. K. Linscott Room 3D418, The Pentagon Washington, DC 20310	1
DCSRDA ATTN: DAMA-DSM-DA, COL Jack King Room 3C444, The Pentagon Washington, DC 20310	1
DCSRDA ATTN: DAMA-CSM-P, Mr. John Mytryshyn Room 3C444, The Pentagon Washington, DC 20310	1
Commander US Army Mobility Equipment R&D Command ATTN: DRDME-VM Fort Belvoir, VA 22060	1
Commander US Army Aviation R & D Command 12th & Spruce Streets St. Louis, MO 63166	1
Commander US Army Materials & Mechanics Research Center ATTN: DRXMR-KB Watertown, MA 02712	1
Commander US Army Armament R&D Command ATTN: DRDAR-LDB-S Watervliet, NY 12189	1



US Army Natick R&D Laboratories  
ATTN: DRDNA-EZM, Mr. Frank Civilikas  
Natick MA 01760

1

Commander  
US Army Test & Evaluation Command  
ATTN: DRSTE-D-M, Mr. John Gehrig  
Aberdeen Proving Ground, MD 21005

1

Commander  
US Army Materials & Mechanics Research Center  
ATTN: DRXMR-PP, Mr. John Gassner  
Watertown, MA j 02172

1

Harry Diamond Laboratories  
ATTN: DELHD-PO, Mr. Julius Hoke  
2800 Powder Mill Road  
Adelphi, MD 20783

1

Commander  
US Army Industrial Base Engineering Activity  
ATTN: SARRI-ENM, Mr. J. W. McGarvey  
Rock Island Arsenal, IL 61299

1

Commander  
Watervliet Arsenal  
ATTN: SARWV-PPI, Mr. T. Wright  
Watervliet, NY 12189

1

US Army Munitions Production Base  
Modernization Agency  
ATTN: SARPM-PBM- DP, Mr. Joseph Taglairino  
Dover, NJ 07801

1

Commander, AVRADCOM  
US Army Applied Technology Laboratory  
ATTN: SAVDL-EU-TAS  
Fort Eustis, VA 23604

1

Commander  
US Army Depot System Command  
ATTN: DRSDS-PE, Mr. Jim Shindle  
Chambersburg, PA 17201

1

Commander  
US Army Industrial Base Engineering Activity  
ATTN: DRXIB-MT, Mr. James Carstens  
Rock Island, IL 61299

1

DCSRDA  
ATTN: DAMA-WSA, LTC Jay Bisbey  
Room 3B454, The Pentagon  
Washington, DC 20310

1

Naval Material Command Industrial Resources Detachment ATTN: Mr. William J. Welsh Philadelphia, PA 19112	1
Naval Weapons Center Code 3624, Mr. Charles Johnson China Lake, CA 93555	1
Naval Air Systems Command NAVAIR 5162C3, Mr. Howard Miller Washington, DC 20361	1
Naval Air Propulsion Center Code PE43, Mr. Joseph Gltz P.O. Box 7176 Trenton, NJ 08628	1
Naval Underwater Systems Center Newport Laboratory, Group Code 363012 ATTN: Mr. Giovanni Silvestri Newport, RI 02804	1
Air Force Materials Laboratory ATTN: AFML/LTM, Mr. Robert Ondercin Wright Patterson AFB, Oh 45433	1
Air Force Materials Laboratory ATTN: AFML/LTM, Mr. F. Miller Wright Patterson AFB, Oh 45433	1
Air Force Materials Laboratory ATTN: AFML/LTM, Mr. William Harris Wright Patterson AFB, OH 45433	1
Air Force Logistics Command ATTN: AFLC/MAX, Mr. James Lawyer Mr. George Shearer Wright Patterson AFB, OH 45433	1
Marshall Space Flight Center Code FSFC/44, Mr. Jim Ehl Huntsville, AL 35812	1
Lewis Research Center 21000 brookpark Road Code LeRC/433, Mr. Charles Blankenship Cleveland, Oh 44135	1
Manufacturing Technology Laboratory Interstate 75, Mail Drop E69 ATTN: Mr. Reed Yount Cincinnati, OH 45215	1

The Cincinatti Milacron, Inc.  
4701 Marburg Avenue  
ATTN: Dr. Richard Kegg  
Manager, Research and Development  
Cincinatti, Oh 45209

1

Aluminum Company of America  
1200 Ring Blvd  
ATTN: Mr. G. B. Barthold  
Washington, DC 20036

1

Western Electric Co., Inc.  
Dept. 316720, Mr. Thomas Gregory  
330 Lexington Road  
Winston-Salem, NC 27102

1

Mr. William Gephardt, Jr.  
4870 Packard Rd.  
Niagara Falls, Ny 14304

1

Mr. John C. Williams  
11522 Running Cedar  
Reston, VA 22091

1

Mr. Paul W. Ramsey  
A.O. Smith Corportion  
Box 584  
Milwaukee, WI 53201

1

Aerojet Electro Systems  
P. O. Box 296  
ATTN: J. F. Keville  
Azusa, CA 91702

1

Mr. Dell K. Allen, Director  
Computer-Aided Manufacturing Lab  
Brigham Young University  
105 D&TB Box 42CB  
Provo, UT 84602

1

Mr. Jerome Fishel  
Circuit Technology, Inc.  
160 Smith Street  
Farmingdale, NY 11735

1

Mr. Michael T. Mittag  
Electrovert Inc.  
P.O. Box 350  
Elmsford, NY 10523

1

Ms. Margaret Scott  
GARD, Inc.  
7449 Natchez Ave.  
Niles, Il 60648

1

Lockheed Missiles & Space Co.  
P. O. Box 504  
ATTN: Mr. Frank Fichter, Mfg. Engr.  
Sunnyvale, CA 94086

1

Mr. Robert Tougas  
Sperry Corporation  
P.O. Box 4648  
Clearwater, FL 33518

1

Commander  
US Army Missile Command  
ATTN: DRCPM-MD-T-I/ Mike Kidd  
BMDSCOM Building, Research Park  
Redstone Arsenal, AL 35898

1

Commander  
Rock Island Arsenal  
ATTN: SARRI-ENM, Mr. J. Benedetto  
Rock Island, IL 61299

1

Chemical System Laboratory  
ATTN: DRDAR-QAC, Mr. Frederick Thompson  
Aberdeen Proving Ground, MD 21010

1

DRSMI-LP, Mr. Voigt  
DRSMI-RPR  
DRSMI-RPT, Record Copy  
DRSMI-RLM

1

15

1

35

**END**

**FILMED**

**10-85**

**DTIC**